



Poznan University of Medical Sciences  
Poland

# **JMS** *Journal of Medical Science*

previously *Nowiny Lekarskie*

Founded in 1889

**2020**  
**Vol. 89, No. 1**

**QUARTERLY**

**Indexed in:**  
Polish Medical Bibliography, Index Copernicus,  
Ministry of Science and Higher Education, Google Scholar

eISSN 2353–9801  
ISSN 2353–9798

[www.jms.ump.edu.pl](http://www.jms.ump.edu.pl)

**EDITOR-IN-CHIEF**

Jarosław Walkowiak

**EDITORIAL BOARD**

David H. Adamkin (USA)  
Adrian Baranchuk (Canada)  
Grzegorz Bręborowicz (Poland)  
Paolo Castiglioni (Italy)  
Wolfgang Dick (Germany)  
Leon Drobnik (Poland)  
Janusz Gadzinowski (Poland)  
Michael Gekle (Germany)  
Przemysław Guzik (Poland)  
Karl-Heinz Herzig (Germany)  
Mihai Ionac (Romania)  
Lucian Petru Jiga (Germany)  
Berthold Koletzko (USA)  
Stan Kutcher (Canada)  
Odded Langer (USA)  
Tadeusz Maliński (USA)  
Leszek Paradowski (Poland)  
Antoni Pruszewicz (Poland)  
Georg Schmidt (Germany)  
Mitsuko Seki (Japan)  
Ewa Stępień (Poland)  
Jerzy Szaflarski (USA)  
Bruno Szczygieł (Poland)  
Kai Taeger (Germany)  
Marcos A. Sanchez-Gonzalez (USA)  
Krzysztof Wiktorowicz (Poland)

**ASSOCIATE EDITORS**

Agnieszka Bienert  
Maria Iskra  
Ewa Mojs  
Adrianna Mostowska

**SECTION EDITORS**

Jaromir Budzianowski – Pharmaceutical Sciences  
Paweł Jagodziński – Basic Sciences  
Joanna Twarowska-Hauser – Clinical Sciences

**LANGUAGE EDITORS**

Margarita Lianeri (Canada)  
Jacek Żywiczka (Poland)

**STATISTICAL EDITOR**

Magdalena Roszak (Poland)

**SECRETARIAT ADDRESS**

27/33 Szpitalna Street  
60-572 Poznań, Poland  
phone: +48 618491432, fax: +48 618472685  
e-mail: jms@ump.edu.pl  
www.jms.ump.edu.pl

**DISTRIBUTION AND SUBSCRIPTIONS**

70 Bukowska Street, 60-812 Poznań, Poland  
phone/fax: +48 618547414  
e-mail: sprzedazwydawnictw@ump.edu.pl

**PUBLISHER**

Poznan University of Medical Sciences

© 2020 by respective Author(s). Production and hosting  
by Journal of Medical Science (JMS)

This is an open access journal distributed under the terms  
and conditions of the Creative Commons Attribution  
(CC BY-NC) licence

eISSN 2353-9801

ISSN 2353-9798

Publishing Manager: Grażyna Dromirecka

Technical Editor: Bartłomiej Wąsiel



WYDAWNICTWO NAUKOWE  
UNIWERSYTETU MEDYCZNEGO  
IM. KAROLA MARCINKOWSKIEGO  
W POZNANIU

60-812 Poznań, ul. Bukowska 70  
tel./fax: +48 618547151  
www.wydawnictwo.ump.edu.pl

Ark. wyd. x,x. Ark. druk. x,x.  
Zam. nr x/19.

The Editorial Board kindly informs that since 2014 *Nowiny Lekarskie* has been renamed to *Journal of Medical Science*.

The renaming was caused by using English as the language of publications and by a wide range of other organisational changes. They were necessary to follow dynamic transformations on the publishing market. The Editors also wanted to improve the factual and publishing standard of the journal. We wish to assure our readers that we will continue the good tradition of *Nowiny Lekarskie*.

You are welcome to publish your basic, medical and pharmaceutical science articles in *Journal of Medical Science*.

**Ethical guidelines**

The Journal of Medical Science applies the ethical principles and procedures recommended by COPE (Committee on Conduct Ethics), contained in the Code of Conduct and Best Practice Guidelines for Journal Editors, Peer Reviewers and Authors available on the COPE website: <https://publicationethics.org/resources/guidelines>

## CONTENTS

### ORIGINAL PAPERS

- Nika V Petrova, Nataliya Y Kashirskaya, Tatyana A Vasilyeva, Elenai I Kondratyeva, Andrey V Marakhonov, Milan Macek Jr, Evgeny K Ginter, Sergey I Kutsev, Rena A Zinchenko*  
**Characteristics of the L138ins (p.Leu138dup) mutation in Russian cystic fibrosis patients . . . . . 7**

- Idris Nasir Abdullahi, Anthony Uchenna Emeribe, Hafeez Aderinsayo Adekola, Habiba Yahaya Muhammad, Abdurrahman El-fulaty Ahmad, Abubakar Umar Anka, Shamsuddeen Haruna, Bamidele Soji Oderinde, Yusuf Mohammed, Halima Ali Shuwa, Adamu Babayo*  
**Leucocytes and Th-associated cytokine profile of HIV-leishmaniasis coinfecting patients attending the Abuja Teaching Hospital, Nigeria . . . . . 12**

- Agnieszka Wiertel-Krawczuk, Juliusz Huber*  
**Iatrogenic injury and regeneration of the facial nerve after parotid gland tumour surgery: a pilot study with clinical and neurophysiological assessment. . . . . 21**

### REVIEW PAPERS

- Roman Lesyk*  
**Drug design: 4-thiazolidinones applications. Part 1. Synthetic routes to the drug-like molecules . . . . . 33**

- Mohammad Yasser Sabbah*  
**The Novel Coronavirus Disease (COVID-19) Outbreak: The Israeli Experience . . . . . 50**

- Jan Niziński, Lukasz Kamieniarz, Piotr Filberek, Greta Sibrecht, Przemysław Guzik*  
**Monitoring the skin NADH changes during ischaemia and reperfusion in humans . . . . . 60**

### THOUSAND WORDS ABOUT...

- Emilia Jakubowska, Sharon Davin, Aleksandra Dumcic Dumcic, Grzegorz Garbacz, Anne Juppo, Bożena Michniak-Kohn, Piotr J. Rudzki, Wojciech Smulek, Clare Strachan, Oleg Syarkevych, Lidia Tajber, Janina Lulek*  
**ORBIS (Open Research Biopharmaceutical Internships Support) – building bridges between academia and pharmaceutical industry to improve drug development . . . . . 71**

## THE RATIONALE, DESIGN AND METHODS OF NEW STUDIES

*Ewa Misterska, Maciej Głowacki*

Longitudinal assessment of changes in psychosocial functioning of patients with adolescent idiopathic scoliosis using virtual reality before, during and after treatment: a quantitative and qualitative study . . . . . 77

Instructions for Authors . . . . . 83

# Characteristics of the L138ins (p.Leu138dup) mutation in Russian cystic fibrosis patients

Nika V Petrova

Research Centre for Medical Genetics, Moscow

 <https://orcid.org/0000-0001-5933-6594>

Nataliya Y Kashirskaya

Research Centre for Medical Genetics, Moscow

 <https://orcid.org/0000-0003-0503-6371>

Corresponding author: kashirskayanj@mail.ru

Tatyana A Vasilyeva

Research Center for Medical Genetics, Moscow

 <https://orcid.org/0000-0002-6744-0567>

Elenai I Kondratyeva

Research Center for Medical Genetics, Moscow

 <https://orcid.org/0000-0001-6395-0407>

Andrey V Marakhonov

Research Center for Medical Genetics, Moscow

 <https://orcid.org/0000-0002-0972-5118>

Milan Macek Jr

2<sup>nd</sup> Faculty of Medicine, Charles University, Prague; Motol University Hospital, Prague

 <https://orcid.org/0000-0002-5173-5280>

Evgeny K Ginter

Research Center for Medical Genetics, Moscow

 <https://orcid.org/0000-0001-6920-6726>

Sergey I Kutsev


Research Center for Medical Genetics, Moscow

 <https://orcid.org/0000-0002-3133-8018>

Rena A Zinchenko

Research Center for Medical Genetics, Moscow; National Institute of Public Health named after N.A. Semashko

 <https://orcid.org/0000-0003-3586-3458>

 DOI: <https://doi.org/10.20883/medical.383>

**Keywords:** cystic fibrosis, haplotype, L138ins (c.411\_412insCTA, p.Leu138dup) mutation

**Published:** 2020-01-30

**How to Cite:** Petrova NV, Kashirskaya NY, Vasilyeva TA, Kondratyeva EI, Marakhonov AV, Macek Jr M, Ginter EK, Kutsev SI, Zinchenko RA. Characteristics of the L138ins (p.Leu138dup) mutation in Russian cystic fibrosis patients. *JMS [Internet]*. 2020 Mar 31;89(1):e383. doi: 10.20883/medical.383



© 2020 by the author(s). This is an open access article distributed under the terms and conditions of the Creative Commons Attribution (CC BY-NC) licence. Published by Poznan University of Medical Sciences

## ABSTRACT

The L138ins mutation, found in Russian cystic fibrosis (CF) patients, is a duplication of three nucleotides (CTA) in exon 4 of the *CFTR* gene and is categorised as a small in-frame insertion/deletion. As a result, the *CFTR* protein molecule elongates by one amino acid residue, leucine, at position 138 (codon 138 (CTA)). In accordance with the new nomenclature, it should be called c.411\_412insCTA (p.Leu138dup). The c.411\_412insCTA (p.Leu138dup, L138ins) mutation is found in CF patients of Slavic origin (Russians, Ukrainians) and has been linked to a single haplotype of the intragenic DNA markers IVS1CA-IVS6aGATT-IVS8CA-IVS17bCA – 22-7-16-13.

## Introduction

Cystic fibrosis (CF; OMIM # 219700) is an autosomal recessive disease caused by a mutation in the *CFTR* gene (OMIM \* 602421), characterised by a variable clinical picture ranging from a rela-

tively mild disease course with monosymptomatic manifestations to severe multiorgan lesions [1]. The prevalence of CF in European countries is about 1 in 2500–4500 newborns and in the Russian Federation, it is 1 in 10,000 newborns [1]. The

spectrum and frequencies of *CFTR* mutations vary widely among different populations and ethnic groups.

The spectrum of *CFTR* mutations specific to Russian CF patients has been recently identified. Moreover, the creation of the Russian Cystic Fibrosis Patient Registry (RCF-PR) and the provisions of the National Consensus documents on CF care have made it possible to combine data from clinical trials and researches conducted in different centres to better clarify the frequency of mutations both in the Russian Federation itself and in specific regions within the Federation [2, 3]. According to the RCF-PR 2016, the ten most common mutations (frequency) are: F508del (52.06%), *CFTR*dele2.3 (5.71%), E92K (2.67%), 2143delT (2.06%), 3849+10kbC>T (2.04%), 2184insA (1.87%), W1282X (1.82%), N1303K (1.47%), 1677delTA (1.44%), and G542X (1.35%). Mutation c.411\_412insCTA (p.Leu138dup, L138ins) can be considered common in Russian patients since its frequency exceeds 1% (1.15%) of the total number of identified mutant alleles (ranging from 0.29–2.89% across different regions) [2, 3]. The frequency of this mutation in Europe has not been determined due to the rarity of this particular pathological allele in European populations [1]. Indeed, the L138ins mutation is not included in the panel of routinely analysed *CFTR* mutations in European countries. The purpose of this study is to describe the genotypic features of the L138ins mutation in Russian CF patients.

## Material and Methods

DNA was isolated from whole blood samples of CF patients using a DNA extraction kit (Promega, USA). Molecular genetic testing for the c.411\_412insCTA (p.Leu138dup, L138ins) mutation was performed using amplified fragment length polymorphism (AFLP) analysis as part of the testing for frequent *CFTR* mutations in 1700 CF patients and was conducted in the Laboratory of Genetic Epidemiology at the Research Centre for Medical Genetics, Moscow [4]. Sanger sequencing to confirm the c.411\_412insCTA (p.Leu138dup, L138ins) mutation presence was performed in 37 CF patients. Analysis of DNA markers IVS1CA, IVS6aGATT, IVS8CA, and IVS17-bCA was performed in 24 CF patients carry-

ing the c.411\_412insCTA (p.Leu138dup, L138ins) mutation and their parents using a previously described procedure [5]. This research project was approved by the Ethics committee of the Research Center for Medical Genetics (Moscow). CF patients, or their fiduciaries, provided written informed consent.

## Results and discussion

In 2000, while testing for the 621+1G>T mutation in a Russian CF patient using RFLP test, the abnormal mobility of the exon 4 fragment of the *CFTR* gene was first observed (**Figure 1**). Sequencing confirmed the presence of a *CFTR* mutation (L138ins) not previously found in the Russian population (**Figure 2**). By 2006, the L138ins mutation was detected in six unrelated CF patients from Moscow and the Moscow region [4]. Subsequently, the L138ins mutation was also identified in two patients from the Krasnodar region [6]. Currently, the L138ins mutation is included in the panel of common *CFTR* mutations routinely tested for in the Russian population [3].

Analysis of the chromatogram (**Figure 1**) shows that the initial sequence of 5'-CACT-GCTCCTACACCCAGCC is changed to 5'-CACT-GCTCCTACTACACCCAGCC. Formally, four dif-

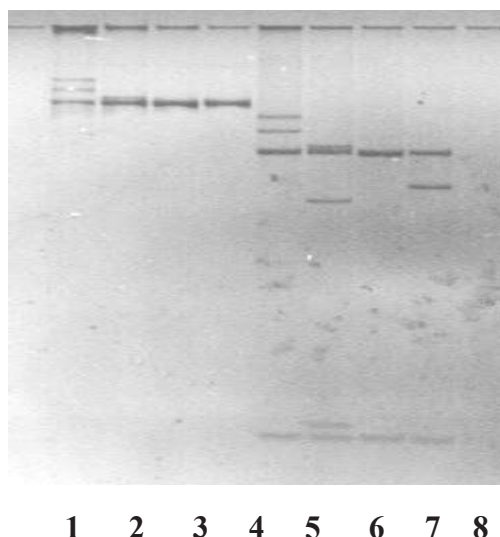
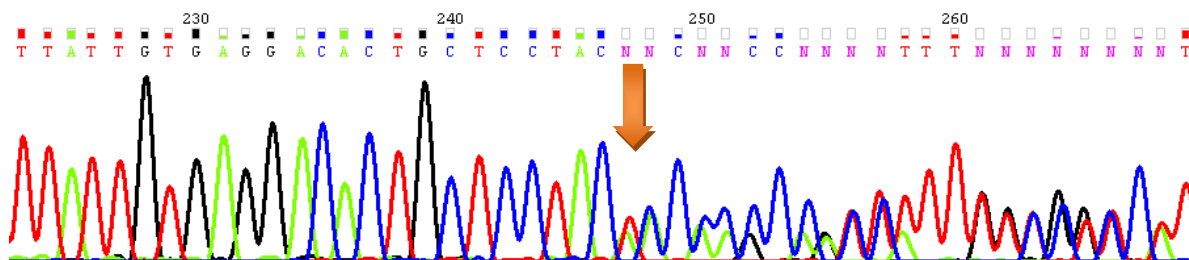


**Figure 1.** Detection of mutations in exon 4 of the *CFTR* gene in patients with CF. Lanes 1–4 are amplification products of exon 4: lanes 1 and 2 are samples with abnormal mobility of amplified fragments. Lanes 5 and 6 are restriction products of amplicons 1–4 using Tru11 endonuclease: 5 – L138insA / normal; 6 – 604insA / normal; 7 – normal / normal; 8 – 621 + 1 G>T / normal



a) from the forward primer



b) from the reverse primer

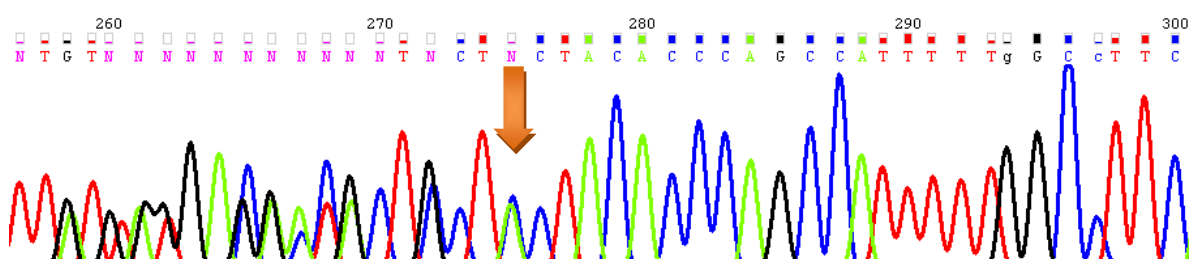


**Figure 2.** Chromatogram of sequencing results of DNA fragment containing exon 4 of the *CFTR* gene with the L138ins (p.Leu138dup) mutation

ferent events can lead to such a rearrangement (**Table 1**): insertion of the CTA triplet between 411 and 412 (1) or 414 and 415 (4) positions of the coding sequence; a TAC insertion between 412 and 413 (2) and an ACT insertion between 413 and 414 (3) positions. Any of these rearrangements will lead to duplication of the CTA codon without changing the reading frame, leading to duplication of leucine at position 138. According to the current nomenclature, the L138ins mutation should be designated as c.411\_412insCTA (p.Leu138dup).

This mutation is located in the second membrane penetrating motif of the first transmem-

brane domain (MSD1) involved in the formation of the pore of the CFTR chloride channel. The likely consequence of this mutation is the impairment of the conductive properties of the chloride channel. The L138ins mutation was first described by Dörk et al. in 1996 in a 34-year-old patient with a congenital bilateral absence of the vas deferens (CBAVD). The patient was pancreatic sufficient, without lung lesions, a sweat chloride level of 53 mmol/l, with the 5T variant in the second allele [7]. The CFTR1 database [8] describes two insertions of three nucleotides in the region under consideration: in one case the mutation, using the legacy nomenclature referred to as

**Table 1.** Mean values of clinical and functional indices in CF patients with different genotypes

|   | L138dup/F508del | 3849+10kbC>T/F508del | F508del/F508del |
|---|-----------------|----------------------|-----------------|
| Sweat chloride (mmol/l)                                 | 86.99 ± 17.02   | 78.29 ± 24.29        | 103.49 ± 22.89  |
| Age at diagnosis (yrs)                                  | 6.71 ± 9.73     | 14.34 ± 8.89         | 1.99 ± 0.16     |
| PI (% of patients)                                      | 19.1            | 33.3                 | 94.1            |
| BMI (kg/m <sup>2</sup> )                                | 21.87 ± 2.58    | 18.84 ± 2.73         | 18.64 ± 2.46    |
| FEV1(%)   | 77.56 ± 29.43   | 54.52 ± 21.88        | 72.34 ± 27.21   |
| Chronic <i>P. aeruginosa</i>                            | 12.5%           | 62.5%                | 37.1%           |
| Age of patients with chronic <i>P. aeruginosa</i> (yrs) | 26.44±10.33     | 27.67 ± 10.18        | 16.24 ± 8.13    |
| Liver damage  | 9.1%            | 6.4%                 | 33.3%           |

L138ins, is an ACT insertion between nucleotides 412 and 413, which leads to the insertion of histidine between two leucines located at 137 and 138 (c.412\_413insACT; p.Leu137\_Leu138insHis). In another case, the 546insCTA (c.414\_415insCTA) mutation was described, however, the wrong amino acid sequence at the protein level was reported as p.Leu139X (i.e., a premature stop codon at position 139); the correct designation of this mutation should be p.Leu138dup (i.e., leucine duplication at position 138).

Since 31<sup>st</sup> August 2018, the mutation under study was included in the CFTR2 database, referred to as c.413\_415dupTAC (p.Leu138dup, L138ins, rs397508679) [9]. It is also included in the EXAC database of 1000 genomes [10] and the ClinVar [11]. The first reference identified was the correct description of the mutation in the work of McGinniss et al. (2011) [12].

In our previous paper regarding the genotype-phenotype correlation in Russian CF

patients with c.411\_412insCTA (p.Leu138dup) mutation, we showed that the p.Leu138dup mutation could be considered as a disease-causing mutation, leading to a variable but relatively mild course of CF (Table 1) [13].

To date, in the Laboratory of Genetic Epidemiology, mutation L138ins (c.411\_412insCTA, p.Leu138dup), *in trans* with other CF-causing mutations, has been detected in 37 Russian CF patients from 33 families. The average patient age is 13.13 ± 11.42 years (1.00–43.00), with a ratio by sex: 0.43 m: 0.57 f (16:21). Eleven different genotypes have been identified and are described in Table 2.

The most common genotype, L138ins/F508del (c.[411\_412insCTA];[1521\_1523delCTT], p.[Leu138dup];[Phe508del]), has been found in 15 CF patients (40.5%); the second allele remains unidentified in four patients. The L138ins (c.411\_412insCTA, p.Leu138dup) mutation is always linked to one haplotype of the intrinsic marker IVS1CA-IVS6aGATT-IVS8CA-IVS17-

**Table 2.** Genotypes of the examined patients

| Genotype   | Number of patients |
|--|--------------------|
| L138ins/F508del (c.[411_412insCTA];[1521_1523delCTT], p.[Leu138dup];[Phe508del])                   | 15                 |
| L138ins/CFTRdele2,3 (c.[411_412insCTA];[54-5940_273+10250del21kb], p.[Leu138dup];[Ser18Arg*fsX16]) | 4                  |
| L138ins/2184insA (c.[411_412insCTA];[2052_2053insA], p.[Leu138dup];Gln685ThrfsX4)                  | 3                  |
| L138ins/2143delT (c.[411_412insCTA];[2012delT], p.[Leu138dup];[Leu671X])                           | 1                  |
| L138ins/N1303K (c.[411_412insCTA];[3909C>G], p.[Leu138dup];[Asn1303Lys])                           | 1                  |
| L138ins/R1162X (c.[411_412insCTA];[3484C>T], p.[Leu138dup];[Arg1162X])                             | 4                  |
| L138ins/712-1G>T (c.[411_412insCTA];[580-1G>T])  | 1                  |
| L138ins/E92K (c.[411_412insCTA];[274G>A], p.[Leu138dup];[Glu92Lys])                                | 1                  |
| L138ins/2183AA->G (c.[411_412insCTA];[2051_2052delAAinsG], p.[Leu138dup];[Lys684SerfsX38])         | 1                  |
| L138ins/L138ins (c.[411_412insCTA];[411_412insCTA], p.[Leu138dup];[Leu138dup])                     | 1                  |
| L138ins/W1282R (c.[411_412insCTA];[3844T>C], p.[Leu138dup];[Trp1282Arg])                           | 1                  |
| L138ins/not identified (c.[411_412insCTA];[?], p.[Leu138dup];[?])                                  | 4                  |

**Table 3.** Distribution of the L138ins (c.411\_412insCTA, p.Leu138dup) mutation in various regions of the Russian Federation

| Federal regions | The number of patients tested in the laboratory of genetic epidemiology | The proportion (%) of the total number of mutant alleles (based on the RCF-PR 2016) |
|-----------------|---|---|
| Central         | 8   | 1.30  |
| Moscow          | 16  | 1.52  |
| North-Western   |   | < 1.00  |
| St. Petersburg  |   | < 1.00  |
| Southern        |   | < 1.00  |
| Volga Region    | 2   | 1.38  |
| Ural            |   | 3.00  |
| Siberian        | 2   | < 1.00  |
| Far Eastern     |   | –   |
| North Caucasus  |   | –   |

bCA – 22–7–16–13, suggesting that the L138ins (c.411\_412insCTA, p.Leu138dup) variant occurred as the result of a single mutation event.

Most CF patients with the L138ins (c.411\_412insCTA, p.Leu138dup) mutation reside in Moscow (17) or the Moscow region (7) and all patients belonged to a Slavic ethnic group (Russians, Ukrainians). The L138ins (c.411\_412insCTA, p.Leu138dup) mutation has been detected in six of the nine Federal Regions (predominantly Russian) of the Russian Federation, with a relative proportion ranging from 0.35% to 3.11%. Relative frequencies of the L138ins (c.411\_412insCTA, p.Leu138dup) mutation (according to RCF-PR 2017) are given in **Table 3** [2].

## Conclusions

The L138ins (c.411\_412insCTA, p.Leu138dup) mutation identified in Russian CF patients (a Slavic ethnic group) is a duplication of three nucleotides (CTA) in exon 4 of the *CFTR* gene and is categorised as a small in-frame insertion/deletion.

## Acknowledgements

### Conflict of interest statement

The authors declare no conflict of interest.

### Funding sources

The work was carried within the state assignment of Ministry of Science and Higher Education of the Russian Federation for Medical Genetics and in part with the financial support of the Russian Fund for Fundamental Research (RFFR) (project No. 20–015–00061) (expeditions, DNA research, writing the manuscript) and Czech Ministry of Health CZ.2.16/3.1.00/24022OPPK; IP00064203/6003 for University Hospital Motol (general management of the project, reviewing the manuscript).

## References

1. Kapranov N, Kashirskaya N, eds. Cystic fibrosis (Mucoviscidosis). Moscow: Medpractika-M; 2014.
2. Krasovsky S, Chernyak A, Voronkova A, Amelina E, Kashirskaya N, Kondratyeva E, Gembitskaya T, eds.

Cystic Fibrosis Patients Registry in Russian Federation. 2016. Moscow: Medpractika-M; 2018.

3. Petrova N, Kondratyeva E, Krasovsky S, Polyakov A, Ivachshenko T, Pavlov A, Zinchenko R, Ginter E, Kutsev S, Odinkova O, Nazarenko L, Kapranov N, Amelina E, Asherova I, Gembitskaya T, Ilyenkova N, Karimova I, Merzlova N, Namazova-Baranova L, Neretina A, Nikonova V, Orlov A, Protasova T, Semykin S, Sergienko D, Simonova O, Shabalova L, Kashirskaya N. National Consensus Project «Cystic fibrosis: definition, diagnostic criteria, treatment» Section «Genetics of Cystic Fibrosis. Molecular genetic diagnosis of cystic fibrosis». *Medical Genetics*. 2016;15(11):29-45.
4. Petrova N. Analysis of four polymorphisms in *CFTR* gene in families of cystic fibrosis patients. *Medical Genetics*. 2006;5(12):27-32.
5. Petrova N, Timkovskaya E, Zinchenko R, Ginter E. Analysis of the frequency of some mutations in the *CFTR* gene in different populations of Russia. *Medical Genetics*. 2006;5(12):32-9.
6. Rukavichkin DV. Clinico-genotypic polymorphism of cystic fibrosis among the population of the Krasnodar Territory. Krasnodar: Diss. Cand. Med. Sciences: 03.00.15; 2007.
7. Dörk T, Dworniczak B, Aulehla-Scholz C, Wieczorek D, Böhm I, Mayerova A, Seydewitz HH, Nieschlag E, Meschede D, Horst J, Pander H, Sperling H, Ratjen F, Passarge E, Schmidtke J, Stuhmann M. Distinct spectrum of *CFTR* gene mutations in congenital absence of vas deferens. *Human Genetics*. 1997 Aug 4;100(3-4):365-377. <https://doi.org/10.1007/s004390050518>
8. Cystic Fibrosis Mutation Database. <http://www.genet.sickkids.on.ca>. Accessed 2019 August 20.
9. Clinical and Functional Translation of *CFTR*. <https://www.cftr2.org>. Accessed 2019 August 20.
10. Exome Aggregation Consortium. <http://exac.broadinstitute.org>. Accessed 2019 August 20.
11. ClinVar; [VCV000053905.2]. <https://www.ncbi.nlm.nih.gov/clinvar/variation/VCV000053905.2>. Accessed 2020 March 2.
12. McGinniss MJ, Buller AM, Quan F, Peng M, Sun W. Cystic Fibrosis Gene Mutations. 2011 Dec 13; US008076078B2 (United States).
13. Petrova N, Kashirskaya N, Vasilyeva T, Voronkova A, Kondratieva E, Sherman V, Novoselova O, Krasovskiy S, Chernyak A, Amelina E, Ginter E, Kutsev S, Zinchenko R. Phenotypic features in patients with cystic fibrosis with L138ins (p.Leu138dup) mutation. *Pediatrics. Journal named after G.N. Speransky*. 2017 Dec 11;96(6):64-72. <https://doi.org/10.24110/0031-403x-2017-96-6-64-72>

# Leucocytes and Th-associated cytokine profile of HIV-leishmaniasis coinfecting patients attending the Abuja Teaching Hospital, Nigeria

Idris Nasir Abdullahi

Department of Medical Laboratory Science, Faculty of Allied Health Sciences, Ahmadu Bello University, Zaria, Nigeria

<https://orcid.org/0000-0002-5511-1272>

Corresponding author: eedris888@yahoo.com

Anthony Uchenna Emeribe

Department of Medical Laboratory Science, University of Calabar, Calabar, Nigeria

<https://orcid.org/0000-0003-2937-8595>

Hafeez Aderinsayo Adekola

Department of Microbiology, Olabisi Onabanjo University, Ogun state, Nigeria

<https://orcid.org/0000-0003-3132-3315>

Habiba Yahaya Muhammad

Department of Medical Laboratory Science, Bayero University Kano, Nigeria

<https://orcid.org/0000-0001-7788-1094>

Abdurrahman El-fulaty Ahmad

Department of Medical Laboratory Science, Faculty of Allied Health Sciences, Ahmadu Bello University Zaria Nigeria

<https://orcid.org/0000-0003-1941-8346>

Abubakar Umar Anka

Department of Medical Laboratory Science, Faculty of Allied Health Sciences, Ahmadu Bello University Zaria Nigeria

<https://orcid.org/0000-0001-7983-8284>

Shamsuddeen Haruna

Department of Medical Laboratory Science, Faculty of Allied Health Sciences, Ahmadu Bello University Zaria Nigeria

<https://orcid.org/0000-0002-8991-6685>

Bamidele Soji Oderinde

Department of Medical Laboratory Science, University of Maiduguri, Maiduguri, Nigeria

<https://orcid.org/0000-0003-4420-8607>

Yusuf Mohammed

Department of Medical Microbiology and Parasitology, Bayero University Kano, Nigeria

<https://orcid.org/0000-0001-9414-9217>

Halima Ali Shuwa

Department of Community Health, Federal University Dutse, Jigawa State, Nigeria

<https://orcid.org/0000-0002-7926-0360>

Adamu Babayo

Department of Medical Microbiology and Parasitology, Bayero University Kano, Nigeria

<https://orcid.org/0000-0003-1039-486X>

DOI: <https://doi.org/10.20883/medical.408>

**Keywords:** cellular immunity, cytokines, leishmaniasis, pro-inflammation, HIV co-infection.

**Published:** 2020-01-30

**How to Cite:** Abdullahi, I. N., A. U. Emeribe, H. A. Adekola, H. Y. Muhammad, A. E. Ahmad, A. U. Anka, S. Haruna, B. S. Oderinde, Y. Mohammed, H. A. Shuwa, and A. Babayo. "Leucocytes and Th-Associated Cytokine Profile of HIV-Leishmaniasis Coinfecting Patients Attending the Abuja Teaching Hospital, Nigeria". *Journal of Medical Science*, vol. 89, no. 1, Jan. 2020, p. e408, doi:10.20883/medical.408.



© 2020 by the author(s). This is an open access article distributed under the terms and conditions of the Creative Commons Attribution (CC BY-NC) licence. Published by Poznan University of Medical Sciences

## ABSTRACT

**Introduction.** T-helper cells (Th)-1& -2 cytokines homeostasis control or predict clinical outcome of infected persons, especially those with HIV /AIDS. This case-control study evaluated the leucocytes differentials, TNF-alpha, interleukin (IL)-2 and -10 levels among HIV infected persons with serological evidence of leishmaniasis attending University of Abuja Teaching Hospital, Nigeria.

**Material and Methods.** Blood samples from 28 HIV infected persons who had *Leishmania donovani* rK39 and IgG positive (group 1), 30 age- & -sex matched HIV infected persons without *Leishmania* antibodies (group 2) and 30 apparently healthy persons without HIV and *Leishmania* antibodies (group 3). Full blood counts, TNF alpha, IL-2 and -10 levels were analyzed using automated hematology analyzer and ELISA, respectively. Structured questionnaires were used to collate biodata and clinical presentations of participants.

**Results.** Ten (35.7%) participants in group 1 were on ART, 15 (50%) in group 2 were on ART, while group 3 were ART naïve. There were significantly higher values in basophil ( $4.4 \pm 2.5\%$ ) and eosinophil counts ( $12.9 \pm 3.8\%$ ) in HIV/*leishmania* coinfecting persons ( $p = 0.005$ ). However, other white cells subpopulation was significantly lower in HIV/*leishmania* co-infected participants ( $p = 0.05$ ). There was significantly reduced CD4+ T cell counts ( $119 \pm 26$  versus  $348 \pm 63$  versus  $605 \pm 116$  cells/mm<sup>3</sup>), TNF-alpha ( $36.82 \pm 8.21$  versus  $64.67 \pm 12.54$  versus  $254.98 \pm 65.59$  pg/mL) and IL-2 levels ( $142.14 \pm 20.91$  versus  $507.6 \pm 84.42$  versus  $486.62 \pm 167.87$  pg/mL) among HIV/*Leishmania* co-infected participants compared to group 2 and group 3 participants, respectively. However, higher IL-10 level ( $80.35 \pm 14.57$  pg/mL) was found in HIV/*Leishmania* co-infected participants as opposed to the HIV mono-infected ( $62.2 \pm 10.43$  pg/mL) and apparently healthy persons ( $23.97 \pm 4.88$  pg/mL) ( $p = 0.001$ ).

**Conclusion.** Eosinophil, basophil counts and serum IL-10 level were high in HIV/*Leishmania* coinfecting persons, demonstrating parasite-induced hypersensitivity and immunosuppression.

## Introduction

HIV-leishmaniasis co-infection poses a major threat in people living with HIV (PLWHV) and vice versa [1]. HIV and leishmaniasis are restricted within the confined of mutual reinforcement [2]. In PLWHV, Leishmaniasis induces, hastens AIDS onset and limits lifespan [3]. Furthermore, HIV infection escalates the risk of clinical Visceral Leishmaniasis (a severe form of leishmaniasis) more than 100 times [4]. Both infections co-existence HIV-leishmaniasis co-infection increase disease burden by inhibiting T helper cell-mediated immune responses [1,4]. In addition, there is a fundamental change in cytokine network signaling pattern [1,4].

Leishmaniasis could be cutaneous (CL), mucocutaneous (ML) or Visceral (VL) depending on the etiologic species and the site or tissue/organ affected. CL pose enormous health challenge in most global regions especially the third world countries [5]. At least 88 countries are considered endemic for leishmaniasis [6]. In sub-Saharan Africa, PLWHV are afflicted more frequently with VL as the third most common infection [7]. As a result of the VL affecting the destitute and indigent patients, under-reporting of the presented cases in several affected regions is usually due to the absence of diagnostic equipment to investigate the co-infection and to inefficient reporting systems [1,7].

Importantly, Individuals living with VL-HIV co-infection are regarded as super-spreaders of VL infection which presents a major challenge to the efforts of eradicating leishmaniasis [1]. Based on these reasons, it was proposed that *Leishmania* organisms are critical in the pathogenesis of HIV-1 infection. In addition, it was observed that *L. donovani* amastigotes enhances HIV replication via TNF-alpha production and activates CD4+ T cells with the aid of its lipophosphoglycan [8]. Put together, it has been proven that anti-leishmanial therapy is efficacious in the inhibition of HIV replication [9]. However, the balances of pro- and anti-inflammatory cytokines are needed to prevent immunopathological disorders [9].

Pro-inflammatory cytokines secreted by Th1 cells are instrumental in regulating the proliferation and differentiation of T-lymphocytes in defense against HIV-leishmania co-infection. Despite the role of these cytokines, it is vital that these population is balance with their anti-inflammatory counterparts so as to avoid unpleasant immunopathological defects.

These defects which could be due to unregulated Th1 cell activity and excessive role of pro-inflammatory cytokines can have negative impact on the survival of T cell clones. The T cells that survive are dysfunctional and lack the ability to increase in number as well as secrete specific interferon-gamma targeted at antigenic stimuli. Previous research has shown that CD4 T lympho-

cytes with diverse lymphokine patterns are more efficient compared to humoral B cells in reducing the burden of leishmania infection. On the other hand, the anti-inflammatory cytokines (IL-4, IL-10) when secreted by Th2 cells in discriminate proportions can promote the survival of parasites within cells and increase disease burden [1,10].

A scientific study currently reported the existence of a dominant cytokine profile secreted by Th1 cells and possess high protective role for pathogens compared to Th2 cytokines in HIV infection. It has been hypothesized that a shift from Th1 to Th2 cytokines depletes CD4 population and enhances viral replication in AIDS [9,11]. In order to determine the expression profile of Th1 and Th2 cytokines in the case of HIV-Leishmaniasis co-infection, this study aims to investigate the plasma levels of both pro- (IL-2, interferon-gamma) and anti-(IL-10) inflammatory cytokines as well as white cell differentials of persons coinfected by the HIV and leishmaniasis University of Abuja Teaching Hospital, Northcentral Nigeria.

## Material and Methods

### Study Area

This hospital-based research was conducted at the University of Abuja Teaching Hospital (UATH) in the Federal Capital Territory (FCT), Abuja, Nigeria. Blood samples were collected at the antenatal clinics and analyzed at the Immunology laboratory. Gwagwalada is about 45 km away from the FCT. It is one of the six area council headquarters of the FCT. The town lies in the downstream of River Usuma and is located between latitude 8°55' and 9°00'N and longitudinal 7°00' and 7°05'E.

The centrality of this town in relation to other area councils' headquarters makes it influential and important in various socio-economic activities. The climate condition of this town is not far-fetched from that of the tropics having several climatic elements in common; most especially the wet and dry season characteristic. The temperature of the area ranges from 30°C to 37°C yearly, with the highest temperature experienced in the month of March and mean total rainfall of approximately 1650 mm/annum. The area council is an industrial zone of FCT that stands out as the second most cosmopolitan city of the FCT, after the capital city with 10 political wards and

consist of over 26 Federal organizations which include University of Abuja, University of Abuja Teaching Hospital etc. These have brought about the inflow of people into the council. About 60% of Gwagwalada residents live in rural settlements and are predominately farmers.

### Study Design and Population

This was a case-control study conducted between the 7<sup>th</sup> of April to the 10<sup>th</sup> of October 2015. Participants were recruited at UATH. Blood samples were collected from 28 HIV infected persons who were clinically diagnosed of VL and were rK39 and anti-leishmania donovani IgG seropositive (group 1), 30 age- & -sex matched HIV infected persons without Leishmania antibodies (group 2) and 30 apparently healthy persons without HIV and Leishmania antibodies (group 3). All participants aged between 15 and 50 years. Unigold® and Determine® were used to confirm the HIV status of participants. Samples from groups 1 and 2 were collected at the HIV Clinic, while samples from group 3 were collected from apparently healthy volunteers, who were interns at the University of Abuja Teaching Hospital (UATH), Gwagwalada, Abuja, Nigeria. Participants were selected by HIV/AIDS physicians and nurses. All participants were re-tested for Kala Azar rK39 and L. donovani IgG antibodies.

### Exclusion and Inclusion Criteria for Selection of Participants

Only Participants who reported with no history of immune system-related diseases, absence of any recent infectious diseases, not on anti-leishmanial treatment prior to sampling, and who gave written consent were enrolled into this study.

### Ethical Issues and Considerations

Ethical approval for this study was obtained from the Human Ethical Research Committee of UATH, while written consent was received either directly from participants (> 18 years) or via their respective parents/guardians (for those < 18 years). Demographics were collected using structured questionnaire. Confidentiality was ensured since samples were stored pseudonymized (study code). All data were analyzed anonymously.

### Sample Collection and Preparation

Five milliliter (5 ml) of whole blood samples were collected aseptically. Two milliliters of ethylene-

diaminetetraacetic acid-preserved blood samples were used for CD4+ cell counts and full blood count, while 3 mL in lithium heparin-preserved blood was used to harvest plasma for cytokine measurement using enzyme immunoassay. Samples were collected between from 7<sup>th</sup> April to 10<sup>th</sup> October 2015. Blood samples were analyzed within 1 hour of collection.

## Laboratory Analytical Procedures

### *White Cell Count and Differentials*

Sysmex™ XS-1000i five parts automated hematology analyzer was used for the total white cell count, monocyte, basophils, eosinophils and lymphocyte differentials using direct current detection method with coincidence correction. The automatic discriminators separated the cell populations based on complex algorithms. The intensity of the electronic pulse from each analyzed cell was proportional to the cell volume.

### *Flow Cytometry Assay for Lymphocyte Population*

Based on the manufacturer's instructions, the CD4+ cell counts in the whole blood were analyzed using a Partec™ CyFlow Analyzer (Sysmex, Nordstedt, Germany) Model SL3. This device used the principle of light scattering property (based on dissimilarity in cell size or granularity) and the fluorescence of cells following staining with monoclonal antibodies to markers on the cell surface bound to fluorescent dyes. Flow cytometry data was analyzed using FlowJo v.7.6.5 software. Cell populations of interest were then gated after identification. The generated percentages were multiplied by the total number of lymphocytes in the haemogram to derive absolute values for circulating lymphocytes. Absolute CD4+ cell counts were subsequently analyzed using a single-platform technique. Values for apparently healthy participants (group 3) were used as a reference.

### *Enzyme-linked Immunosorbent Assay for Anti-Leishmania IgG antibody*

Indirect ELISA was carried out according to the method described by kit manufacturer (product code: KA3295) (Abnova®, USA). The Leishmania ELISA test is a three-incubation process whereby the first incubation involved the coating of the wells with Leishmania spp antigen. During

this step, all antibodies that are reactive with the L. donovani antigens bind to the wells. Next, the wells were washed to remove test sample and other non-IgG antibodies. At this point Enzyme Conjugate was added. During this second incubation, the Enzyme Conjugate specifically bound to IgG antibodies present.

Before the third incubation step, 3 more washings were done. Then a chromogen (tetramethylbenzidine or TMB) was added. With the presence of Enzyme Conjugate and the peroxidase causing the consumption of peroxide, the chromogen changed to a blue color. The blue color turned to a bright yellow color after the addition of the stop solution, which ended the reaction. ELISA plate reader was used for the optical densities (ODs) of every well and results calculated from the ODs.

### *Detection of Leishmania donovani rK39 antibodies by Immunochromatography*

This test was conducted using the Inbios® Kalazar Detect™ Rapid Test (USA). The Kalazar Detect™ Test for VL is a qualitative, membrane-based immunoassay for the detection of antibodies to Visceral Leishmaniasis in human serum. The membrane was pre-coated with rK39 on the test line region and chicken anti-protein A on the control line region. During testing, the serum sample reacted with the dye conjugate (protein A-colloidal gold conjugate) which has been pre-coated in the test device.

The mixture then migrates upward on the membrane chromatographically and reacted with recombinant VL antigen on the membrane and generates a red line. The presence of this red line indicated a positive result, while its absence indicated a negative result. Regardless of the presence of antibody to rK39, as the mixture continues to migrate across the membrane to the immobilized chicken anti-protein A region, a red line at the control line region will always appear. The presence of this red line served as verification for sufficient sample volume and proper flow and as a control for the reagents. In addition, external control sera with known L. donovani result were ran alongside the samples. This test has sensitivity of 89.8% and specificity of 100%.

### *Enzyme-linked Immunosorbent Assay for Cytokines*

ELISA was carried out according to the method described by kit manufacturer (Abcam®, UK).

Accordingly, IL-2 (product code: ab174444), IL-10 (product code: ab100549) and TNF-alpha (product code: ab181421) were investigated.

The Simple-step ELISA® employs an affinity tag labeled capture antibody and a reporter conjugated detector antibody which immunocapture the sample analyte in solution. This entire complex (capture antibody/analyte/detector antibody) is in turn immobilized via immunoaffinity of an anti-tag antibody coating the well. To perform the assay, samples or standards were added to the wells, followed by the antibody mix. After incubation, the wells were washed to remove unbound material. TMB Development Solution was added and during incubation the reaction was catalyzed by HRP, generating blue coloration. This reaction was then stopped by addition of Stop Solution completing any color change from blue to yellow. Signal is generated proportionally to the amount of bound analyte and the intensity was measured at 450 nm.

## Statistical analysis

SPSS (version 24, IBM Corporation, USA) was used to analyze data which was expressed as mean  $\pm$  SD and statistical significance was considered for p-values  $\leq$  0.05. One-way ANOVA was used to compare categorical variables. P values  $<$  0.05 at a confidence interval of 95% were considered statistically significant.

## Results

### HIV-Leishmaniasis co-infected participants showed preponderance of female gender

The evaluation of the preponderance of female gender on the basis of the ratio of all the participant groups (1–3), indicated that the female to male ratio (19:9) was mainly maximum in participants co-infected with HIV and Leishmaniasis.

The mean  $\pm$  SD age of participants was  $26.6 \pm 4.9$  years,  $28.2 \pm 5.8$  years, and  $26.9 \pm 5.1$  years for groups 1, 2 and 3, respectively. Only 10 (35.7%) participants in group were on ART, 15 (50%) in group 2 were on ART, while group 3 were ART naïve (Table 1).

### HIV-Leishmaniasis co-infected participants indicated varied leukocyte profile concentrations in whole blood

Serum levels of neutrophil ( $p = 0.04$ ), and lymphocytes ( $p = 0.001$ ), where significantly decreased in Leishmania-HIV co-infected participants compared to the HIV mono-infected participants. On the other hand, the serum levels of basophils ( $p = 0.001$ ), eosinophils ( $p = 0.001$ ), and monocytes ( $p = 0.001$ ) where significantly raised in the Leishmania-HIV co-infected group of participants as opposed to the HIV mono-infected group of participants (Table 2).

### CD4+ T cell population decline in response to HIV-Leishmaniasis

CD4+ T cell population significantly ( $p = 0.001$ ) decreased in participants with HIV/Leishmaniasis co-infection compared to their HIV-mono-infected counterparts. All HIV sero-positive participants with or with anti-Leishmania antibodies had their CD4+ T-lymphocyte below the reference lower limit of 500 cells/mm<sup>3</sup> (Table 3).

### HIV-Leishmaniasis co-infected participants showed varied cytokine profile in plasma

In a similar case with CD4+ T cell population, pro-inflammatory cytokines [IL-2 ( $p = 0.001$ ) and TNF-alpha ( $p = 0.001$ )] significantly decreased, while anti-inflammatory cytokine [IL = 10 ( $p = 0.001$ )] significantly increased in participants with HIV/Leishmaniasis co-infection compared to their HIV-mono-infected counterparts. On the other hand, significantly increased serum levels of anti-inflammatory cytokine (IL-10 ( $p = 0.001$ ))

**Table 1.** Demographic of participants with and without anti-*Leishmania donovani* seropositivity

| Variable                      | HIV and Leishmania Coinfected Persons (n = 28) | HIV Infected Persons without Leishmania antibodies (n = 30) | Persons without HIV and Leishmania antibodies (n = 30) |
|-------------------------------|--|---|--|
| Age (years) Mean $\pm$ SD     | 26.6 $\pm$ 4.9                                 | 28.2 $\pm$ 5.8  | 26.9 $\pm$ 5.1   |
| Male to female ratio          | 9:19   | 9:21  | 9:21   |
| Number of participants on ART | 9  | 15  | 0  |



**Table 2.** Comparison of White cell count and differentials of participants with and without *Leishmania donovani* seropositivity

| Parameter              | Value (mean ± SD)                              |   |  | F-value | p-value |
|------------------------|--|---|--|---------|---------|
|                        | HIV and Leishmania Coinfected Persons (n = 28) | HIV Infected Persons without Leishmania antibodies (n = 30) | Persons without HIV and Leishmania antibodies (n = 30) |         |         |
| WBC 10 <sup>9</sup> /L | 3.7 ± 1.2                                      | 4.2 ± 1.9   | 5.9 ± 2.1  | 12.23   | 0.0001  |
| Neutrophils (%)        | 58.9 ± 11.6                                    | 61.6 ± 10.4   | 64.1 ± 13.2  | 5.834   | 0.040   |
| Lymphocytes (%)        | 22.5 ± 9.8                                     | 29.9 ± 10.6   | 30.7 ± 9.9   | 9.994   | 0.001   |
| Basophils (%)          | 4.4 ± 2.5                                      | 3.1 ± 1.2   | 1.4 ± 0.8  | 11.01   | 0.001   |
| Eosinophils (%)        | 12.9 ± 3.8                                     | 4.3 ± 2.6   | 3.2 ± 2.3  | 62.63   | 0.001   |
| Monocytes (%)          | 1.3 ± 3.5                                      | 1.1 ± 0.2   | 0.6 ± 0.1  | 13.97   | 0.001   |

**Table 3.** Comparison of Cytokines and CD4+T cell count and differentials of participants with and without *Leishmania donovani* seropositivity

| Parameter                                  | Value (mean ± SD)                              |   |  | F value | p-value |
|--|--|---|--|---------|---------|
|  | HIV and Leishmania Coinfected Persons (n = 28) | HIV Infected Persons without Leishmania antibodies (n = 30) | Persons without HIV and Leishmania antibodies (n = 30) |         |         |
| CD4+ T cell count (cells/mm <sup>3</sup> ) | 119±26   | 348±63  | 605±116  | 278.0   | 0.001   |
| IL-2 (pg/ml)                               | 142.14±20.91                                   | 507.6±84.42   | 486.62±167.87  | 291.0   | 0.001   |
| IL-10 (pg/ml)                              | 80.35±14.57                                    | 62.2±10.43  | 23.97±4.88   | 211.0   | 0.001   |
| TNF-alpha (pg/ml)                          | 36.82±8.21                                     | 64.67±12.54   | 254.98±65.59   | 269.0   | 0.001   |

was observed in the Leishmania-HIV co-infected participants as opposed to the HIV mono-infected participants (Table 3).

## Discussion

Leishmania/HIV's capability to influence host cellular immunity and co-exist in the lymphoid tissues indicates their ability to mutually communicate by mutually re-enforcing their replication when co-existing in the same host cells [11]. To the best of our knowledge, this is one of a few studies that demonstrates for the first time the influence of the interaction of these pathogens on cytokines and leukocytes which are orchestrators of the host defense system and play vital functions in modulating the host immune response against Leishmania/HIV co-infection. Comparative analysis of leukocyte and cytokine profiles from co- and mono-infected participants highlighted significant variations in immune response mounted against co-infection, confirming the ability of Leishmania and HIV to mutually interact at the immunological level.

Participants co-infected with Leishmania and HIV responded with an overall decrease in pro-inflammatory cytokine (IL-2, TNF-alpha) and the increase in anti-inflammatory cytokine (IL-10)

release. Low level of these pro-inflammatory cytokines have been reported in Indian patients with active Leishmaniasis and elevated levels observed in those treated of Leishmaniasis [12]. IL-2 and TNF-alpha have been implicated in protective immunity towards parasitic and viral infections [13]. TNF-alpha, a vital mediator of both innate and adaptive inflammatory responses [14], is observed to possess a crucial role in the formation and maintenance of granuloma against visceral leishmania. This anti-parasitic function of TNF-alpha is mediated by the activation of infected macrophages for the killing of intracellular Leishmania amastigote [15]. IL-2, which is produced by activated CD4+ Th cells and was formally referred to as "T-cell growth factor", have been thought to induce the proliferation and differentiation of Th2 cells (B-cells, natural killer cells, monocyte/macrophages, oligodendrocytes and lymphocyte activated killer cells) and aid in the release of IgG1 and IgE-producing cells which is vital for the resolution Leishmaniasis [16], suggesting that this cytokine may be crucial for Leishmania clearance. Hence decreased concentrations of IL-2 observed in the co-infected versus the mono-infected cohort, apart from the already diminished levels of TNF-alpha, may be indicative of a non-favourable, poor prognosis for Leishmania.

However, an increase in the level of IL-10 (an anti-inflammatory cytokine), and reduction in cell-mediated immunity are seen in Leishmania infection. IL-10 dampens the production of many pro-inflammatory cytokines (including TNF-alpha, IL-1, IL-6, and IL-12), it also decreases the expression of MHC-II and other co-stimulatory molecules on the surface of macrophages, and these inhibit macrophage-mediated activation of CD4+ helper T cells leading to a reduction in both adaptive and innate immune responses [17].

The immunosuppressive role of IL-10 in human visceral leishmaniasis leads to a drastic decrease in the accumulation of monocyte-derived macrophages, which is controlled by the migration inhibition factor. Furthermore, IL-10 is observed to encourage the Th1 cell dysfunction which enhance intracellular infection for interferon-gamma production, deactivating parasitized tissue macrophages, and downregulating antigen presentation by dendritic cells [17].

IL-10 have also been implicated in inhibiting the leishmanicidal roles of macrophages by decreasing the synthesis and release of pro-inflammatory molecules (reactive nitrogen intermediates by macrophages, interferon-gamma by T/natural killer cells, and IL-12 mediated activation of macrophages). These suppressive roles of IL-10 which is released by alternatively activated macrophages and interferon-gamma co-producing CD4+ T cells (type 1 regulatory T cells) at moderate to high levels due to the low to zero levels of pro-inflammatory cytokines and the decreased number of multifunctional CD4+ T cells [17]. During the initial phases of infection justifies why it is associated with decreased immunity against Leishmania infection. Due to suppressive role of IL-10, the parasite burden continues to build up even when interferon-gamma levels are elevated [18].

In addition to the varying levels of cytokine profile, this study revealed a higher secretion of IL-10 which was associated with increased viremia and depleted CD4+ T cell population in Leishmania/HIV co-infected participants compared to those of the HIV mono-infected group. This corroborated with a recent study, which reported CD4+ T cell count as low as 49 cells/mm<sup>3</sup> in HIV/Leishmaniasis asymptomatic immune responders compared to the non-responders [19]. The marked fall in CD4+ T cell number is associated with the reduced leishmanicidal capacity of mac-

rophages, and the replication and uncontrolled systemic spread of the parasite throughout the body [20] which increases the risk of progression to visceral leishmaniasis by 100 to 2320 times based on the mutual interaction between HIV and Leishmania [21].

Based on the leukocyte profile, HIV/Leishmania co-infected participants had significantly lower lymphocyte and neutrophil counts with significantly higher monocyte, basophil and eosinophil counts as observed in this study. These observations were in line with a study conducted in Brazil [22] which demonstrated significantly lower levels of lymphocyte and haemoglobin counts at diagnosis, and considerably higher levels of eosinophil count in the initial hematologic evaluation in over 50% of co-infected participants. Similar observations were observed in the liver of genetically susceptible mice infected with experimental visceral leishmaniasis [19].

The primary cells of mice that are infected by Leishmania donovani amastigotes are the liver resident tissue macrophages (Kupffer cells). These cells are observed to produce cytokine and chemokines which recruit monocytes and neutrophils to the infection site during the initial days of infection, thus, further amplifying the production of more chemokines [23]. Neutrophils (primary antimicrobial cells) control infections by phagocytising and killing invading pathogens. While some of these pathogens are killed by the lysosomal effect of the neutrophil, others which are either obligate or facultative intracellular organism become resistant to the lysosomal enzymes and replicate in these cells which become apoptotic. These apoptotic neutrophils (without parasiticidal effect) either control Leishmania growth by undergoing depletion to reduce the load of this parasite and delaying the onset of leishmaniasis [24] or act as Trojan horses with delayed apoptosis by the parasite for onward transmission, infection and replications of these parasites in monocytes and macrophages that phagocytize the infected apoptotic neutrophils.

Another exciting outcome observed in this study is the decrease in neutrophil count. Leishmania infection interferes with several signaling pathways in immune cells [25]. Monocytes have been observed to possess antiparasitic function based on their plasticity and ability to differentiate into potent antigen-presenting or regulatory

cells [26]. The recruitment of neutrophils, monocytes, and then the T cells into the Kupffer cells is crucial for the formation of granuloma around these cells which is required for controlling the growth of Leishmania/HIV co-infection [27].

The cellular immune-mediated interactions between Leishmania spp and HIV seem to determine the extent of immunological response that occur in the co-infected biological system as well as the intensity of the onset of the accompanying infection. Similar circumstances have been observed with other Leishmania co-infections, revealing that the inherent consequences that emerge from several pathogen-host relations need to resolve when designing Leishmania vaccine trials. Proper consideration of parasite interplays should be adopted when determining the best strategy for the treatment of Leishmania-HIV co-infections to achieve immune stability without inflicting harm during the clinical course of the infected individual.

### Acknowledgements

Authors appreciate Head of Immunology Laboratory of University of Abuja Teaching Hospital for Logistic and technical support.

### Conflict of interest statement

The authors declare no conflict of interest.

### Funding sources

There are no sources of funding to declare.

### References

1. Adriaansen W, Dorlo TPC, Vanham G, Kestens L, Kaye PM, van Griensven J. Immunomodulatory Therapy of Visceral Leishmaniasis in Human Immunodeficiency Virus-Coinfected Patients. *Frontiers in Immunology*. 2018 Jan 12;8. <https://doi.org/10.3389/fimmu.2017.01943>
2. Monge-Maillo B, Norman FF, Cruz I, Alvar J, López-Vélez R. Visceral Leishmaniasis and HIV Coinfection in the Mediterranean Region. Valenzuela JG. *PLoS Neglected Tropical Diseases*. 2014 Aug 21;8(8):e3021. <https://doi.org/10.1371/journal.pntd.0003021>
3. Lindoso JA, Cota GF, da Cruz AM, Goto H, Maia-Elkhoury ANS, Romero GAS, de Sousa-Gomes ML, Santos-Oliveira JR, Rabello A. Visceral Leishmaniasis and HIV Coinfection in Latin America. Valenzuela JG. *PLoS Neglected Tropical Diseases*. 2014 Sep 18;8(9):e3136. <https://doi.org/10.1371/journal.pntd.0003136>
4. Craft N, Ezra N, Ochoa MT. Human immunodeficiency virus and leishmaniasis. *Journal of Global Infectious Diseases*. 2010;2(3):248. <https://doi.org/10.4103/0974-777x.68528>
5. de Vries HJC, Reedijk SH, Schallig HDFH. Cutaneous Leishmaniasis: Recent Developments in Diagnosis and Management. *American Journal of Clinical Dermatology*. 2015 Feb 17;16(2):99-109. <https://doi.org/10.1007/s40257-015-0114-z> WHO Report on Global Surveillance of Epidemic-prone Infectious Diseases - Leishmaniasis. [https://www.who.int/csr/resources/publications/CSR\\_ISR\\_2000\\_1leish/en/](https://www.who.int/csr/resources/publications/CSR_ISR_2000_1leish/en/). Accessed 2019 August 20.
6. Shafiei R, Mohebbali M, Akhoundi B, Galian MS, Kalantar F, Ashkan S, Fata A, Hosseini Farash BR, Ghasemian M. Emergence of co-infection of visceral leishmaniasis in HIV-positive patients in northeast Iran: A preliminary study. *Travel Medicine and Infectious Disease*. 2014 Mar;12(2):173-178. <https://doi.org/10.1016/j.tmaid.2013.09.001>
7. Forestier C, Gao Q, Boons G. Leishmania lipophosphoglycan: how to establish structure-activity relationships for this highly complex and multifunctional glycoconjugate? *Frontiers in Cellular and Infection Microbiology*. 2015 Jan 21;4. <https://doi.org/10.3389/fcimb.2014.00193>
8. Rodrigues MZA, Grassi MFR, Mehta S, Zhang X, Gois LL, Schooley RT, Badaro R. Th1/Th2 Cytokine Profile in Patients Coinfected with HIV and Leishmania in Brazil. *Clinical and Vaccine Immunology*. 2011 Aug 10;18(10):1765-1769. <https://doi.org/10.1128/cvi.00076-11>
9. Gois LL, Mehta S, Rodrigues MZA, Schooley RT, Badaró R, Grassi MFR. Decreased memory T-cell response and function in human immunodeficiency virus-infected patients with tegumentary leishmaniasis. *Memórias do Instituto Oswaldo Cruz*. 2014 Feb;109(1):9-14. <https://doi.org/10.1590/0074-0276130174>
10. Andargie TE, Diro Ejara E. Pro- and Anti-inflammatory Cytokines in Visceral Leishmaniasis. *Journal of Cell Science & Therapy*. 2016;6(2). <https://doi.org/10.4172/2157-7013.1000206>
11. Abbas AK, Lichtman A, Pillai S. *Cellular and Molecular Immunology 7<sup>th</sup> Edition*. Philadelphia: Elsevier; 2012.
12. Costa ASA, Costa GC, Aquino DMCD, Mendonça VRRD, Barral A, Barral-Netto M, Caldas ADJM. Cytokines and visceral leishmaniasis: a comparison of plasma cytokine profiles between the clinical forms of visceral leishmaniasis. *Memórias do Instituto Oswaldo Cruz*. 2012 Sep;107(6):735-739. <https://doi.org/10.1590/s0074-02762012000600005>
13. Dayakar A, Chandrasekaran S, Kuchipudi SV, Kalangi SK. Cytokines: Key Determinants of Resistance or Disease Progression in Visceral Leishmaniasis: Opportunities for Novel Diagnostics and Immunotherapy. *Frontiers in Immunology*. 2019 Apr 5;10. <https://doi.org/10.3389/fimmu.2019.00670>
14. Murray HW, Jungbluth A, Ritter E, Montelíbano C, Marino MW. Visceral Leishmaniasis in Mice Devoid of Tumor Necrosis Factor and Response to Treatment. *Mansfield JM. Infection and Immunity*. 2000 Nov 1;68(11):6289-6293. <https://doi.org/10.1128/iai.68.11.6289-6293.2000>
15. Stegall T. *Cytokines, Clinical Immunology & Serology (4<sup>th</sup> edn)*. Philadelphia: F.A. Davis Company; 2010.

16. Nylén S, Sacks D. Interleukin-10 and the pathogenesis of human visceral leishmaniasis. *Trends in Immunology*. 2007 Sep;28(9):378-384. <https://doi.org/10.1016/j.it.2007.07.004>
17. Mesquita I, Ferreira C, Barbosa AM, Ferreira CM, Moreira D, Carvalho A, Cunha C, Rodrigues F, Dinis-Oliveira RJ, Estaquier J, Castro AG, Torrado E, Silvestre R. The impact of IL-10 dynamic modulation on host immune response against visceral leishmaniasis. *Cytokine*. 2018 Dec;112:16-20. <https://doi.org/10.1016/j.cyto.2018.07.001>
18. Botana L, Ibarra-Meneses AV, Sánchez C, Castro A, San Martín JV, Molina L, Ruiz-Giardin JM, Carrillo E, Moreno J. Asymptomatic immune responders to *Leishmania* among HIV positive patients. Rafati S. *PLOS Neglected Tropical Diseases*. 2019 Jun 3;13(6):e0007461. <https://doi.org/10.1371/journal.pntd.0007461>
19. Okwor I, Uzonna JE. The immunology of *Leishmania*/HIV co-infection. *Immunologic Research*. 2013 Mar 16;56(1):163-171. <https://doi.org/10.1007/s12026-013-8389-8>
20. van Griensven J, Carrillo E, López-Vélez R, Lynen L, Moreno J. Leishmaniasis in immunosuppressed individuals. *Clinical Microbiology and Infection*. 2014 Apr;20(4):286-299. <https://doi.org/10.1111/1469-0691.12556>
21. Henn GADL, Ramos Júnior AN, Colares JKB, Mendes LP, Silveira JGC, Lima AAF, Aires BP, Façanha MC. Is Visceral Leishmaniasis the same in HIV-coinfected adults?. *The Brazilian Journal of Infectious Diseases*. 2018 Mar;22(2):92-98. <https://doi.org/10.1016/j.bjid.2018.03.001>
22. Smelt SC, Cotterell SEJ, Engwerda CR, Kaye PM. B Cell-Deficient Mice Are Highly Resistant to Leishmaniadonovani Infection, but Develop Neutrophil-Mediated Tissue Pathology. *The Journal of Immunology*. 2000 Apr 1;164(7):3681-3688. <https://doi.org/10.4049/jimmunol.164.7.3681>
23. McFarlane E, Perez C, Charmoy M, Allenbach C, Carter KC, Alexander J, Tacchini-Cottier F. Neutrophils Contribute to Development of a Protective Immune Response during Onset of Infection with *Leishmania donovani*. *Infection and Immunity*. 2007 Dec 3;76(2):532-541. <https://doi.org/10.1128/iai.01388-07>

# Iatrogenic injury and regeneration of the facial nerve after parotid gland tumour surgery: a pilot study with clinical and neurophysiological assessment

Agnieszka Wiertel-Krawczuk

Department of Pathophysiology of Locomotor Organs, Poznan University of Medical Sciences

 <http://orcid.org/0000-0002-4587-0822>

Juliusz Huber

University of Medical Sciences, Poznań, Poland  
Department of Pathophysiology of Locomotor Organs


 <http://orcid.org/0000-0002-8671-0497>

Corresponding author: [juliusz.huber@ump.edu.pl](mailto:juliusz.huber@ump.edu.pl)

**How to Cite:** Wiertel-Krawczuk A, Huber J. Iatrogenic injury and regeneration of the facial nerve after parotid gland tumour surgery: a pilot study with clinical and neurophysiological assessment. *JMS* [Internet]. 2020 Mar 31;89(1):e385. doi:10.20883/medical.385



© 2020 by the author(s). This is an open access article distributed under the terms and conditions of the Creative Commons Attribution (CC BY-NC) licence. Published by Poznan University of Medical Sciences

 DOI: <https://doi.org/10.20883/medical.385>

**Keywords:** parotid gland, benign tumor surgery, conservative treatment, neurophysiological examination, facial nerve regeneration

**Published:** 2020-01-30

## ABSTRACT

**Introduction.** Benign tumour surgery of the parotid gland may cause iatrogenic injury of the facial nerve, with results of postoperative treatment depending on the type of injury. The study aimed to clarify the mechanism of facial nerve injury after benign tumour surgery of parotid gland.

**Materials and Methods.** The effectiveness was verified preoperatively and 1, 3, 6 and 17 months postoperatively. House-Brackmann scales, electroneurography, blink reflex study and needle electromyography were performed. Pharmacological treatment (Galantamine, Cocarboxylase, Dexamethasone, Triamcinolone) and supervised physiotherapeutic procedures (Facial-Oral-Tract-Therapy, Proprioceptive neuromuscular facilitation) were applied for six months.

**Results.** Tumour removal led to the total paralysis of the left facial nerve, IV, III and III House-Brackmann grades were ascertained at the subsequent 3<sup>rd</sup>–5<sup>th</sup> periods of observation. In postoperative studies, electroneurography results showed full functional recovery of the frontal branch and incomplete regeneration in the marginal mandibular branch. Blink reflex examination showed proper parameters of evoked potentials only during preoperative and the last observation period. Residual voluntary activity of the frontal muscle and weak voluntary activity of orbicularis oris muscle were recorded in the needle electromyography examination. Contracture of mimic muscles at rest and improvement of their voluntary activity on the left side was observed six months after surgery compared to the early period of observation.

**Conclusion.** Consecutive studies showed the predominant axonal type of injury in the marginal mandibular branch and neuropraxia effect of the facial nerve, allowing the creation of a rehabilitation programme optimal for the functional recovery of the nerve.

## Introduction

Iatrogenic injury of the facial nerve accompanied by benign tumours surgery occurs rarely [1], with the size and location of the tumour within the parotid gland determining the scope and duration of surgery which may contribute to postoperative complications [2]. Nerve oedema and ischaemia during surgery, as well as mechanical and thermal manipulations within surrounding tissues may result in persistent or temporary facial nerve injuries in the postoperative period [3,4], which can lead to axonotmesis or neuropraxia, conditioning the degree of facial nerve damage. Neuropraxia is present when a conduction block appears without macroscopic nerve damage, which may reflect a demyelinating lesion without a Wallerian degeneration distal to the injury. In the case of axonotmesis, the nerve fibers, including motor axons are damaged, but the epineurium and perineurium remain intact, with the Wallerian degeneration occurring distal to the zone of injury [5]. Data regarding the type of iatrogenic injury, neuropraxia or axonotmesis dominating during parotid gland tumour surgery is lacking. Elmadawy, Hegab, Alahmady and Shuman [6] pointed to electromyographic (EMG) and electroneurographic (ENG) assessment as valuable tools for the evaluation of facial nerve function after different surgeries. Axonotmesis and conduction block in motor fibers may lead to degenerative changes in muscles which can be detected in needle electromyographic recordings. Conduction block as result of neuropraxia can be functionally reversible. Similarly, in the case of axonotmesis, the regeneration process is possible due to the surviving proximal stump of the nerve. The improvement of motor function in facial nerve and face muscles after 12 weeks of conservative treatment may indicate a functional recovery [6,7]. Additionally, late complications related to improper functional regeneration of the facial nerve are crucial for successful treatment [8,9].

## Aim

This study aimed to explain the mechanism of facial nerve iatrogenic injury by means of axonotmesis versus neuropraxia taking into consideration results of clinical and neurophysiological

observations performed 1, 3, 6 and 17 months after benign parotid gland tumour surgery. Also, conservative treatment results with pharmacotherapy which may influence nerve functional recovery in one patient with the iatrogenic facial palsy are presented.

## Material and Methods

The pilot study included thirteen patients with a benign parotid gland tumour, which was recognised based on clinical and ultrasonographic examinations. The study group consisted of thirteen patients, including six women and seven men aged 16 to 67 (the average age was 47), with tumours of small or medium size, from 1.5 cm to 3.5 cm, located in the superficial lobe of the parotid gland (N = 12) except one patient, where the tumour was located in both lobes. Results of histopathological examination, surgical treatment as well as the clinical and neurophysiological studies of this particular patient are presented and discussed in detail in this paper. The surgeon removed the tumour located in the lower pole of the left parotid gland in this particular case. Ultrasound Doppler imaging revealed poorly demarcated and rich vascularised pathological structure 1.5 cm under the skin, 35 x 30 mm in size measured transversally and 40 mm sagittally in computer tomography, without signs of the destruction of the mandible and mastoid process (Figure 1). The anteromedial part of the tumour closely adhered to the left pterygoid muscle; a clear border between them was not visible in several scans. The tumour did not adhere to the masseter muscle, external auditory meatus and lymph nodes, as well as other salivary glands showed no pathologies.

Observations including clinical and neurophysiological examinations of the facial nerve function were performed preoperatively and 1, 3, 6 months postoperatively. Additionally, a patient with deep localisation of the tumour and facial nerve palsy underwent a neurophysiological examination of the facial nerve 17 months after nerve damage. The investigation took place as part of the routine diagnostics ordered by the physician. The stage of injury was also determined by the House-Brackmann (H-B) scale [10], which is used for the clinical evaluation of the



**Figure 1.** Photograph of CT scan with the left parotid gland tumour marked by a white arrow, the mandible is marked by a black arrow

degree of nerve damage in facial nerve palsy. The measurement is determined by analysis of the face muscle movement, symmetry, and muscle tone, with the presence of deficits like synkinesis, contracture of face muscle, or hemifacial spasm also determining the degree of nerve dysfunction. The scale is based on functional impairment, ranging between I (normal function) and VI (no movement, total paralysis).

Neurophysiological tests were recorded with a Keypoint system (Medtronic A/S, Skovlunde,

Denmark). Standard (AgCl) 5 mm<sup>2</sup> surface electrodes were used for recording compound muscle action potentials (CMAP) from frontal and orbicularis oris muscles (Figure 2 A and B) during ENG examination. The active electrode (cathode) was placed on the muscle belly, with the reference electrode positioned on contralateral frontal muscle or the chin, the ground electrode on the neck. A stimulating bipolar electrode was applied to the stylomastoid foramen area along the anatomical passage of the facial nerve [11]. The time base was set at 5 ms/D, recording sensitivity at 2 mV/D, 20 Hz upper and 10 kHz lower filters of recorder amplifier were used during ENG.

The intensity of the single electrical stimuli (with 0.2 ms duration and 1 Hz frequency) was increased from 30 mA to a value evoking the potential with the largest amplitude. Values of amplitude [12] and standardised latency [13-15] were analysed in CMAP recordings. The decrease of CMAP amplitude was the result of axonal loss (axonotmesis), whereas an increase in the standardised latency parameter was initiated by the demyelination process (neuropraxia). Twenty-one healthy volunteers (fourteen females and seven males) aged 21 to 51 years (mean age was 28) underwent neurophysiological tests to establish reference values.

The Blink reflex examination (BR) was used as a supplementary method for facial nerve testing. The blink reflex test is an essential element of a comprehensive neurophysiological assessment of the facial nerve peripheral damage with 81% sensitivity and 94% specificity. The improvement in parameters of the recorded potentials

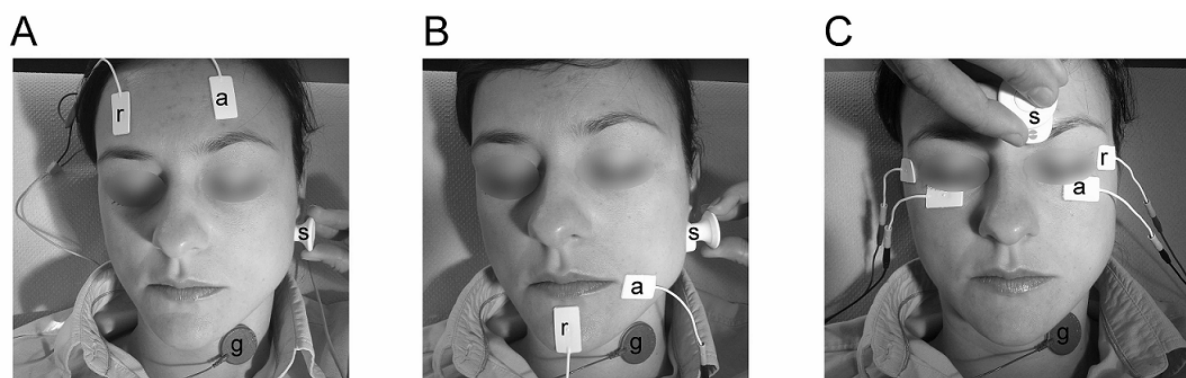


**Figure 2.** Photographs illustrating principles of electroneurographic studies: location of stimulating (s), ground (g) and recording (a-active, r-reference) electrodes during the examination of neural transmission in motor fibers of the facial nerve within the frontal branch (A), marginal mandibular branch (B) and the blink reflex study (C).

to the reference values suggests that the nerve impulse conduction disorder concerns the myelin sheath of the nerve without signs of axon damage. The blink reflex study is also an indicator of the improvement in the function of the facial nerve fibers. Recording electrodes were placed bilaterally on the orbicularis oculi muscles and a ground electrode on the neck. Electrical stimulus was applied over the supraorbital nerve (Figure 2 C) and required rectangular stimulus at 1 Hz with intensity of 20 mA and 0.5 ms duration. The short-latency ipsilateral R1 response and two long-latency R2 responses were analysed in recordings both ipsi- and contralaterally [11,16].

Statistical calculations for neurophysiological tests were performed using the STATISTICA version 9.1 programme (StatSoft Inc., 2009). The compliance of parameters with the normal distribution was checked by the Shapiro-Wilk test. Descriptive statistics of measurable parameters concerned minimum and maximum values, arithmetic means and standard deviation values. Simple comparison of parameters was used in all observation periods.

Confirmation of axonal changes in the facial nerve required needle EMG examination from the frontal and orbicularis oris muscles [11]. The study included the analysis of the muscle spontaneous activity at rest and evaluation of twenty motor unit action potentials (MUAPs) parameters (amplitude in mV, duration in ms and Size Index in mV/ms) recorded during weak voluntary contraction [15]. Two parameters of MUAPs with values greater than reference values determined the neurogenic advancement of their injury and reinnervation process in examined muscle. The last stage of EMG examination included measurements of amplitude and frequency of motor unit recruitment during maximal voluntary contraction lasting 5 seconds [17]. Conducting the two last stages of EMG examination was possible only in face muscles presenting voluntary activity.

The modified Blair's skin incision was applied, with patients (N = 12) treated surgically by the extracapsular tumour removing technique. General anaesthesia with volatile anaesthetics was applied during the surgery in all patients, with no complications in patients during anaesthesia. Superficial parotidectomy with tumour removal was performed in one patient where the tumour

was located in the lower parotid pole in the superficial and deep lobes. The facial nerve was identified and dissected using an anterograde technique due to its location in the parotid gland. Facial nerve branches were located on the surface of tumour and were "peeled off" during the intervention which lasted 180 minutes.

In one patient with the tumour located in both lobes, the pharmacological treatment included injections with Galantamine (5 mg per day, for 30 days), Cocarboxylase (50 mg per day, for 10 days), Dexamethasone (4 mg twice a day, for 10 days) and Triamcinolone (orally 4 mg twice a day, for 3 weeks). The above conservative treatment, as well as physiotherapy, was used because of iatrogenic facial nerve palsy which occurred in this particular patient.

Physiotherapeutic treatment was introduced two days after the surgery, performed twice a day for eight days. Two therapeutic procedures were applied, the Facial-Oral-Tract-Therapy (F.O.T.T.) [18], which stimulated muscle receptors on the paralysed side together with relaxation and stretching, as well as with muscle tension decrease on the asymptomatic side, and Proprioceptive neuromuscular facilitation (PNF) [19], which included activation of facial muscles on both sides to evoke their synergy, similar to the conditions of their normal innervation. Proper face muscle function on the asymptomatic side influences contractile properties of muscles on the paralysed side. The patient continued the exercises at home (2–3 times a day for 10 minutes) using a facial mirror biofeedback technique, focusing on the symmetry of facial movements. Supervised treatment was continued for the next 6 months.

The remaining patients did not receive the treatment, as mentioned earlier, due to the lack of complications after surgery in the form of facial nerve palsy.

Ethical considerations were according to the Helsinki Declaration. The research was approved by the Bioethical Committee of the University of Medical Sciences including studies on healthy people. Each patient was informed about the aim of study and provided written consent for examinations and data publication. Statistical analysis included comparison of mean values and ranges of parameters with reference to the tumour size and analysed results of neurophysiological studies.



## Results

In nine out of thirteen patients, the histopathological study revealed pleomorphic adenoma, adenolymphoma (Warthin's tumour) in three patients and myoepithelioma was recognised in the preliminary histological study in one patient. The type of tumour was indicated by the immunohistochemical examination. Tumour was not malignant; its total excision was not confirmed. The anatomical tumour-nerve relation and surgery difficulty were factors determining the iatrogenic facial nerve injury.

In twelve patients, the clinical examination using the H-B scale showed the proper function of the facial nerve bilaterally (H-B I) in all periods of observations. One of the co-existing symptoms was analgesia of auricle; this symptom remitted 6 months after surgery.

The data presented in Table 1 concerns one patient with a tumour located in both lobes of the parotid gland, which shows that before the surgery, despite proper facial nerve function (H-B grade I), the only weakness of the orbicularis oculi muscle was found on the symptomatic side. Xerostomia, as well as numbness and itching of the left cheek, were reported by the patient. Tumour removal led to the total paralysis of left facial nerve fibers (grade VI of H-B scale), which was accompanied by additional symptoms

such as hypoesthesia of auricle and numbness. Recovery of the facial nerve function (H-B grades IV, III and III, respectively) was found at the subsequent 3<sup>rd</sup>–5<sup>th</sup> periods of observation. Late complications such as Frey's syndrome and oral-ocular synkinesis were detected 3 months after surgery (Table 1). The H-B score was IV, although the improvement of facial nerve function was detected in ENG (Figure 6) and BR examination (Table 3), as well as in the residual bioelectrical activity of mimic muscles (Table 4). Following (4<sup>th</sup> and 5<sup>th</sup>) periods of observation, the H-B score was III with further improvement of nerve function and muscle activity. Moreover, contracture of mimic muscles on the symptomatic side was observed in these observation periods. The patient reported regression of auricle hypoesthesia in the 5<sup>th</sup> period (Table 1).

The results of the ENG and BR examination in twelve patients were within physiological limits (Table 2), with no significant differences between the symptomatic and asymptomatic sides in the four periods of observation.

In the case of one patient, data in Figure 3 shows that the amplitudes of CMAP evoked after stimulation of the frontal branch were comparable to the reference values at all periods of observation. In postoperative studies, CMAP amplitudes recorded after the marginal mandibular branch stimulation were always lower compared to refer-

**Table 1.** Clinical assessment of facial nerve function on the tumour side according to the H-B scale as well as the coexisting symptoms in one particular patient as an example

| Periods of observation | Coexisting symptoms   | H-B scale |
|------------------------|---|-----------|
| 1 <sup>st</sup>        | Slightly weaker eye clenching against the resistance<br>Xerostomia<br>Numbness and itching of the left cheek                | I         |
| 2 <sup>nd</sup>        | Hypoesthesia of the auricle<br>Numbness on the left side of the face  | VI        |
| 3 <sup>rd</sup>        | Hypoesthesia of the auricle<br>Oral-ocular synkinesis<br>Frey's syndrome  | IV        |
| 4 <sup>th</sup>        | Hypoesthesia of the auricle<br>Oral-ocular synkinesis<br>Frey's syndrome<br>Contracture of the facial muscles               | III       |
| 5 <sup>th</sup>        | The correct sense of touch in the auricle<br>Oral-ocular synkinesis<br>Frey's syndrome<br>Contracture of the facial muscles | III       |

H-B scale: (House-Brackmann scale): I normal function, II slight dysfunction, III moderate dysfunction, IV moderately severe dysfunction, V severe dysfunction, VI total dysfunction. Periods of observation: 1<sup>st</sup> before the surgery, 2<sup>nd</sup> one month after the surgery, 3<sup>rd</sup> three months after the surgery, 4<sup>th</sup> six months after the surgery, 5<sup>th</sup> seventeen months after the surgery.

ence values. Additionally, the dispersion of CMAP potential duration recorded from the orbicularis oris muscle was noted 6 months after surgery, which coexisted with mimic muscles contracture on the symptomatic side (Table 1). Values of CMAP standardised latencies after stimulation of both nerve branches were higher when compared

to the controls, indicating decreasing conduction velocity of the nerve impulses in subsequent postoperative periods. Values of the standardised latency were normal 17 months after surgery only in studies of the frontal branch.

The value of CMAP amplitude evoked after stimulation of the frontal branch on the symp-

**Table 2.** Summary of normative values (mean and range) for the clinical neurophysiology studies in the control group of healthy subjects (N = 21)

| Type of neurophysiological examination     | Type of parameters    |  |
|--|-----------------------|--|
|  | Amplitude (mV)        | Standardized latency (ms/cm) or latency (ms) |
| ENG – CMAP from frontal branch             | 1.53 mV<br>0.7–2.3 mV | 0.29 ms/cm<br>0.23–0.35 ms/cm                |
| ENG – CMAP from marginal mandibular branch | 4.37 mV<br>2.2–6.2 mV | 0.28 ms/cm<br>0.24–0.32 ms/cm                |
| BR – R1 response                           | NA                    | 11.06 ms<br>9.4–12.56 ms                     |
| BR – R2 response                           | NA                    | 30.05 ms<br>25–35 ms                         |
| BR – R2c response                          | NA                    | 30.6 ms<br>25–36 ms                          |

ENG – electroneurography, CMAP - compound muscle action potential, EMG – electromyography, BR– blink reflex, R1 - short-latency ipsilateral response, R2 - long-latency ipsilateral response, R2c - long-latency contralateral response, NA - not analyzed.

**Table 3.** Latencies of the blink reflex potentials recorded on the side symptomatic side in all periods of observation in one particular patient as an example

| Evoked potential latency (ms) | Periods of observation |                 |                    |                 |                 |
|-------------------------------|------------------------|-----------------|--------------------|-----------------|-----------------|
|                               | 1 <sup>st</sup>        | 2 <sup>nd</sup> | 3 <sup>rd</sup>    | 4 <sup>th</sup> | 5 <sup>th</sup> |
| R1                            | 9.8                    | No potential    | Residual potential | 15.7            | 9.2             |
| R2                            | 29.2                   | No potential    | 43.8               | 37.7            | 28.3            |
| R2c                           | 28.2                   | No potential    | 45.7               | 35.5            | 28.3            |

Periods of observation: 1<sup>st</sup> before the surgery, 2<sup>nd</sup> one month after the surgery, 3<sup>rd</sup> three months after the surgery, 4<sup>th</sup> six months after the surgery, 5<sup>th</sup> seventeen months after the surgery. R1 and R2 - ipsilaterally recorded potentials, R2c – contralaterally recorded potential.

**Table 4.** Results of EMG studies recorded from frontal and orbicularis oris muscles in the four periods of observation in one particular patient as an example

|                                | Periods of observation |                  |                   |                                      |                                      |
|--------------------------------|------------------------|------------------|-------------------|--------------------------------------|--------------------------------------|
|                                | 1 <sup>st</sup>        | 2 <sup>nd</sup>  | 3 <sup>rd</sup>   | 4 <sup>th</sup>                      | 5 <sup>th</sup>                      |
| <b>Frontal muscle</b>          |                        |                  |                   |                                      |                                      |
| Spontaneous activity           | Not examined           | Numerous F + PSV | F + PSV           | Single F + PSV                       | Single F + PSV                       |
| Voluntary activity             | Not examined           | No Activity      | Residual activity | Moderate activity Neurogenic MUAPs   | Moderate activity Neurogenic MUAPs   |
| <b>Orbicularis oris muscle</b> |                        |                  |                   |                                      |                                      |
| Spontaneous activity           | Not examined           | Numerous F + PSV | F + PSV S         | Single F + PSV S                     | Single F + PSV S                     |
| Voluntary activity             | Not examined           | No activity      | Weak activity     | Moderate activity Neurogenic MUAP MC | Moderate activity Neurogenic MUAP MC |

Periods of observation: 1<sup>st</sup> before the surgery, 2<sup>nd</sup> one month after the surgery, 3<sup>rd</sup> three months after the surgery, 4<sup>th</sup> six months after the surgery, 5<sup>th</sup> seventeen months after the surgery. F – fibrillations, PSV – positive sharp waves, S – synkinesis, MC – muscular contracture.

tomatic side was 38% lower compared to the asymptomatic side one month after surgery. Despite the lack of difference in amplitude, above 50% between sides, the result of H-B score (VI), the presence of denervation signs and no voluntary activity in EMG examinations from frontal muscle confirmed an axonal injury within the frontal branch of the facial nerve. Furthermore, values of CMAP amplitudes were comparable to those recorded on the asymptomatic side in subsequent periods of observation. Amplitudes of CMAPs after stimulation of the marginal mandibular branch were lower at 86%, 58%, 47% and 27% in subsequent postoperative observation periods in comparison to the values recorded on the asymptomatic side.

According to Esslen [20], CMAP amplitude value reflects a 1:1 proportion of active axons within the examined nerve branch. In the case of one patient, we ascertained the progression of nerve regeneration based on the results of CMAP amplitude variability (expressed in percentages) after marginal mandibular branch stimulation in subsequent postoperative observation periods compared to the preoperative recording. These values were 14%, 43%, 49% and 68%, indicating the advancement of the regeneration process

which was most prominent at 29% between the first and third month after surgery.

The Blink reflex examination showed proper parameters of evoked potentials only during the preoperative and the final observation periods (17 months after surgery; Table 3, Figure 4 AB1, 4). One month after tumour resection, R1 and R2 ipsilateral evoked potentials were not recorded on the symptomatic side (Figure 4 A2), nor was the R2 contralateral response after stimulation on the asymptomatic side (Figure 4 B2). This reflects the consequences of injury in the efferent pathway of the reflex arc (the facial nerve on the symptomatic side). In addition, low amplitude potentials with prolonged latencies in the BR study were recorded three months after surgery (Figure 4 AB3), indicating the recovery of nerve impulses transmission.

Data presented in Table 4 for a case of one patient proves the recovery of mimic muscles activity, which was observed 3 months after surgery. Residual voluntary activity of the frontal muscle and weak voluntary activity of the orbicularis oris muscle were recorded in the EMG examination. Analysis of MUAP parameters 6-months after surgery showed properties of neurogenic changes secondary to nerve injuries. Positive sharp waves

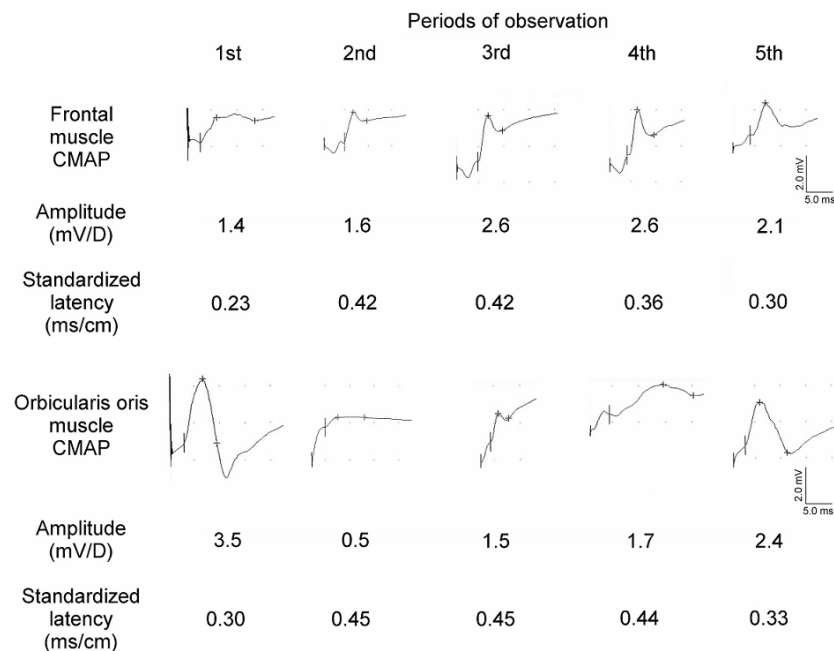


**Figure 3.** Results of ENG study on the symptomatic side with examples of CMAP recordings from the frontal and orbicularis oris muscles in the five stages of observation. CMAP: compound muscle action potential; Periods of observation: 1<sup>st</sup> before the surgery, 2<sup>nd</sup> one month after the surgery, 3<sup>rd</sup> three months after the surgery, 4<sup>th</sup> six months after the surgery, 5<sup>th</sup> seventeen months after the surgery.

and fibrillation potentials indicating the denervation of face muscles were recorded in the remaining postoperative observation periods. This activity was particularly frequent in the 1<sup>st</sup> and 3<sup>rd</sup> months after surgery, thus confirming the acute neurogenic injury. Signs of denervation process were weaker in other postoperative observation periods (Figure 5).

Assessment of EMG spontaneous activity 6 and 17 months after surgery was particularly complicated in terms of the orbicularis oris muscle due to the coexistence of oral-ocular synkinesis and facial muscles contracture (Figure 6). The synkinesis on the symptomatic side appeared after 3 months, whereas muscles contracture

was present 6 months after the parotid gland tumour surgery (Table 1).

A decrease of asymmetry between the symptomatic and asymptomatic side was observed in the long-lasting postoperative observation, being visible during the total relaxation of facial muscles. During attempts of voluntary contraction, the asymmetry increased particularly in the lower part of face. Asymmetry was deepened by the muscle contracture on the symptomatic side six months after surgery. Weak voluntary activity and the clearly visible narrowing of the eyelid fissure during activation of orbicularis oris muscle (oral-ocular synkinesis) were observed.

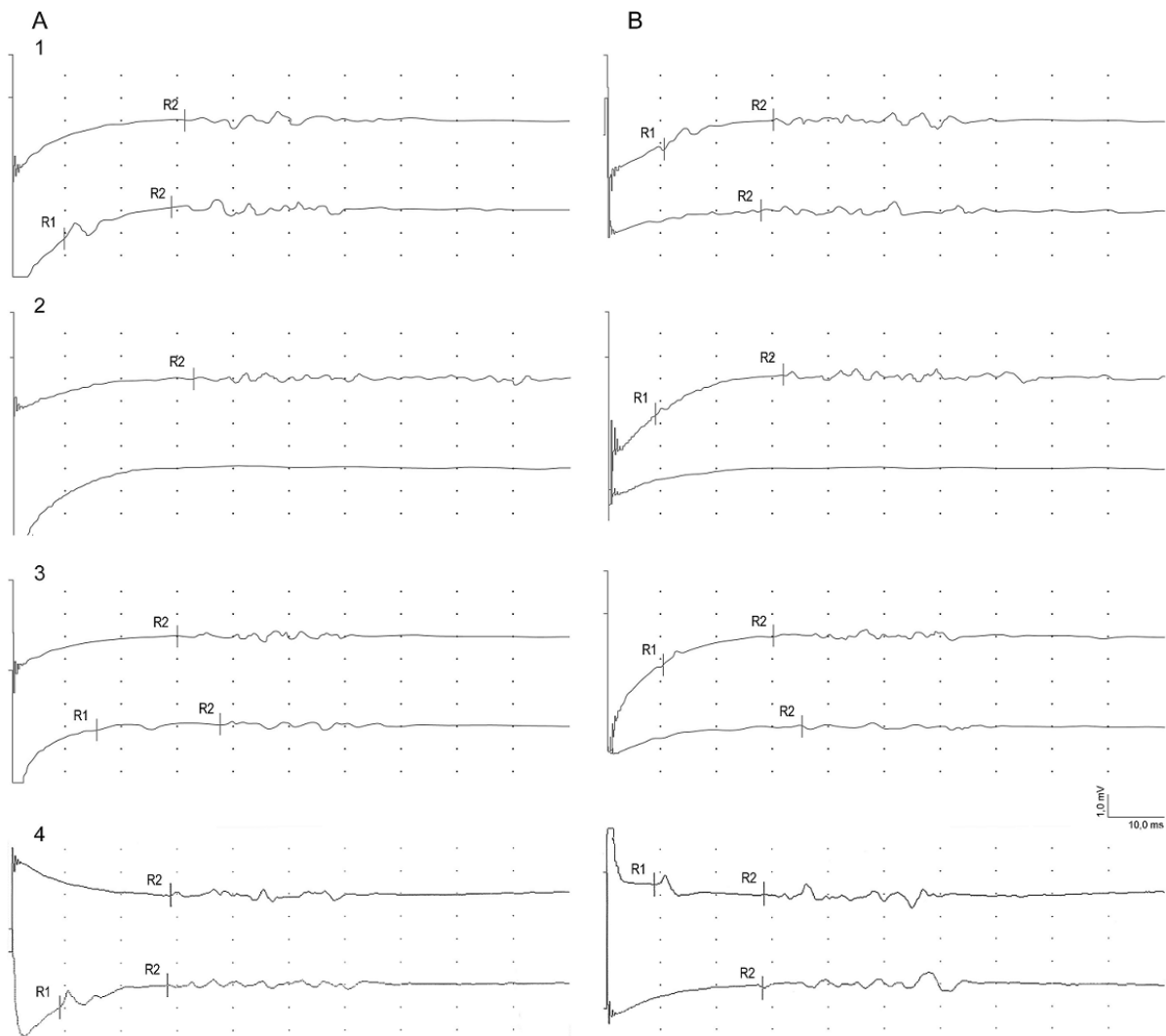


**Figure 4.** Examples of blink reflex studies in the three stages of observation: before surgery (1), one month after surgery (2), three months after surgery (3) and seventeen months after surgery (4) recorded on the symptomatic (A) and asymptomatic side (B)

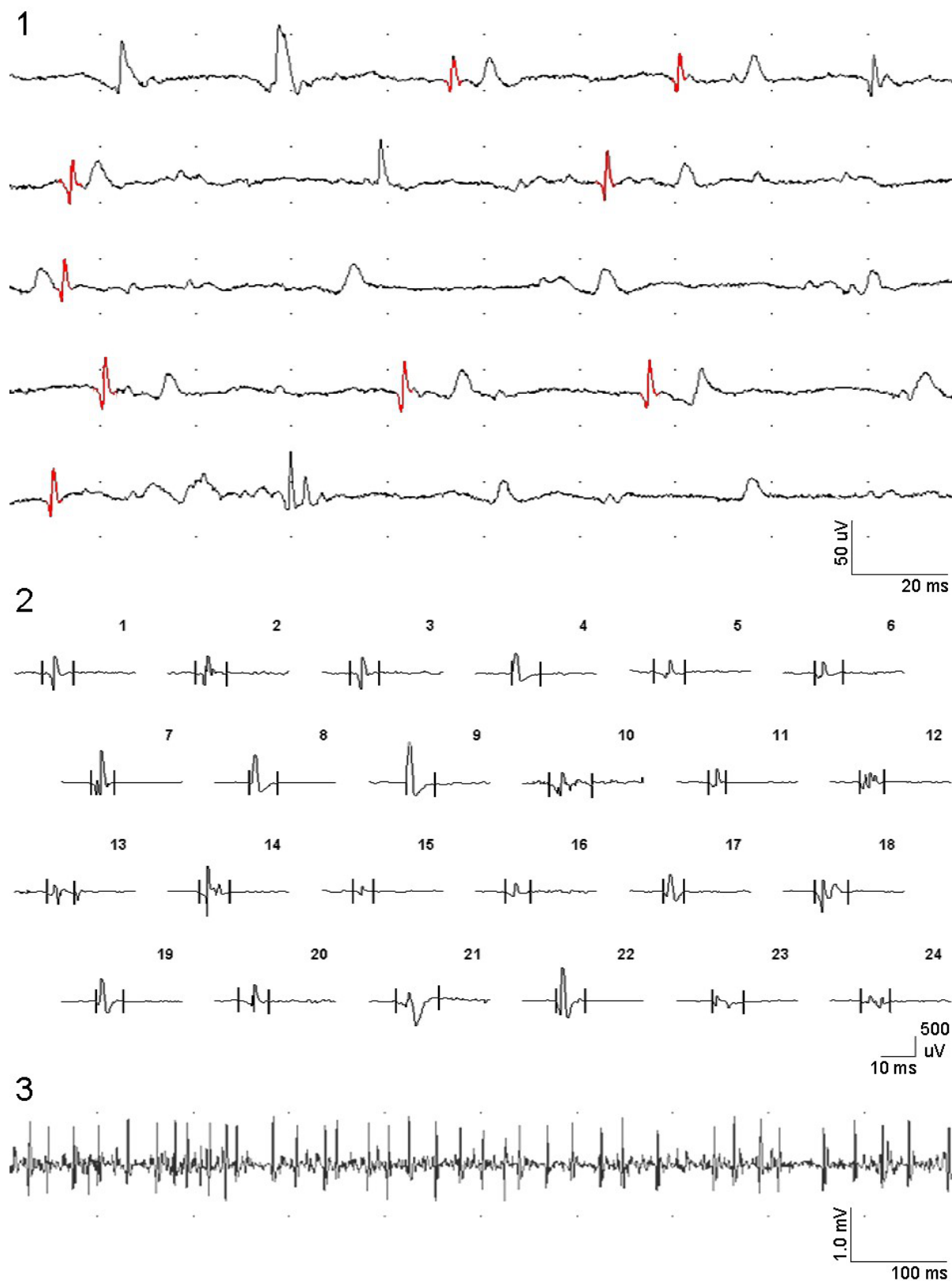


**Figure 5.** Examples of recordings in the EMG study from the orbicularis oris muscle 6 months after the parotid gland tumour removal showing the spontaneous denervation activity at rest with fibrillations marked in red (1), motor unit action potentials (MUAP) during attempts of voluntary contraction (2) and frequency pattern of MUAPs discharges during the maximal contraction (3). Note the increase in duration in single MUAPs (2) and frequency decrease of MUAPs recruitment (3) confirming the advancement of neurogenic pathology.

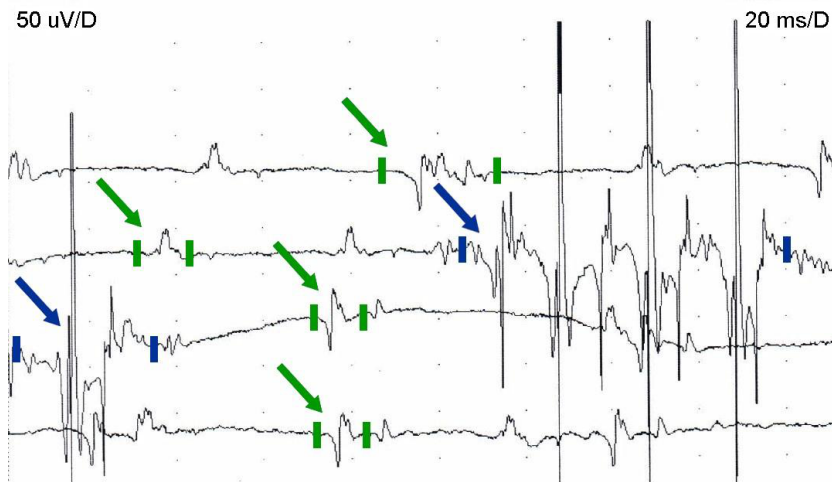


**Figure 6.** Example of the spontaneous activity recorded from the orbicularis oris muscle at rest. Muscle spasms associated with the presence of oral-ocular synkinesis (marked with the blue arrows) and single MUAP discharges resulting from orbicularis oris contractures (indicated by the green arrows) are presented.

## Discussion

Differentiation of the facial nerve injury type presented in this study based only on ENG results is difficult. CMAP amplitude may be reduced in the case of axonotmesis and conduction block. The latter refers to neuropraxia with decreasing axonal conductive properties at the site and above compression. Possibilities of regeneration differ in these types of injuries, according to Hughes et al. [21], 50% reduction of CMAP amplitude recorded proximally to the site of nerve block confirms this phenomenon. If the distal point of facial nerve stimulation overlaps with the site of parotid gland tumour surgery, ascertaining the conduction block is not possible. In our study, the analysis of facial nerve regeneration progress with its clear exponent of CMAP amplitude increase in the period between the 1<sup>st</sup> and the 3<sup>rd</sup> month suggests that the most probable mechanism of nerve injury was coexistence of conduction block and mild axonotmesis. Diminished conduction block in the 3<sup>rd</sup> month after surgery resulted in a significant increase of CMAP amplitude which, in the case of frontal branch examination, reached a value comparable to normal. The increase in CMAP amplitude recorded from the marginal mandibular branch in all periods of observation was also recorded, but this value has never reached the reference, confirming mild axonotmesis. The advancement in facial nerve regeneration was also observed in the results of

the blink reflex examination, validated by recordings of R1 and R2 responses on the symptomatic side 3 months after surgery.

The rate and dynamics of changes recorded in the frontal and orbicularis oris muscles during EMG studies also indicate the possibility of coexistence of both axonotmesis and neuropraxia. The spontaneous activity at rest showing denervation and lack of muscle voluntary activity was observed 1 month after surgery. The appearance of voluntary activity of face muscles, which was the symptom of nerve regeneration with still existing denervation, were recorded 3 months after surgery. Similar to observations of Martin and Helsper [22], in our study, the first symptoms of reinnervation were better expressed in muscles located closer to the injured area. At the same time, oral-ocular synkinesis was also observed in EMG, suggesting an axonotmesis mechanism of nerve injury and reflects the abnormal proliferation of axons during regeneration. Considering the location of the tumour in the parotid gland and possible mechanical and thermal reasons of injury during surgery, it is likely that axonotmesis involved the marginal mandibular branch to a greater extent than the whole nerve trunk. This can be validated by a better function of the frontal than marginal mandibular branch ascertained in the neurophysiological examination. The marginal mandibular branch is located nearest to the area of surgery, hence it may be exposed to more damage than another branch of the facial nerve.

Moreover, the marginal mandibular branch has the least anatomical connections between other branches of the facial nerve, so the regenerative capacity may be limited. Similar results pointing to the iatrogenic injury of the marginal mandibular branch during parotid gland tumour surgery were described in other studies [2,23].

The results presented in this study and findings of Reddy et al. [24] indicate the importance of physiotherapeutic treatment introduced immediately after surgery for creation of the appropriate conditions for facial nerve regeneration and muscle atrophy prevention. Spontaneous regeneration is successful when nerve branches undergo intensive afferent and efferent functional stimulation, consequently accelerating neurogenesis and activating the cortical centres in a feedback way. Exercises to activate face muscles promote regenerating axonal endings to create new connections at neuromuscular junction [25].

The study findings also suggest that precautions undertaken during surgery, including intraoperative monitoring of facial nerve function, and application of appropriate conservative treatment are essential for the final nerve regeneration. Neurophysiological examination performed 1, 3, 6 and 17 months after surgery allowed for objective determination of the facial nerve injury type, the progress of its regeneration and face muscles reinnervation. Comparative studies showed the predominant mild axonotmesis, especially with reference to the marginal mandibular branch. This type of injury was also confirmed by detecting post-regenerative deficits previously mentioned by other authors [26-29]. In this study, complications after surgical removal of the parotid gland tumour affected only one patient. The rarity of this phenomenon in the case of benign parotid tumours prompted the authors to present this case and propose optimal therapeutic and diagnostic processes.

In the case of axonotmesis, spontaneous regeneration of the nerve may be incomplete, therefore, a detailed neurophysiological diagnosis is non-invasive and a valuable diagnostic and prognostic tool for assessing facial nerve function.

### Acknowledgements

#### Conflict of interest statement

The authors declare no conflict of interest.

#### Funding sources

There are no sources of funding to declare.

### References

1. Aimoni C, Lombardi L, Gastaldo E, Stacchini M, Pastore A. Preoperative and Postoperative Electroneurographic Facial Nerve Monitoring in Patients With Parotid Tumors. *Archives of Otolaryngology–Head & Neck Surgery*. 2003 Sep 1;129(9):940. <https://doi.org/10.1001/archotol.129.9.940>
2. Wiertel-Krawczuk A, Huber J, Wojtysiak M, Golusiński W, Pierkowski P, Golusiński P. Correlations between the clinical, histological and neurophysiological examinations in patients before and after parotid gland tumor surgery: verification of facial nerve transmission. *European Archives of Oto-Rhino-Laryngology*. 2014 Apr 17;272(5):1219-1229. <https://doi.org/10.1007/s00405-014-3032-4>
3. Koide C, Imai A, Nagaba A, Takahashi T. Pathological Findings of the Facial Nerve in a Case of Facial Nerve Palsy Associated With Benign Parotid Tumor. *Archives of Otolaryngology - Head and Neck Surgery*. 1994 Apr 1;120(4):410-412. <https://doi.org/10.1001/archotol.1994.01880280038006>
4. Marchesi M, Biffoni M, Trinci S, Turriziani V, Campana FP. Facial Nerve Function After Parotidectomy for Neoplasms with Deep Localization. *Surgery Today*. 2006 Mar 24;36(4):308-311. <https://doi.org/10.1007/s00595-005-3146-9>
5. Ozgur A, Semai B, Hidir UU, Mehmet Fatih O, Tayfun K, Zeki O. Which electrophysiological measure is appropriate in predicting prognosis of facial paralysis?. *Clinical Neurology and Neurosurgery*. 2010 Dec;112(10):844-848. <https://doi.org/10.1016/j.clineuro.2010.07.001>
6. Elmadawy A, Hegab A, Alahmady H, Shuman M. Clinical and electromyographic assessment of facial nerve function after temporomandibular joint surgery. *International Journal of Oral and Maxillofacial Surgery*. 2015 Oct;44(10):1275-1280. <https://doi.org/10.1016/j.ijom.2015.04.013>
7. Martins RS, Bastos D, Siqueira MG, Heise CO, Teixeira MJ. Traumatic injuries of peripheral nerves: a review with emphasis on surgical indication. *Arquivos de Neuro-Psiquiatria*. 2013 Oct;71(10):811-814. <https://doi.org/10.1590/0004-282x20130127>
8. Terzis JK, Karypidis D. Therapeutic Strategies in Post-Facial Paralysis Synkinesis in Adult Patients. *Plastic and Reconstructive Surgery*. 2012 Jun;129(6):925e-939e. <https://doi.org/10.1097/prs.0b013e318230e758>
9. Campbell WW. Evaluation and management of peripheral nerve injury. *Clinical Neurophysiology*. 2008 Sep;119(9):1951-1965. <https://doi.org/10.1016/j.clinph.2008.03.018>
10. House JW. Facial nerve grading systems. *The Laryngoscope*. 1983 Aug;93(8):1056-1069. <https://doi.org/10.1288/00005537-198308000-00016>
11. Lee HJ, DeLisa JA. *Manual of nerve conduction study and surface anatomy for needle electromyography*. Philadelphia: Lippincott Williams & Wilkins; 2005.

12. Di Bella P, Logullo F, Lagalla G, Sirolla C, Provinciali L. Reproducibility of normal facial motor nerve conduction studies and their relevance in the electrophysiological assessment of peripheral facial paralysis. *Neurophysiologie Clinique/Clinical Neurophysiology*. 1997 Sep;27(4):300-308. [https://doi.org/10.1016/s0987-7053\(97\)85828-5](https://doi.org/10.1016/s0987-7053(97)85828-5)
13. Kimura J. *Electrodiagnosis in Diseases of Nerve and Muscle: Principles and Practice* (4 ed.). Oxford University Press; 2001. <https://doi.org/10.1093/med/9780199738687.001.0001>
14. Preston D, Shapiro B. *Electromyography and neuromuscular disorders. Clinical-electrophysiological correlations*. 2<sup>nd</sup> Ed. Elsevier, Butterworth & Heinemann; 2005.
15. Rubin DI, Daube JR. *Clinical neurophysiology*. Oxford University Press; 2009.
16. Brown W, Bolton C, Aminoff M. *Neuromuscular function and disease. Basic, clinical and electrodiagnostic aspects*. Vol. 1. Philadelphia: W.B. Saunders; 2002.
17. Stlberg E, Falck B. The role of electromyography in neurology. *Electroencephalography and Clinical Neurophysiology*. 1997 Dec;103(6):579-598. [https://doi.org/10.1016/s0013-4694\(97\)00138-7](https://doi.org/10.1016/s0013-4694(97)00138-7)
18. Nusser-Müller-Busch R. *Die Therapie des Facio-Oralen Trakts. F.O.T.T. nach Kay Coombes*. Heidelberg: Springer Medizin Verlag; 2011.
19. Adler SS, Beckers D, Buck M. *PNF in Practice*. Heidelberg: Springer Medizin Verlag; 2008.
20. Esslen E. *The Acute Facial Palsies. Investigations on the Localization and Pathogenesis of Meato-Labyrinthine Facial Palsies*. Berlin: Springer; 1977.
21. Hughes GB, warnock GR, glasscock ME, jackson CG, ray WA, sismanis A. *Clinical electroneurography*. *The Laryngoscope*. 1981 Nov;91(11):1834-1846. <https://doi.org/10.1288/00005537-198111000-00007>
22. Martin H, helsper JT. Spontaneous Return of Function Following Surgical Section or Excision of the Seventh Cranial Nerve in the Surgery of Parotid Tumors. *Annals of Surgery*. 1957 Nov;146(5):715-727. <https://doi.org/10.1097/00000658-195711000-00001>
23. Bendet E, Talmi YP, Kronenberg J. Preoperative electroneurography (ENoG) in parotid surgery: Assessment of facial nerve outcome and involvement by tumor—A preliminary study. *Head & Neck*. 1998 03;20(2):124-131. [https://doi.org/10.1002/\(sici\)1097-0347\(199803\)20:2<124::aid-hed5>3.0.co;2-4](https://doi.org/10.1002/(sici)1097-0347(199803)20:2<124::aid-hed5>3.0.co;2-4)
24. Reddy PG, Arden RL, Mathog RH. Facial nerve rehabilitation after radical parotidectomy. *The Laryngoscope*. 1999 06;109(6):894-899. <https://doi.org/10.1097/00005537-199906000-00010>
25. Shafshak T. The Treatment of Facial Palsy From the Point of View of Physical and Rehabilitation Medicine. *Europa Medicophysica*. 2006;42(1):41-7. PMID 16565685
26. Dulguerov P, Quinodoz D, Cosendai G, Piletta P, Marchal F, Lehmann W. Prevention of Frey Syndrome During Parotidectomy. *Archives of Otolaryngology—Head & Neck Surgery*. 1999 Aug 1;125(8):833. <https://doi.org/10.1001/archotol.125.8.833>
27. Marchese-Ragona R, De Filippis C, Marioni G, Staffieri A. Treatment of Complications of Parotid Gland Surgery. *Acta Otorhinolaryngol Ital*. 2005 Jun;25(3):174-8. PMID 16450773
28. Pourmomeny AA, Asadi S. Management of synkinesis and asymmetry in facial nerve palsy: a review article. *Iran J Otorhinolaryngol*. 2014 Oct;26(77):251-6. PMID 25320703
29. Peitersen E. Bell's Palsy: The Spontaneous Course of 2,500 Peripheral Facial Nerve Palsies of Different Etiologies. *Acta Oto-laryngologica. Supplementum*. 2002;(549):4-30. PMID 12482166




# Drug design: 4-thiazolidinones applications. Part 1. Synthetic routes to the drug-like molecules

Roman Lesyk

Danylo Halytsky Lviv National Medical University, Ukraine

 <https://orcid.org/0000-0002-3322-0080>

**How to Cite:** Lesyk R. Drug design: 4-thiazolidinones applications. Part 1. Synthetic routes to the drug-like molecules. JMS [Internet]. 2020 Mar 31;89(1):e406. doi:10.20883/medical.406

 DOI: <https://doi.org/10.20883/medical.406>

**Keywords:** Structure-based drug design, 5-Ene-4-thiazolidinones, Thiopyrano[2,3-d]thiazoles, biological activity, SAR analysis, Michael acceptors

**Published:** 2020-01-31



© 2020 by the author(s). This is an open access article distributed under the terms and conditions of the Creative Commons Attribution (CC BY-NC) license. Published by Poznan University of Medical Sciences

## ABSTRACT

4-Thiazolidinones, as examples of privileged scaffolds, have been the focus of medicinal chemistry since 60<sup>th</sup>. Among them, 5-substituted thiazolidinones with a C5 exocyclic bond (5-ene derivatives) are of special interest due to chemical characteristics and pharmacological profiles, possessing anticancer, antimicrobial, and antiviral properties, as well as being high-affinity ligands to a number of biological targets. A new medicinal chemistry trend claims that the aforementioned compounds are frequent hitters or pan assay interference compounds, which are useless because of the possible low selectivity. This is argued by the Michael acceptor property of 5-ene-4-thiazolidinones, which is actively discussed in the literature and requires further investigation. Based on SAR analysis, the main vectors for the design of 5-ene-4-thiazolidinone-based molecules were proposed: complication of C5 fragment; introduction of the substituents in the N3 position; synthesis of isosteric heterocycles; combination with other pharmacologically attractive fragments; annealing of thiazolidinone core; utilisation of 5-ene-thiazolidinones in synthesis of other compounds. The affinity of 5-ene-4-thiazolidinones toward various targets can be regarded as an advantage in polypharmacological approaches. Michael acceptors are considered as the "new old tool" for new drug creation, especially anticancer agents. One of the possible solutions within privileged substructure-based diversity-oriented synthesis is the fixation of 5-ene-4-thiazolidinone fragment in the fused heterocycles, for example, thiopyrano[2,3-d]thiazoles obtained from 5-ene-thiazolidinones.

The 4-thiazolidinone core is well known privileged scaffold in medicinal chemistry and is a powerful tool in the design of new drug-like molecules, especially within rational privileged substructure-based diversity-oriented synthesis [1-6]. Among the diversity of 4-thiazolidinone derivatives, 5-ene-4-thiazolidinone-based com-

pounds (Figure 1) are of special interest (most 4-thiazolidinone-based drugs, drug-candidates and lead-compounds belong to the mentioned subtypes). This is outlined in the thesis regarding the crucial role of the C5 substituent's nature in biological activity realisation. The conjugation of the C5-ene fragment to the C4 carbonyl group

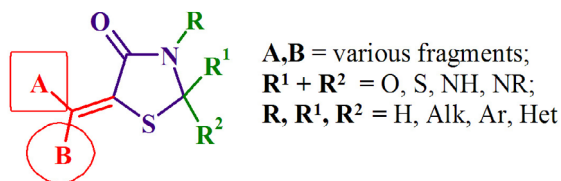


**Figure 1.** Structure of target 5-ene-4-thiazolidinones

makes such compounds electrophilic and potentially reactive due to the possible Michael addition of the nucleophilic protein residues to the exocyclic double bond compound. Thus, 5-ene-4-thiazolidinones can be treated as Michael acceptors (MA) [7]. The MA in modern medicinal chemistry possessed dualistic features, which characterises 5-ene-4-thiazolidinones as frequent hitters (promiscuous inhibitors) or pan assay interference compounds (PAINS) that are useless in the drug discovery process because of their possible insufficient selectivity due to the interaction with the biotargets (receptors, enzymes, etc.) [8-11]. However, the low selectivity toward various targets can be regarded as an advantage and baseline for further optimisation, especially in a polypharmacological approach. Many MA are confirmed covalent inhibitors (EGFR-, PI3K-, BTK-, MEK-inhibitors etc.) with anticancer properties, with the presence of the MA-moiety increasing the selectivity of known ligands. MA are inducers of phase 2 enzymes and inducible phase 2 proteins that can be treated as new approach for cancer treatment. Such MA are effective activators of Nrf2 through the Keap1 modification that opens new perspectives in the treatment of inflammation, cancer and chemoprevention. Moreover, MA properties, calculated or predicted *in silico*, are often not confirmed experimentally (under conditions close to physiological). Currently, the MA are assigned as "old new tool" for anticancer agent design [12,13].

In an attempt to solve this confusion ("negative and positive" profiles of 5-ene-4-thiazolidinones) in the spirit of drug design and discovery, we propose two approaches, "biological" and "chemical". The biological approach is based on the hypothesis regarding the crucial role of the presence/nature of the C-5 substituent of the 4-thiazolidinone core for biological activity realisation and involves the design of new active molecules and the development of directions of

4-thiazolidinone core modification to increase the selectivity and activity level of compounds. The advantage of this approach is that most hit- and lead-compounds belong to the 5-ene-4-thiazolidinones [12-14]. The chemical approach is based on our hypothesis that active 5-ene-4-thiazolidinone fixation in fused thiopyrano[2,3-d]thiazoles allows conservation of the activity vector, therefore opens new possibilities of molecule optimisation. Thus, fused thiazolidinone-based heterocycles could be of special interest as cyclic mimetics of 5-ene-4-thiazolidinone precursors without MA properties [15]. For this reason, rows of different thiopyrano[2,3-d][1,3]thiazoles were designed and synthesised and their anticancer potential was confirmed.

The synthetic strategy is grounded on thiazolidinone-based design, involving a combinatorial approach, diversity-oriented synthesis as well as privileged sub-structure-based diversity-oriented synthesis (bioisostere replacement, natural compounds modifications etc.). Additionally, molecular hybridisation as one of the most employed approaches in new anticancer drug design, allows the design of hybrid molecules where the combination of several privileged scaffolds has been regarded as a benefit.

## The "biological" method of drug-like molecule design

SAR analysis outlined the main directions for 4-thiazolidinone optimisation: complication of C5 fragment; modification of N3 and C2 positions; the isosteric replacement; creation of hybrid molecules via combination of thiazolidinone core with other "pharmacologically attractive" fragments (pyrazoline, pyridine, indole, benzothiazole, etc.). Thus, the reaction of (benzothiazol-2-yl)hydrazine with trithiocarbonyl diglycolic acid yielded starting 3-(benzothiazol-2-ylamino)-2-thioxo-4-thiazolidinone 1, which was subsequently utilised in a Knoevenagel condensation to obtain a series of 5-arylidene derivatives 2 (Scheme 1, Figure 2) [16,17]. The acetylation of exocyclic nitrogen was observed (3) following acetic anhydride addition to reactive mixture. A similar pattern with the formation of N-acetylsubstituted 5-ethoxymethylene-2-thioxo-4-thiazolidinone 4 was observed in the condensation of 1 with triethyl orthoformate in

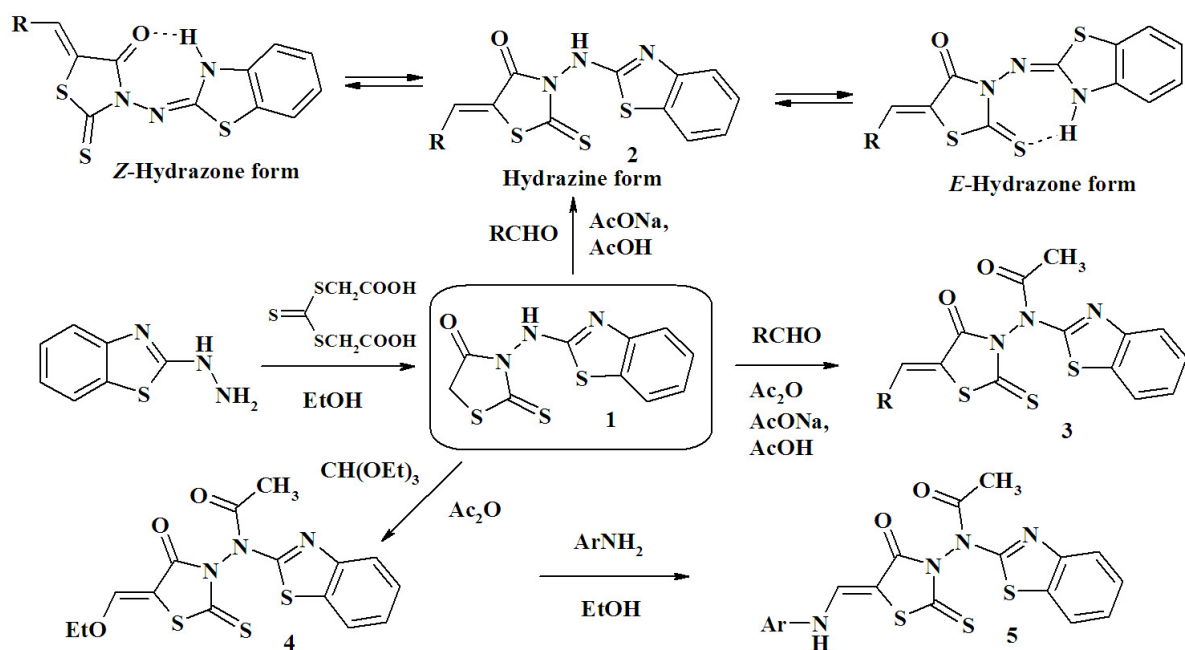


Figure 2. Scheme 1

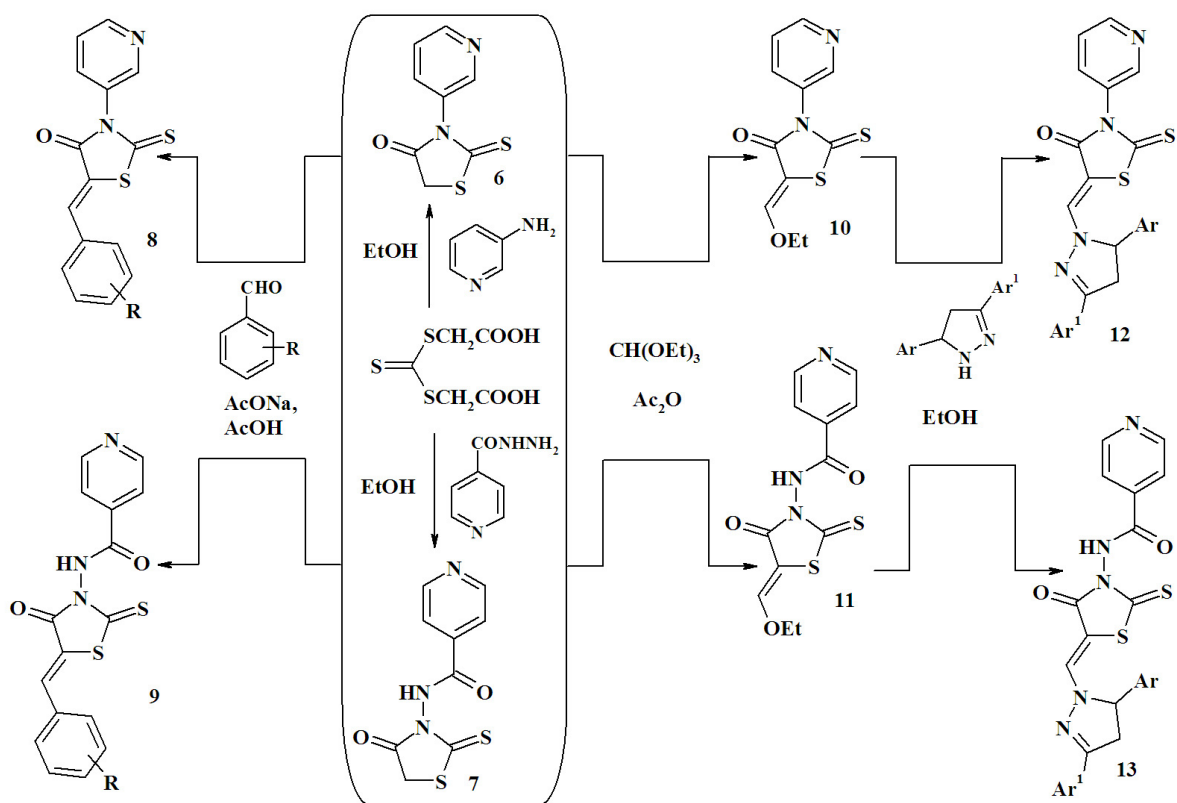


Figure 3. Scheme 2

acetic anhydride. The 5-ethoxymethylene derivative 4 was converted into appropriate enamines 5.

Following the reaction of 3-aminopyridine or isoniazid with trithiocarbonyl diglycolic acid in an ethanol medium, 3-pyridine substituted rhodanines 6, 7 were obtained. Derivatives 6 and 7 are methylene active heterocycles, which yield a series of 5-arylidene derivatives 8, 9 in the Knoevenagel reaction. Moreover, the 5-ethoxymethylene derivatives 10 and 11 were synthesised by the condensation of 6 and 7 with triethyl orthoformate in acetic anhydride. As the amine component in the aminolysis reaction, we tested some 3,5-diarylpyrazolines, which allowed the synthesis of new pyrazoline-thiazolidinone conjugates 12 and 13 (Scheme 2, Figure 3) [18-21].

Condensation of 2-(4-oxo-2-thioxothiazolidin-3-yl)-3-phenylpropionic acid 14 with triethyl orthoformate yielded 5-ethoxymethylene derivative 15. Interestingly, the simultaneous esterification of the carboxylic group resulted in the ester formation. Compound 15 was converted into appropriate enamines 16–18 (Scheme 3, Figure 4) [22].

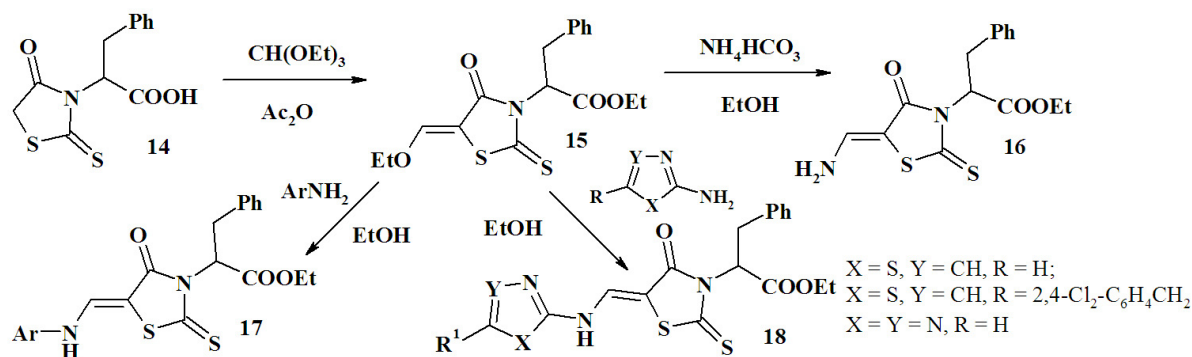


Figure 4. Scheme 3

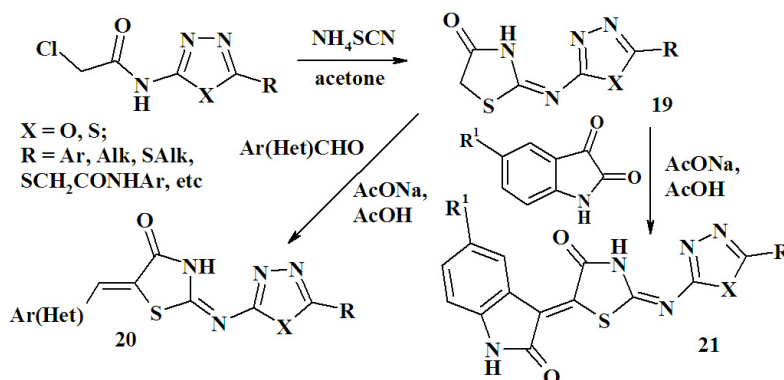


Figure 5. Scheme 4

It is known that the reaction of 2-chloroacetamides with thiocyanates does not stop at the nucleophilic substitution stage, but passes spontaneous heterocyclisation with the formation of a 4-thiazolidinone ring and the Dimroth rearrangement with the migration of the substituents in positions 2 and 3. Using this method, various 1,3,4-thia(oxa)diazol-substituted 2-imino-4-thiazolidinones 19 were synthesised (Scheme 4, Figure 5) [18,23]. Compounds 19 were utilised to obtain 5-ene derivatives 20, 21.

Spiro-substituted 4-thiazolidinone-isatins 22 were obtained in a three-component one-pot reaction of isatin, corresponding to aromatic amine and thioglycolic acid (Scheme 5, Figure 6). The synthesis of 5-arylidene-4-thiazolidinones 23 is described in the Knoevenagel reaction under different conditions. Although commonly used conditions (sodium acetate as catalyst in acetic acid) are not effective in the case of 2-substituted-4-thiazolidinone because of the low reactivity of the methylene group in comparison with rhodanine or 2,4-thiazolidinedione derivatives, the reac-

tion was performed in isopropanol with the presence of potassium tert-butyrate as a catalyst [24].

The interaction of 3,5-diaryl-4,5-dihydro-1H-pyrazoles with 4-thioxo-2-thiazolidinones (isorhodanines) yielded 4-pyrazoline-substituted-1,3-thiazole-2-one 24, which were utilised for the synthesis of 5-arylidene derivatives 25 (Scheme 6, Figure 7) [25].

Detailed biological activity evaluation of pyrazoline-thiazolidinone conjugates 28-32 (Scheme 7, Figure 8) synthesised via the [2+3]-cyclocondensation of 4,5-dihydropyrazole-1-carbothioamides 26 as S,N-bi-nucleophiles and dielectrophilic synthon [C2]2+ allowed the identification of compounds with antimicrobial, antiviral, anti-inflammatory and antitumor activities. For the

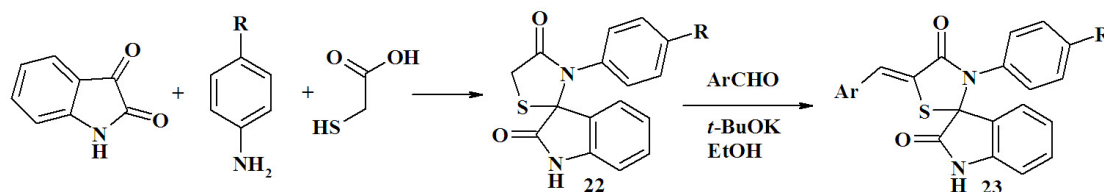


Figure 6. Scheme 5

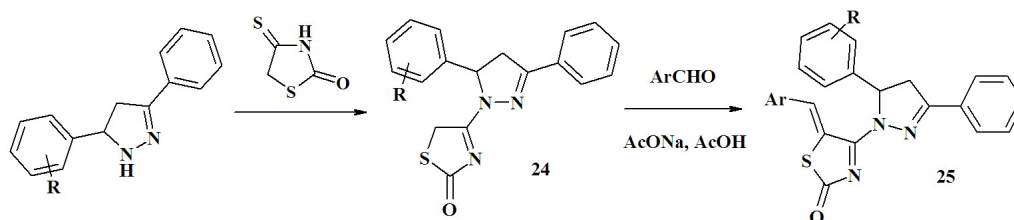


Figure 7. Scheme 6

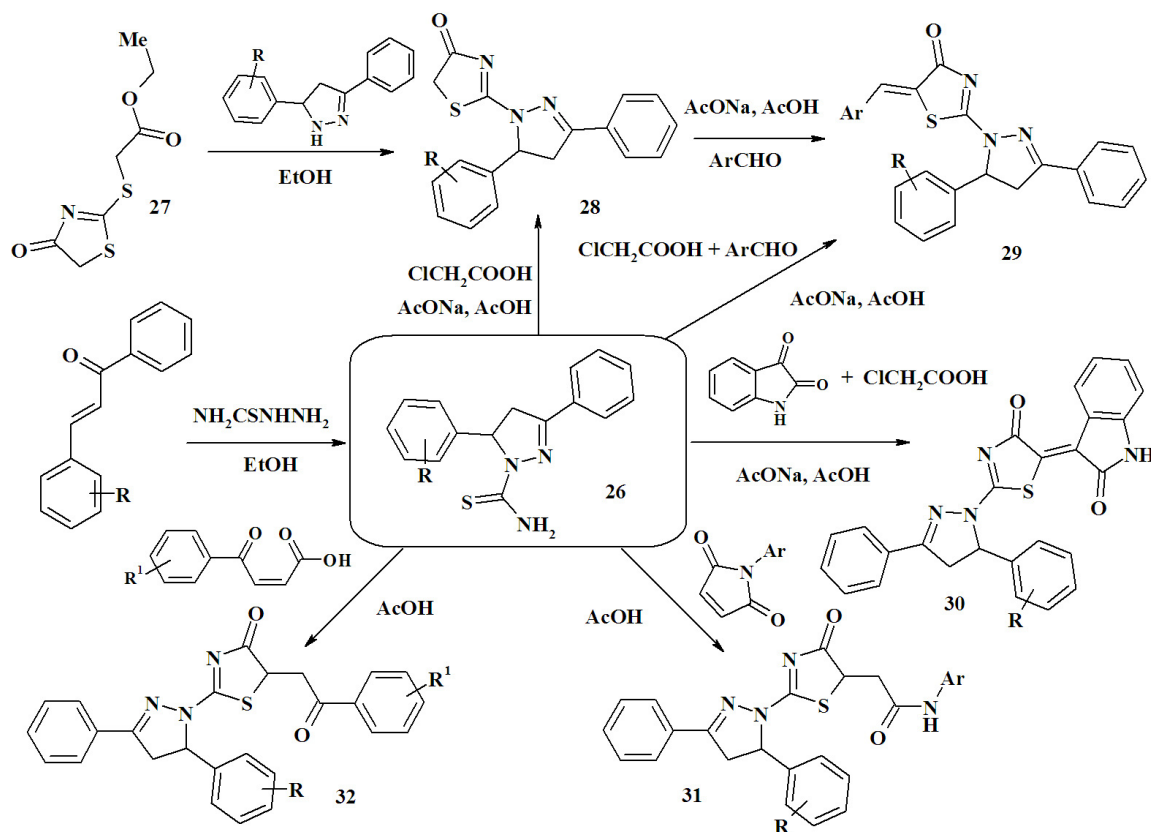


Figure 8. Scheme 7

synthesis of target derivatives, chloroacetic acid, maleic anhydride, maleimides and  $\beta$ -aroylacrylic acids were used as equivalents of dielectrophilic synthon [C2]2+. The three-component one-pot reaction including [2+3]-cyclocondensation of 4,5-dihydropyrazole-1-carbotioamides 26 with chloroacetic acid and the further Knoevenagel reaction with aromatic aldehydes or isatin derivatives is an effective approach for the design of new anticancer agents from pyrazoline-thiazolidinones 29, 30. Alternatively, 2-(5-aryl-3-phenyl-4,5-dihydro-1H-pyrazol-1-yl)-1,3-thiazol-4(5H)-ones 28 were obtained following the reaction of 2-carbomethoxymethylthio-2-thiazoline-4-one 27 with appropriate 5-aryl-3-phenyl-2-pyrazolines in ethanol [25-27].

Continuing systematic synthetic studies of heterylsubstituted 4-thiazolidinone, a series of thiosemicarbazones 34 was obtained based on 6-arylimidazo[2,1-b]thiadiazole-5-carbaldehydes 33. The synthesis of the target thiazolidinone/thiazole-indole/imidazothiadiazole hybrids 35-38 was performed via the reaction of [2+3]-cyclocondensation.  $\alpha$ -Halogenocarboxylic acids, ethyl-2-chloroacetoacetate, 2-bromoacetophenone, and 2-bromobutyrolactone were used as [C2]2+ reagents. When utilising 2-bromobutyrolactone, compounds with free or acetylated OH group were obtained depending on the reaction medium (Scheme 8, Figure 9). The synthesis of

these compounds was confirmed by our preliminary data on the high antitrypanosomal activity of 2-hydrazone-4-thiazolidinones with arylindole moiety in position 2, which are bioisosteric to 6-arylimidazo[2,1-b]thiadiazole [28].

Next, new oleanolic acid (OA) derivatives with 4-thiazolidinone-carboxylic acids fragments were designed as new potential anticancer agents. The design of the target compounds is outlined on Scheme 10 (Figure 11) and consists of the modification of OA A-ring-linking group by heterocyclic acids, with the use of oxime group as a linker. Starting oximes 43 were synthesised by reacting hydroxylamine hydrochloride with 3-oxooleanolic acid 39, its methyl ester 40, morpholide 41 or 12-bromolactone 42 in ethanol in the presence of anhydrous sodium acetate. The mentioned 3-oxooleananes 39-42 were obtained from OA extracted from *Viscum album*, L. For the synthesis of target 3-O-acyloleanolic acid derivatives 44, the oximes 43 were acylated by 4-thiazolidinone-based heterocyclic acids in the presence of *N,N'*-dicyclohexylcarbodiimide (DCC) in dioxane or THF at room temperature (Scheme 9, Figure 10). As a result, we designed and synthesised new semi-synthetic compounds with possible satisfactory ADME-tox parameters. Moreover, the oleanane fragment of these derivatives could be considered as an element of drug-delivery systems [29].

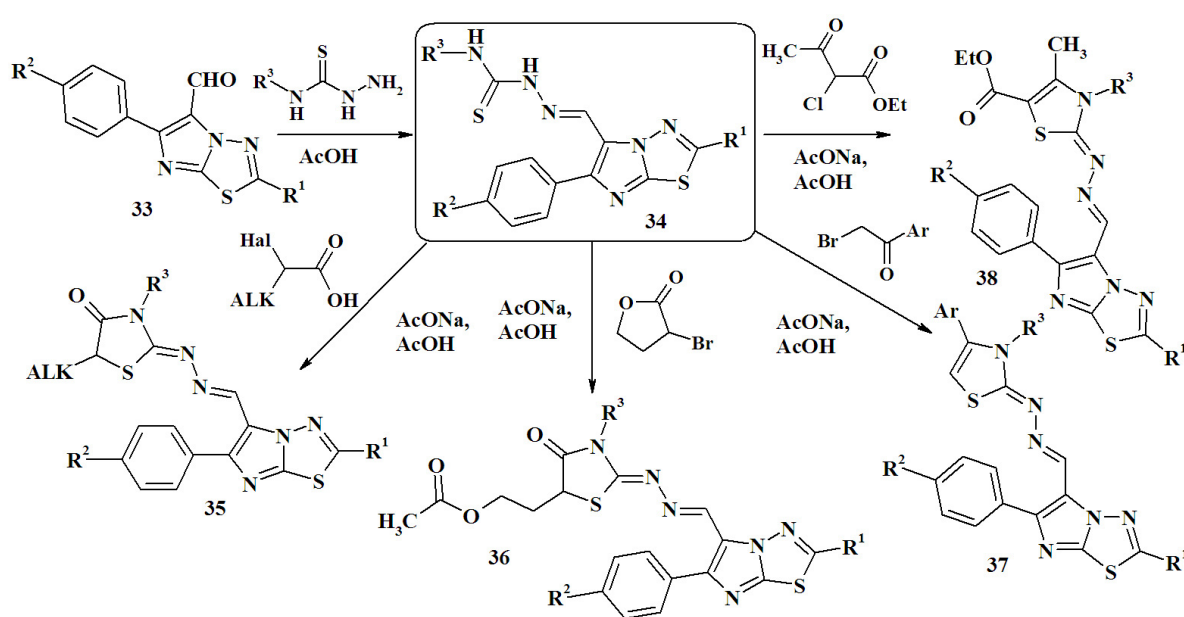


Figure 9. Scheme 8

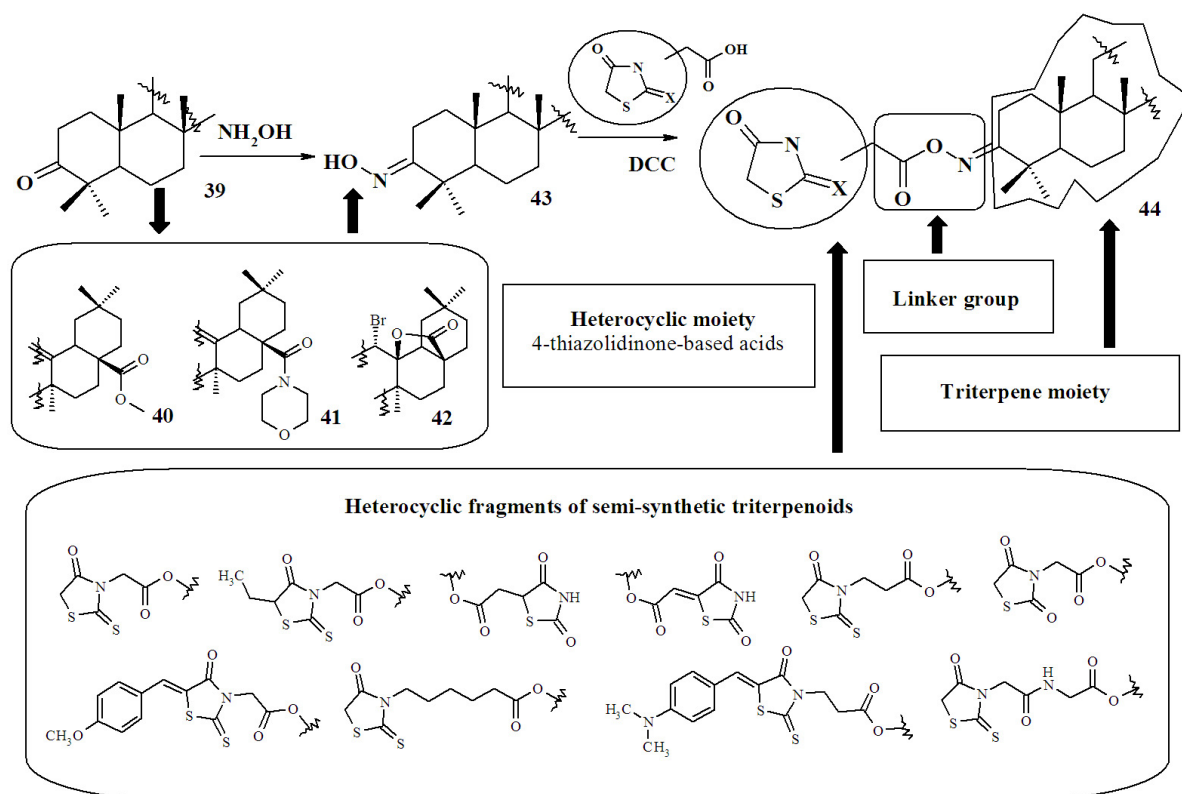


Figure 10. Scheme 9

## "Chemical" approach for the design of drug-like molecules

The "Chemical" approach is based on the hypothesis that thiopyranthiazole scaffold can be treated as "fixed" 4-thiazolidinone biophore in a "rigid" fused heterocyclic system, thereby preserving the biological activity of synthetic precursors, namely 5-ene-4-thiazolidinones. Thiopyranthiazoles can be considered as biomimetics of pharmacologically active 5-ene-4-thiazolidinones without MA properties (Scheme 10, Figure 11). The combination of thiazole and thiopyran cycles in a condensed heterosystem is a precondition for the creation of "centres conservative" of the ligand-target binding complex and promotes potential selectivity to biotargets.

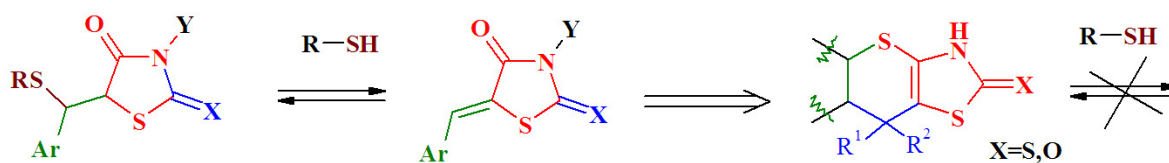


Figure 11. Scheme 10

Considering the aforementioned arguments, the directed search for new drugs among fused thiazole-based derivatives is justified and a promising direction in modern medicinal chemistry [15].

The most efficient approach to thiopyrano-[2,3-d]thiazoles design is the use of the hetero-Diels-Alder reaction, and 5-ene-4-thioxo-2-thiazolidinones (5-ene-isorhodanines) with 5-ene-2,4-thiazolidinedithiones (5-ene-thiorhodanines) as heterodienes (Scheme 11, Figure 12). These reagents contain in their structure  $\alpha,\beta$ -unsaturated thiocarbonyl fragment similar to the 1-thio-1,3-butadiene which leads to their high reactivity in the [4+2]-cycloadditions. The important condition is the presence of a strong dienophile with electron acceptor properties to decrease the energy difference between diene's

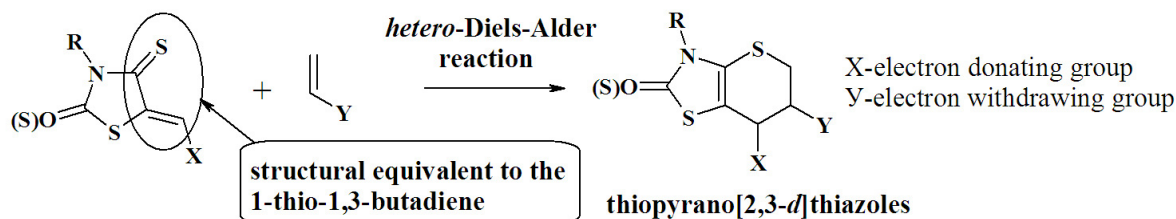


Figure 12. Scheme 11

"HOMO" and "LUMO" or "HOMO" of the dienophile. For these reasons, reactions are highly regioselective [30].

In the pioneering works of our department, the dienophile component was represented by maleic acid and its derivatives (maleic anhydride, maleinimides) and acrylic acid and its derivatives (methyl acrylate, ethyl acrylate, acrylonitrile) [31-33]. Currently, we have significantly expanded the list of dienophiles. Thus, the use of cinnamic acids and their amides [34], acrylylic

[35] and arylidenepyruvic acids [36] as well as dimethyl acetylenedicarboxylate [37], propiolic acid and its ethyl ester [38], acrolein [39], 2-norbornene [40,41] and 5-norbornene-2,3-dicarboxylic acid imides [42] as dienophiles yielded new thiopyrano[2,3-d]thiazoles 45-52 (Scheme 12, Figure 13).

We established that the reaction of 5-arylideneisorhodanines with 2(5H)furanone yielded mixtures of endo/exo adducts 53,54 (Scheme 13, Figure 14). Considering the moderate diastereo-

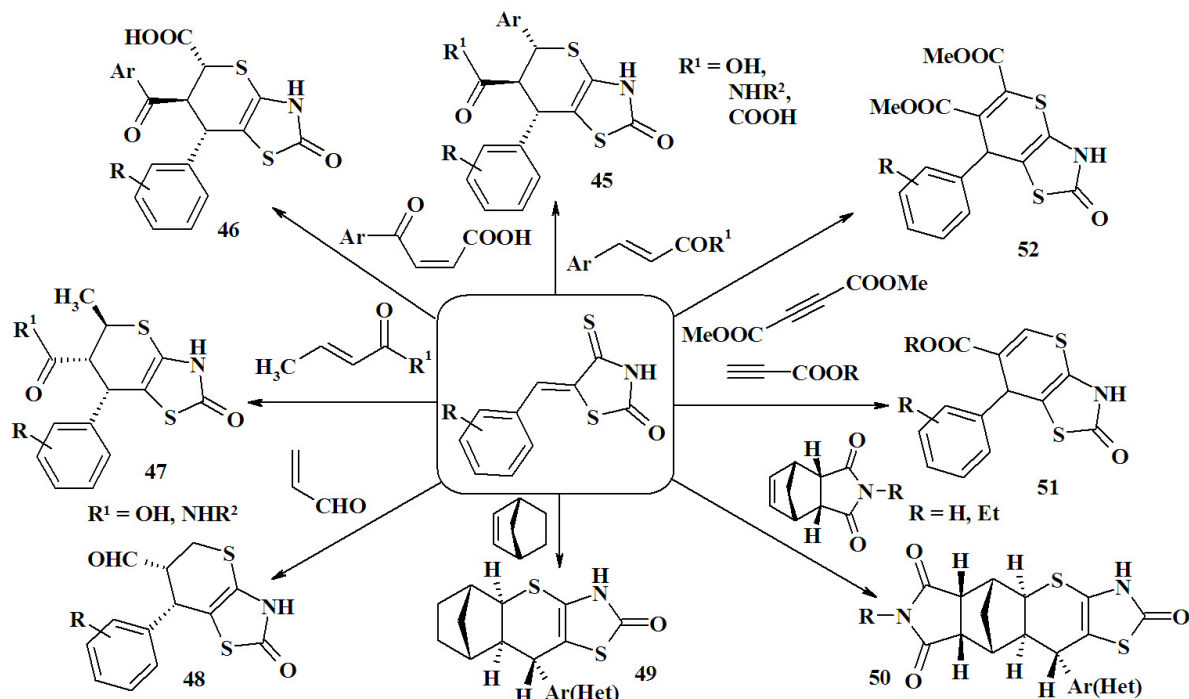


Figure 13. Scheme 12

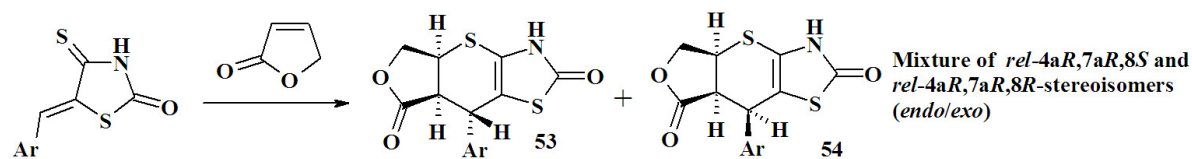


Figure 14. Scheme 13



selectivity, the reaction can occur through endo or exo transition states. Thus, the endo transition state leads to anti configuration, while the exo geometry results in syn configuration of the 8-H respectively [43].

The reaction of 5-arylideneisorhodanines with trans-aconitic acid proceeds as a regio- and diastereoselective [4+2]-cycloaddition with spontaneous decarboxylation of the adduct 55 to furnish rel-(6R,7R)-diastereomers 56. The same products were synthesised using itaconic acid as dienophile. Interestingly, the one-pot three-component reaction of 5-arylideneisorhodanines, trans-aconitic acid and anilines diastereoselectively yielded rel-(5'R,6'R,7'R)-spiro[pyrrolidin-3,6'-thiopyrano[2,3-d]thiazol]-2,2',5-triones 57 without decarboxylation of adducts. The

thiopyrano[2,3-d]thiazoles 90 were synthesised using (2,5-dioxo-1-arylpyrrolidin-3-ylidene)-acetic acids as dienophiles. It should be noted that unlike free trans-aconitic acid or its imides, the corresponding trimethyl ester (trimethyl 1-propene-1,2,3-tricarboxylate) reacted with opposite regioselectivity resulting in [4+2]-cycloadducts (58) (Scheme 14, Figure 15) [44].

In the case of utilisation of 1,4-naphthoquinone as a dienophile, intermediates of the [4+2]-cycloaddition reaction undergo spontaneous oxidation with the formation of tetracyclic thiopyrano[2,3-d]thiazoles 59 (Scheme 15, Figure 16) [45].

It is known that [4+2]-cycloaddition of 5-ethoxymethylidene-4-thiazolidinethiones with dienophiles in boiling acetic acid passes with

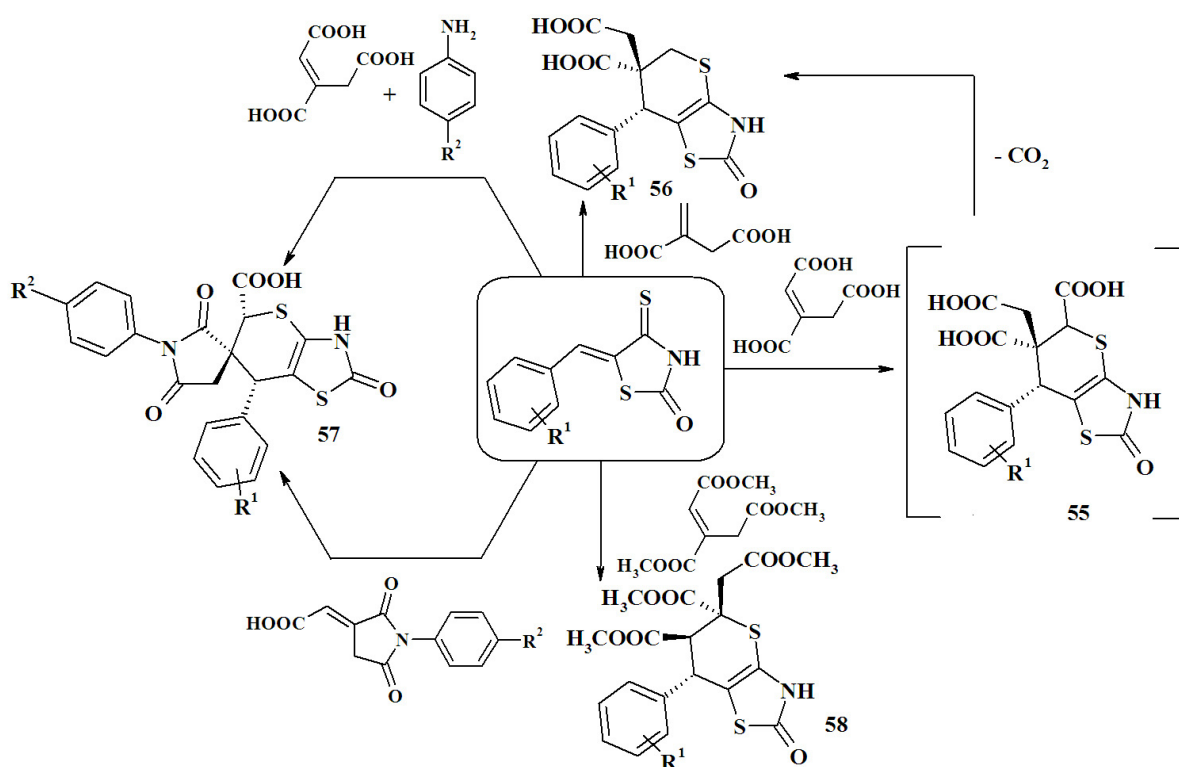


Figure 15. Scheme 14

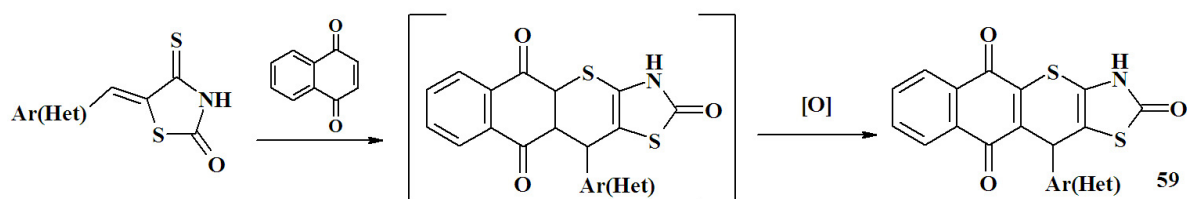


Figure 16. Scheme 15

spontaneous ethanol elimination and the formation of 3,5-dihydro-2H-thiopyrano[2,3-d]thiazoles. Analogously, we observed in the [4+2]-cycloaddition with acrolein, crotonic aldehyde, 2-norbornene and 5-norbornene-2,3-dicarboxylic acid imides (60–62). When the interaction of 5-ethoxymethylene-4-thioxo-2-thiazolidinones with propiolic acid is accompanied by not only the ethanol elimination, but the rearrangement of double bonds with the formation of 2-oxo-2H-thiopyrano[2,3-d]thiazole-6-carboxylic acid 63, compound 63 is also formed when using acetylene dicarboxylic acid, which may be explained by additional adduct decarboxylation. [4+2]-Adducts of aroylacrylic acids also undergo elimination of ethanol and decarboxylation with regioselective formation of 64. Interaction with the 1,4-naphthoquinone was accompanied by spontaneous dehydrogenation and ethanol elimination yielding derivative 98 (Scheme 16, Figure 17) [46].

One of the relatively new areas in thiopyrano[2,3-d]thiazole chemistry is the usage of 5-(cyclo)alkylideneisorhodanines as key reagents (Scheme 17, Figure 18). Thus, the starting heterodienes 66 were obtained in the reaction of isorhodanine with acetone, cyclopentanone or cyclohexanone at room temperature and in the

presence of triethylamine as a catalyst. Interestingly, performing the reaction in ethanol at the solvent boiling point leads to the formation of tricyclic heterosystems 67. When thiorhodanine is used, only fused derivatives 68 are formed regardless of the reaction conditions. [4+2]-Cycloaddition of 66 with maleinamides, 2-norbornene and (3,5-dioxo-4-azatricyclo[5.2.1.0<sup>2,6</sup>]decen-8-yl-4)-acetic acid yielded derivatives 69–71 [47].

As a phase of study of the hetero-Diels-Alder reaction, we suggested new tandem and domino processes for the synthesis of polycondensed thiopyranothiazole-based compounds. These reactions allow the synthesis of structurally complex molecules with high selectivity, while the usage of solvents, reagents, adsorbents and energy is significantly reduced compared to traditional multistage synthetic approaches.

The presence of active groups in the o-position of 5-arylidene-4-thiazolidinethiones is an important feature contributing to the passing of tandem processes based on the hetero-Diels-Alder reaction. Among the tandem reactions, we distinguished two types of processes: acylation- and hemiacetal-based reactions (Scheme 18, Figure 19). The first approach requires the use of

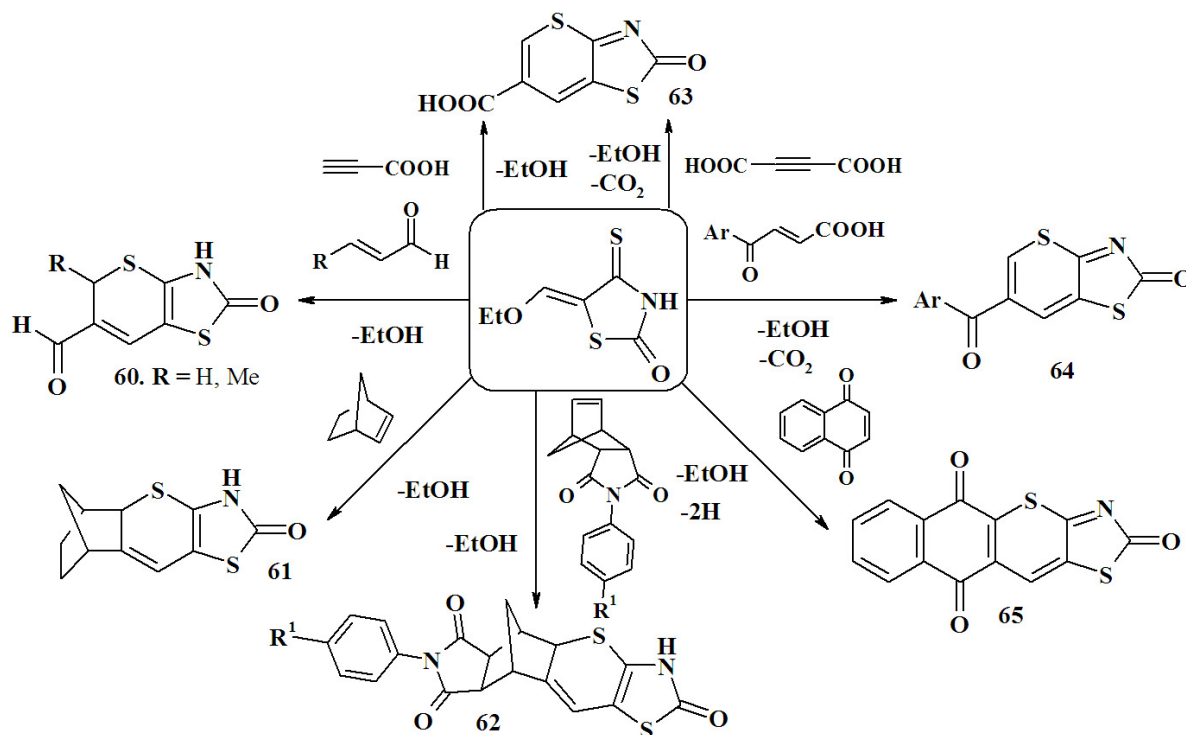


Figure 17. Scheme 16

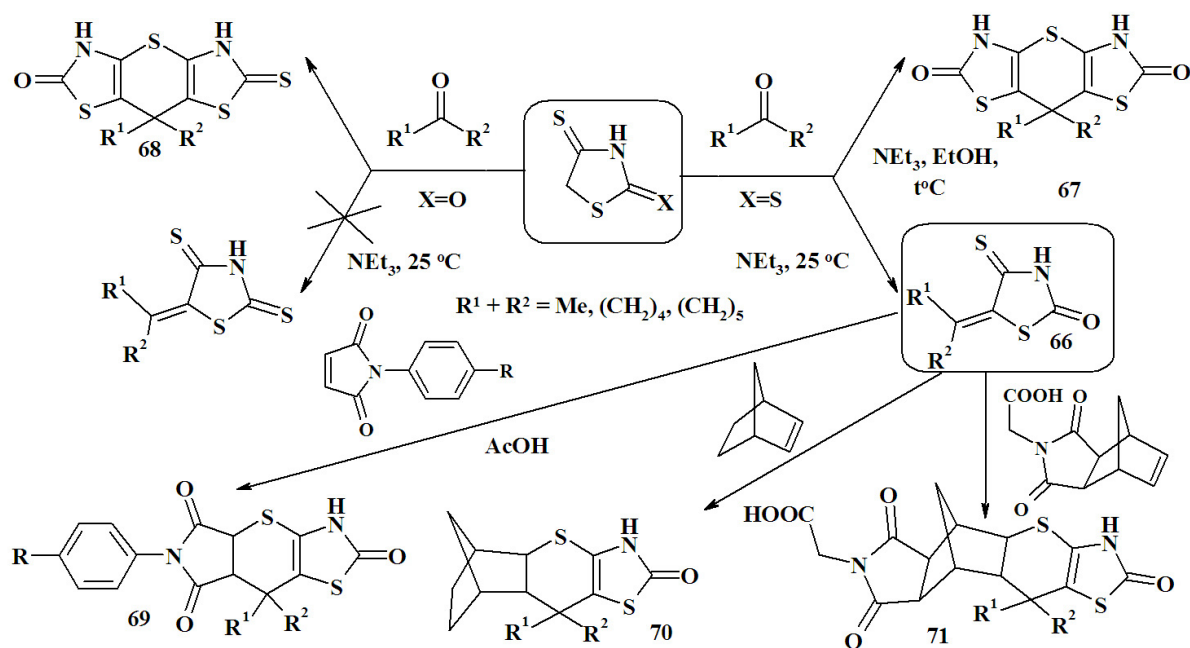


Figure 18. Scheme 17

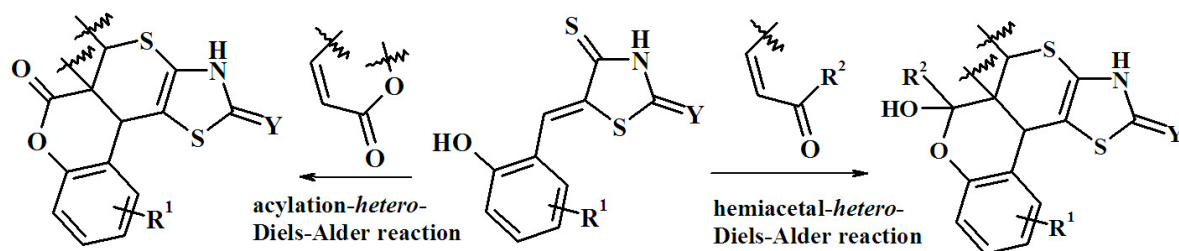


Figure 19. Scheme 18

derivatives of  $\alpha,\beta$ -unsaturated carboxylic acids as dienophiles, and  $\alpha,\beta$ -unsaturated oxo compounds (aldehydes and ketones) in the second.

Thus, when studying hetero-Diels-Alder-acylation tandem reactions of 5-(2-hydroxyphenylmethylidene)isorhodanines 72 with unsaturated carboxylic acids and their derivatives more precisely, a number of stereochemical peculiarities of these processes were established (Scheme 19, Figure 20). For example, in the reaction of crotonic acid, its amides or anhydride, a mixture of *rel*-5R,5aR,11bS and *rel*-5S,5aR,11bS diastereomers (73) was formed. The reaction of heterodiene 72 with maleic and fumaric acids and their derivatives (maleic anhydride, esters) passed diastereoselectively. Moreover, independently of the stereoisomerism of the dienophile, a racemic mixture of *rel*-(5R,5aR,11bS) derivatives 74 was formed. Itaconic acid and its anhydride as well as *trans*-aconitic acid reacted in a similar manner forming

derivative 75. In the case of *trans*-aconitic acid, the reaction proceeded with spontaneous decarboxylation at position 5 of thiopyrano[2,3-d]thiazole core. *rel*-(5S,5aR,11bS) derivative 76 was the product of tandem hetero-Diels-Alder-acylation reaction of 72 and cinnamic acids. Compound 75 proved to be an effective reagent for the next chemical transformations. The reaction of 75 with primary amines in acetic acid passed through the amidation stage, followed by spontaneous recycling in spiroimides 77. The thiopyrano[2,3-d]thiazoles 77 were also obtained by the alternative method from itaconic acid imides [38,44,48,49].

It is important to note that in the reaction of propiolic acid, a classic hetero-Diels-Alder reaction takes place to form 78. The presence of a double bond at positions 5–6 causes planar structure of the bicyclic fragment and creates the spatial obstacles for acylation of the phenolic group. Dehydrogenation of the basic hetero-

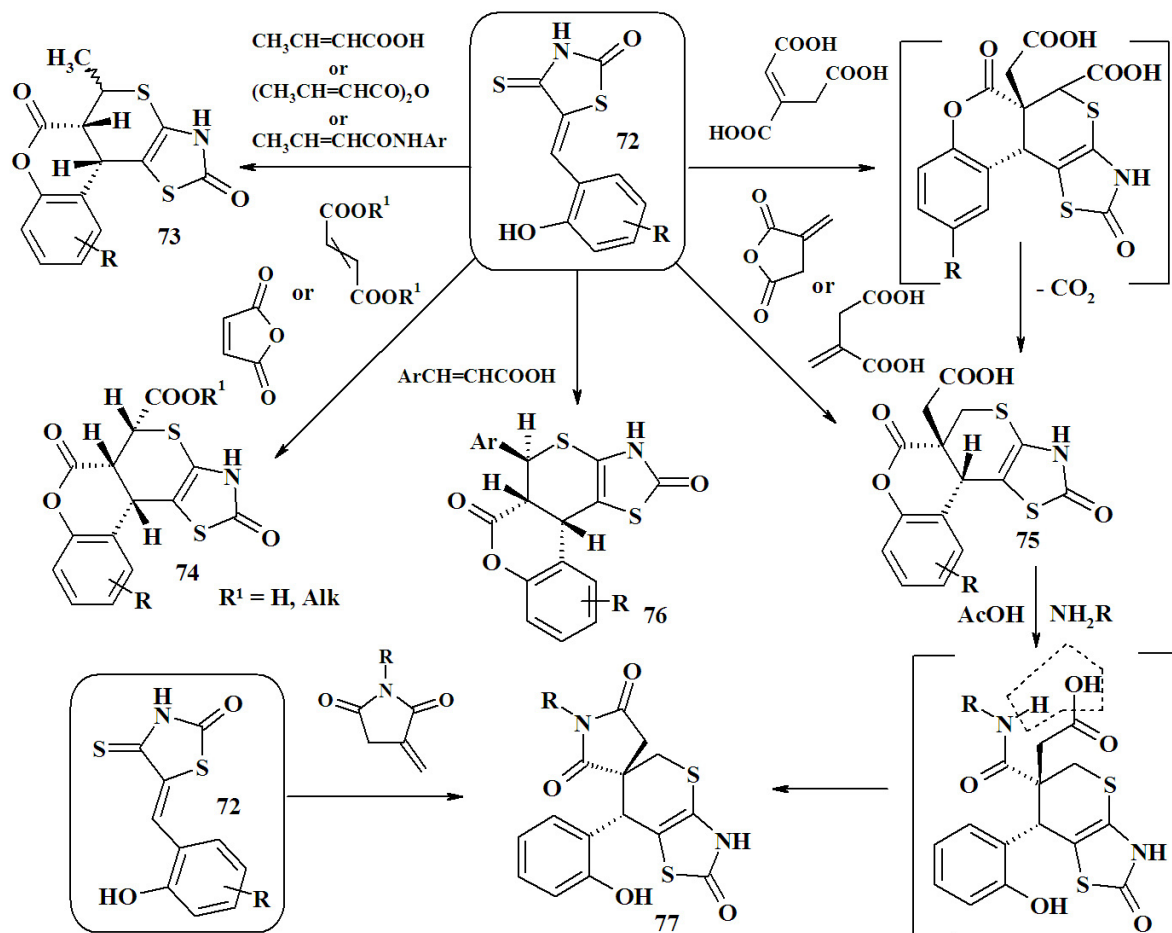


Figure 20. Scheme 19

cycle with bromine in acetic acid removes these obstacles to obtain the derivative 79 (Scheme 20, Figure 21) [38].

The reaction of 5-(2-hydroxyphenylmethylene)isorhodanines with 2(5H)furanone proceeded as a diastereoselective tandem acylation-hetero-Diels-Alder reaction providing novel rel-(5R,5aR,11bS) derivatives 80 (Scheme 21, Figure 22) [43].

The reactions between 5-(2-hydroxybenzylidene)-4-thioxo-2-thiazolidinones and arylidene pyruvic acids (Scheme 22, Figure 23) yielded the mixture of rel-(5S,5aR,11bR) 81 and rel-(5R,5aS,11bR) 81\* diastereoisomers in a 2:1 ratio [50]. At the same time, acrolein, crotonic and cinnamic aldehydes in this tandem hetero-Diels-Alder-hemiacetal reaction (Scheme 23) diastereoselectively yielded rel-(5aR,6R,11bS)-6-hydroxy-

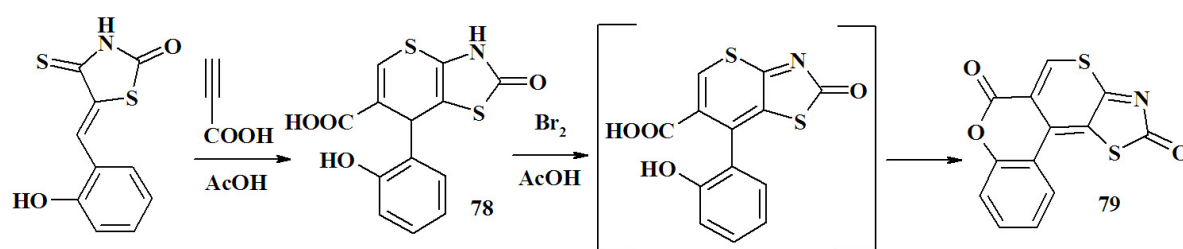


Figure 21. Scheme 20

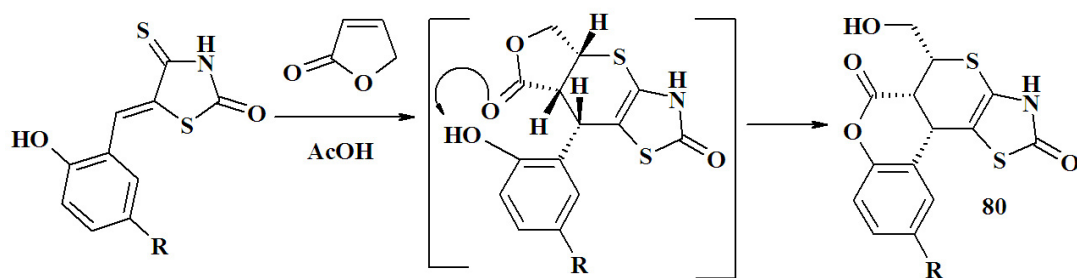


Figure 22. Scheme 21

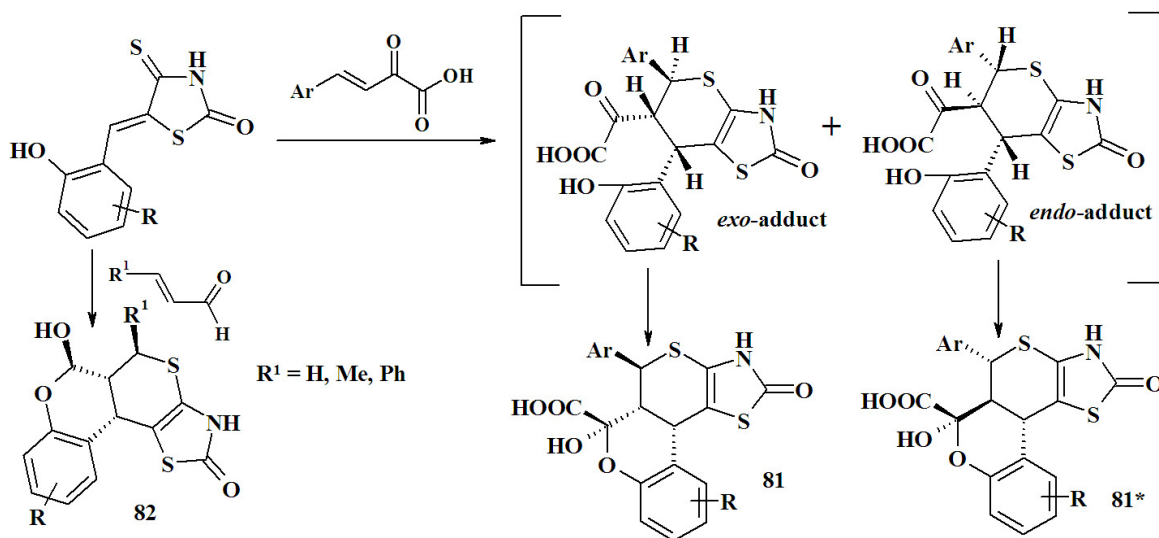


Figure 23. Scheme 22

3,5a,6,11b-tetrahydro-2H,5H-chromeno[4',3':4,5]thiopyrano[2,3-d]thiazole-2-ones 82.

In addition to tandem reactions, domino reactions also play an important role in the synthesis of thiopyrano[2,3-d]thiazole-based compounds. A domino reaction involves two or more transformations, which result in the formation of bonds (usually C-C bonds) and occur under the same reaction conditions without adding new reagents and/or catalysts. In this process, the subsequent reactions take place as a consequence of the functionality formed in the previous step, for example, obtaining isothiochromeno[4a,4-d]thiazole-2-ones 83 and chromeno[4',3':4,5]thiopyrano[2,3-d]thiazole-2-(thi)ones 84,85 in the domino Knoevenagel-hetero-Diels-Alder reaction (Scheme 23, Figure 24) of isorhodanine with 3,7-dimethyl-6-octenal ((±)citronelal) and 2-allyloxybenzaldehyde [51]. It should be noted that the reaction of isorhodanine with 2-allyloxybenzaldehyde yielded a mixture of trans- 84 and cis- 84a

isomers (5:1). Recrystallization from dioxane can provide individual trans-isomer 84. Alternatively, tetracyclic derivatives 84,85 were synthesised via the domino thionation-hetero-Diels-Alder reaction of 5-(2-allyloxyphenylmethylidene)-4-thiazolidinones 86.

Another example of the domino Knoevenagel-hetero-Diels-Alder reaction is the interaction of isorhodanine with 2-(2-methylallyloxy)- and 2-(cyclohexene-2-yloxy)benzaldehydes, 2-allyloxynaphthalaldehyde as well as 2-formylphenyl-(E)-3- aryl-2-propenoates (Scheme 24, Figure 25). These reactions allowed the preparation of a series of pentacyclic derivatives characterised by trans- (87-89) or cis-configuration (90) of 5a and 11b protons. Interestingly, when 2-formylphenyl-(E)-3-aryl-2-propenoates are used as reagents, stereo-configuration of the final products 90 were similar to the derivatives 76 obtained in tandem acylation-hetero-Diels-Alder reaction (Scheme 20, Figure 21). The stereochemistry of the final compounds

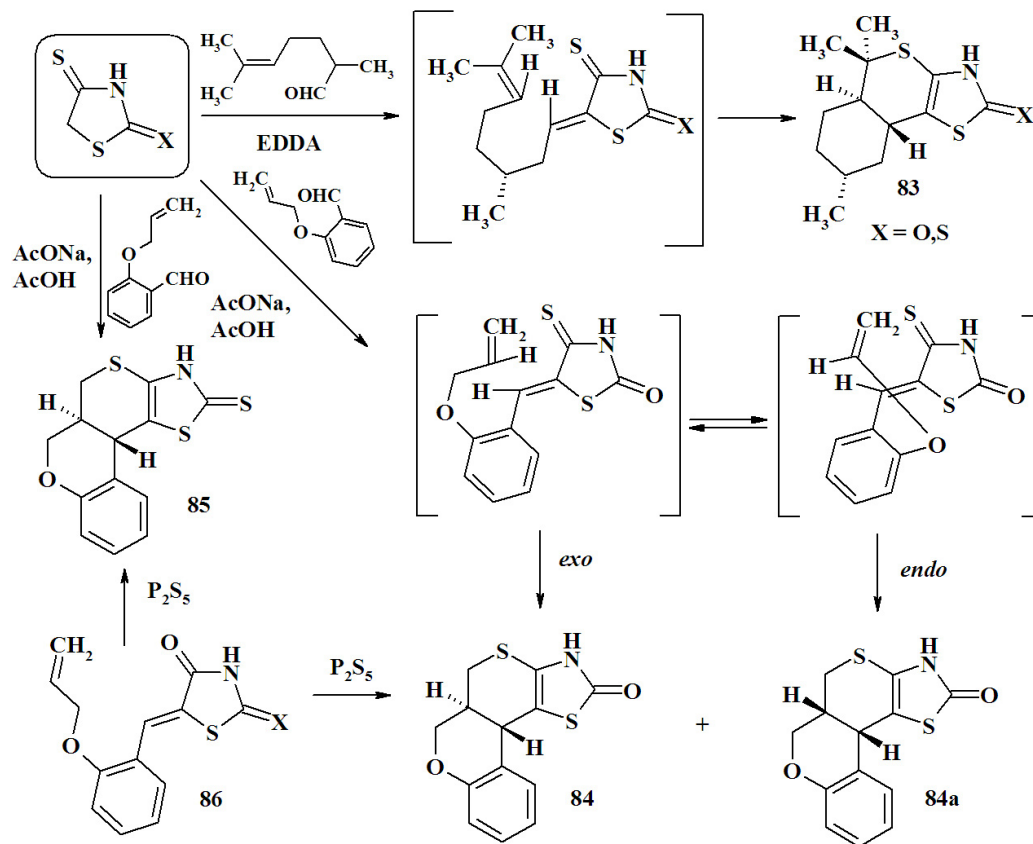


Figure 24. Scheme 23

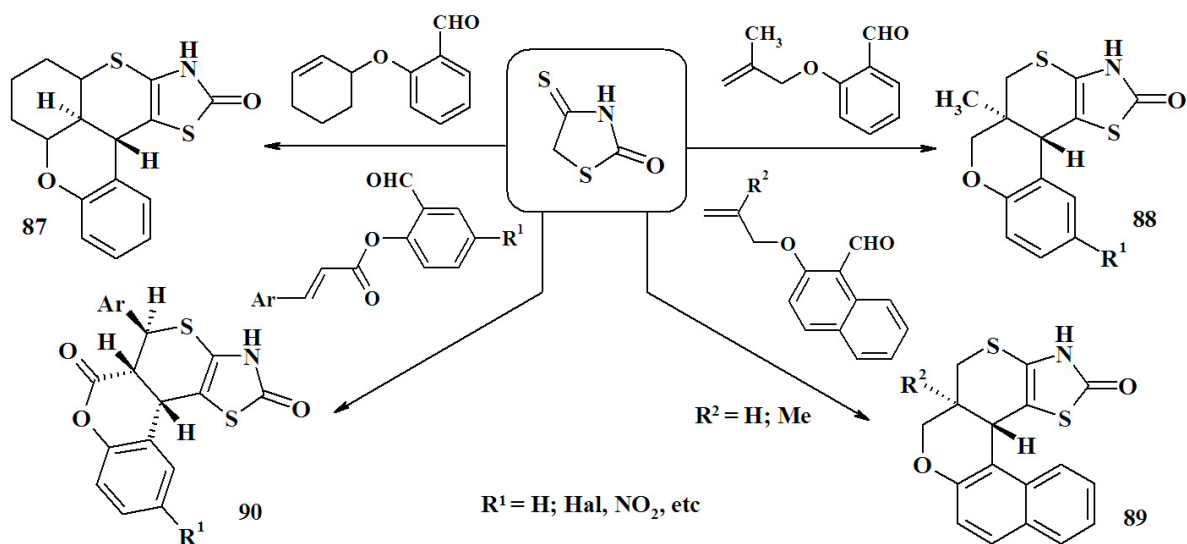


Figure 25. Scheme 24

depends on the endo- and exo-orientation of the dienophile in the transition state. The presence of the allyl moiety in the molecule induces an exo transition state, in contrast to the cinnamoyl fragment which causes endo-orientation of the dienophile due to the orbital interactions [51].

## Conclusions and further perspectives

The combination of several reactive centres in the main core led to different 4-thiazolidinone-based compound subtypes. The main routes for 5-ene-thiazolidinones synthesis and modification, mainly within a structure-based approach, can be compiled into the following groups:

- › complication of the C5 fragment (following the thesis regarding the crucial impact of the C5 moiety for pharmacological activity);
- › introduction of the substituents in the N3 position (especially fragments with carboxylic/amino/hydroxy groups);
- › synthesis of isosteric heterocycles;
- › combination with other pharmacologically attractive fragments within hybrid pharmacophore approach;
- › annealing in complex heterocyclic systems;
- › utilisation of 5-ene-thiazolidinones for the synthesis of other heterocycles.

The realisation of the presented routes is based on a combinatorial approach, privileged substructure-based diversity-oriented synthesis and molecular hybridisation. The chemical transformations cover mainly the reactions which involve the exocyclic double bond in C5 position of the main core and correspond to the above-mentioned direction of the 5-ene-4-thiazolidinones modification.

## Acknowledgements

### Conflict of interest statement

The authors declare no conflict of interest.

### Funding sources

There are no sources of funding to declare.

## References

1. Lesyk R, Zimenkovsky B. 4-Thiazolidinones: Centenarian History, Current Status and Perspectives for Modern Organic and Medicinal Chemistry. *Current Organic Chemistry*. 2004 Nov 1;8(16):1547-1577. <https://doi.org/10.2174/1385272043369773>
2. Havrylyuk D, Zimenkovsky B, Lesyk R. Synthesis, Biological Activity of Thiazolidinones Bearing Indoline Moiety and Isatin Based Hybrids. *Mini-Reviews in Organic Chemistry*. 2014 Dec 24;12(1):66-87. <https://doi.org/10.2174/1570193x11666141028231910>
3. Havrylyuk D, Roman O, Lesyk R. Synthetic approaches, structure activity relationship and biological applications for pharmacologically attractive pyrazole/pyrazoline-thiazolidine-based hybrids. *European Journal of Medicinal Chemistry*. 2016 May;113:145-166. <https://doi.org/10.1016/j.ejmech.2016.02.030>
4. Tripathi AC, Gupta SJ, Fatima GN, Sonar PK, Verma A, Saraf SK. 4-Thiazolidinones: The advances continue.... *European Journal of Medicinal Chemistry*. 2014 Jan;72:52-77. <https://doi.org/10.1016/j.ejmech.2013.11.017>
5. Tomasic T, Masic L. Rhodanine as a Privileged Scaffold in Drug Discovery. *Current Medicinal Chemistry*. 2009 May 1;16(13):1596-1629. <https://doi.org/10.2174/092986709788186200>
6. Verma A, Saraf SK. 4-Thiazolidinone – A biologically active scaffold. *European Journal of Medicinal Chemistry*. 2008 May;43(5):897-905. <https://doi.org/10.1016/j.ejmech.2007.07.017>
7. Tomašić T, Peterlin Mašič L. Rhodanine as a scaffold in drug discovery: a critical review of its biological activities and mechanisms of target modulation. *Expert Opinion on Drug Discovery*. 2012 May 19;7(7):549-560. <https://doi.org/10.1517/17460441.2012.688743>
8. Mendgen T, Steuer C, Klein CD. Privileged Scaffolds or Promiscuous Binders: A Comparative Study on Rhodanines and Related Heterocycles in Medicinal Chemistry. *Journal of Medicinal Chemistry*. 2012 Jan 11;55(2):743-753. <https://doi.org/10.1021/jm201243p>
9. Baell JB. Observations on screening-based research and some concerning trends in the literature. *Future Medicinal Chemistry*. 2010 Oct;2(10):1529-1546. <https://doi.org/10.4155/fmc.10.237>
10. Baell JB, Holloway GA. New Substructure Filters for Removal of Pan Assay Interference Compounds (PAINS) from Screening Libraries and for Their Exclusion in Bioassays. *Journal of Medicinal Chemistry*. 2010 Apr 8;53(7):2719-2740. <https://doi.org/10.1021/jm901137j>
11. Baell J, Walters MA. Chemistry: Chemical con artists foil drug discovery. *Nature*. 2014 Sep;513(7519):481-483. <https://doi.org/10.1038/513481a>
12. Kaminsky D, Kryshchshyn A, Lesyk R. 5-Ene-4-thiazolidinones – An efficient tool in medicinal chemistry. *European Journal of Medicinal Chemistry*. 2017 Nov;140:542-594. <https://doi.org/10.1016/j.ejmech.2017.09.031>
13. Kaminsky D, Kryshchshyn A, Lesyk R. Recent developments with rhodanine as a scaffold for drug discovery. *Expert Opinion on Drug Discovery*. 2017 Oct 11;12(12):1233-1252. <https://doi.org/10.1080/17460441.2017.1388370>
14. Lesyk RB, Zimenkovsky BS, Kaminsky DV, Kryshchshyn AP, Havrylyuk DY, Atamanyuk DV, Subtel'na

- IY, Khyluk DV. Thiazolidinone motif in anticancer drug discovery. Experience of DH LNMU medicinal chemistry scientific group. *Biopolymers and Cell*. 2011 Mar 20;27(2):107-117. <https://doi.org/10.7124/bc.000089>
15. Kryshchshyn A, Roman O, Lozynskiy A, Lesyk R. Thiopyrano[2,3-d]Thiazoles as New Efficient Scaffolds in Medicinal Chemistry. *Scientia Pharmaceutica*. 2018 Jun 14;86(2):26. <https://doi.org/10.3390/scipharm86020026>
  16. Mosula L, Zimenkovsky B, Havrylyuk D, Missir A, Chiriță I, Lesyk R. Synthesis and antitumor activity of novel 2-thioxo-4-thiazolidinones with benzothiazole moieties. *Farmacia*. 2009;57(3):321-30.
  17. Havrylyuk D, Mosula L, Zimenkovsky B, Vasylenko O, Gzella A, Lesyk R. Synthesis and anticancer activity evaluation of 4-thiazolidinones containing benzothiazole moiety. *European Journal of Medicinal Chemistry*. 2010 Nov;45(11):5012-5021. <https://doi.org/10.1016/j.ejmech.2010.08.008>
  18. Kaminskyy D, den Hartog GJ, Wojtyra M, Lelyukh M, Gzella A, Bast A, Lesyk R. Antifibrotic and anticancer action of 5-ene amino/iminothiazolidinones. *European Journal of Medicinal Chemistry*. 2016 Apr;112:180-195. <https://doi.org/10.1016/j.ejmech.2016.02.011>
  19. Senkiv J, Finiuk N, Kaminskyy D, Havrylyuk D, Wojtyra M, Krill I, Gzella A, Stoika R, Lesyk R. 5-Ene-4-thiazolidinones induce apoptosis in mammalian leukemia cells. *European Journal of Medicinal Chemistry*. 2016 Jul;117:33-46. <https://doi.org/10.1016/j.ejmech.2016.03.089>
  20. Wojtyra MN, Lesyk RB. Синтез 3-піридилзаміщених 4-тіазолідинонів як потенційних біологічно активних сполук. *Фармацевтичний часопис*. 2017 Mar 24;(1). <https://doi.org/10.11603/2312-0967.2017.1.7533>
  21. Wojtyra M, Lesyk R, Zimenkovsky B, Grellier P. (Z)-(5-[5-(3,5-diaryl-4,5-dihydropyrazol-1-yl-methylidene)-3-(pyridine-3-yl)-2-thioxothiazolidin-4-ones exhibiting antitrypanosomal action. 2017 Oct 10; UA 119822 (Ukraine).
  22. Holota S, Kryshchshyn A, Derkach H, Trufin Y, Demchuk I, Gzella A, Grellier P, Lesyk R. Synthesis of 5-enamine-4-thiazolidinone derivatives with trypanocidal and anticancer activity. *Bioorganic Chemistry*. 2019 May;86:126-136. <https://doi.org/10.1016/j.bioorg.2019.01.045>
  23. Lelyukh M, Havrylyuk D, Lesyk R. Synthesis and Anticancer Activity of Isatin, Oxadiazole and 4-Thiazolidinone Based Conjugates. *Chemistry & Chemical Technology*. 2015 Mar 15;9(1):29-36. <https://doi.org/10.23939/chcht09.01.029>
  24. Kaminskyy D. A Facile Synthesis and Anticancer Activity Evaluation of Spiro[Thiazolidinone-Isatin] Conjugates. *Scientia Pharmaceutica*. 2011;79(4):763-777. <https://doi.org/10.3797/scipharm.1109-14>
  25. Havrylyuk D, Zimenkovsky B, Vasylenko O, Zaprutko L, Gzella A, Lesyk R. Synthesis of novel thiazolone-based compounds containing pyrazoline moiety and evaluation of their anticancer activity. *European Journal of Medicinal Chemistry*. 2009 Apr;44(4):1396-1404. <https://doi.org/10.1016/j.ejmech.2008.09.032>
  26. Ouyang G, Cai X, Chen Z, Song B, Bhadury PS, Yang S, Jin L, Xue W, Hu D, Zeng S. Synthesis and Antiviral Activities of Pyrazole Derivatives Containing an Oxime Moiety. *Journal of Agricultural and Food Chemistry*. 2008 Nov 12;56(21):10160-10167. <https://doi.org/10.1021/jf802489e>
  27. Havrylyuk D, Zimenkovsky B, Vasylenko O, Gzella A, Lesyk R. Synthesis of New 4-Thiazolidinone-, Pyrazoline-, and Isatin-Based Conjugates with Promising Antitumor Activity. *Journal of Medicinal Chemistry*. 2012 Oct 9;55(20):8630-8641. <https://doi.org/10.1021/jm300789g>
  28. Kryshchshyn A, Kaminskyy D, Karpenko O, Gzella A, Grellier P, Lesyk R. Thiazolidinone/thiazole based hybrids – New class of antitrypanosomal agents. *European Journal of Medicinal Chemistry*. 2019 Jul;174:292-308. <https://doi.org/10.1016/j.ejmech.2019.04.052>
  29. Kaminskyy D, Bednarczyk-Cwynar B, Vasylenko O, Kazakova O, Zimenkovsky B, Zaprutko L, Lesyk R. Synthesis of new potential anticancer agents based on 4-thiazolidinone and oleanane scaffolds. *Medicinal Chemistry Research*. 2011 Nov 25;21(11):3568-3580. <https://doi.org/10.1007/s00044-011-9893-9>
  30. Komarista I. Synthesis, transformations and biological activity of some azolidones and their condensed derivatives. Moscow, USSR: I.M. Sechenov First State Medical Institute; 1989.
  31. Komaritsa ID, Baranov SN, Grishuk AP. 4-Thiazolidinones, derivatives and analogs. *Chemistry of Heterocyclic Compounds*. 1967 Jul;3(2):533-534. <https://doi.org/10.1007/bf00481594>
  32. Plevachuk NE, Komaritsa ID. A study of azolidones and their derivatives. *Chemistry of Heterocyclic Compounds*. 1970 Feb;6(2):144-145. <https://doi.org/10.1007/bf00474983>
  33. Grischuk AP, Komaritsa ID, Baranov SN. 4-Thionazolidones, derivatives and analogs. *Chemistry of Heterocyclic Compounds*. 1968;2(5):541-543. <https://doi.org/10.1007/bf00477515>
  34. Lozynskiy A, Zimenkovsky B, Lesyk R. Synthesis and Anticancer Activity of New Thiopyrano[2,3-d]thiazoles Based on Cinnamic Acid Amides. *Scientia Pharmaceutica*. 2014;82(4):723-733. <https://doi.org/10.3797/scipharm.1408-05>
  35. Lozynskiy A, Zasadko V, Atamanyuk D, Kaminskyy D, Derkach H, Karpenko O, Ogurtsov V, Kutsyk R, Lesyk R. Synthesis, antioxidant and antimicrobial activities of novel thiopyrano[2,3-d]thiazoles based on aroylacrylic acids. *Molecular Diversity*. 2017 Apr 19;21(2):427-436. <https://doi.org/10.1007/s11030-017-9737-8>
  36. Lozynskiy A, Zimenkovsky B, Nektegayev I, Lesyk R. Arylidene pyruvic acids motif in the synthesis of new thiopyrano[2,3-d]thiazoles as potential biologically active compounds. *Heterocyclic Communications*. 2015 Jan 1;21(1). <https://doi.org/10.1515/hc-2014-0204>
  37. Zelisko N, Atamanyuk D, Ostapiuk Y, Bryhas A, Matyichuk V, Gzella A, Lesyk R. Synthesis of fused thiopyrano[2,3-d][1,3]thiazoles via hetero-Diels-Alder reaction related tandem and domino process-



- es. *Tetrahedron*. 2015 Dec;71(50):9501-9508. <https://doi.org/10.1016/j.tet.2015.10.019>
38. Zelisko N, Atamanyuk D, Vasylenko O, Bryhas A, Matiychuk V, Gzella A, Lesyk R. Crotonic, cynamonic, and propiolic acids motifs in the synthesis of thiopyrano[2,3-d][1,3]thiazoles via hetero-Diels–Alder reaction and related tandem processes. *Tetrahedron*. 2014 Jan;70(3):720-729. <https://doi.org/10.1016/j.tet.2013.11.083>
  39. Lozynskiy A, Golota S, Zimenkovsky B, Atamanyuk D, Gzella A, Lesyk R. Synthesis, anticancer and antiviral activities of novel thiopyrano[2,3-d]thiazole-6-carbaldehydes. Phosphorus, Sulfur, and Silicon and the Related Elements. 2016 Mar 30;191(9):1245-1249. <https://doi.org/10.1080/10426507.2016.1166108>
  40. Kryshchshyn AP, Atamanyuk DV, Kaminskyy DV, Grellier P, Lesyk RB. Investigation of anticancer and anti-parasitic activity of thiopyrano[2,3-d]thiazoles bearing norbornane moiety. *Biopolymers and Cell*. 2017 Jun 30;33(3):183-205. <https://doi.org/10.7124/bc.00094f>
  41. Lesyk R, Zimenkovsky B, Atamanyuk D, Jensen F, Kieć-Kononowicz K, Gzella A. Anticancer thiopyrano[2,3-d][1,3]thiazol-2-ones with norbornane moiety. Synthesis, cytotoxicity, physico-chemical properties, and computational studies. *Bioorganic & Medicinal Chemistry*. 2006 Aug;14(15):5230-5240. <https://doi.org/10.1016/j.bmc.2006.03.053>
  42. Atamanyuk D, Zimenkovsky B, Lesyk R. Synthesis and anticancer activity of novel thiopyrano[2,3-d]thiazole-based compounds containing norbornane moiety. *Journal of Sulfur Chemistry*. 2008 Apr;29(2):151-162. <https://doi.org/10.1080/17415990801911723>
  43. Lozynskiy A, Zimenkovsky B, Karkhut A, Polovkovich S, Gzella AK, Lesyk R. Application of the 2(5H)furanone motif in the synthesis of new thiopyrano[2,3-d]thiazoles via the hetero-Diels–Alder reaction and related tandem processes. *Tetrahedron Letters*. 2016 Jul;57(30):3318-3321. <https://doi.org/10.1016/j.tetlet.2016.06.060>
  44. Zelisko N, Karpenko O, Muzychenko V, Gzella A, Grellier P, Lesyk R. trans-Aconitic acid-based hetero-Diels–Alder reaction in the synthesis of thiopyrano[2,3-d][1,3]thiazole derivatives. *Tetrahedron Letters*. 2017 May;58(18):1751-1754. <https://doi.org/10.1016/j.tetlet.2017.03.062>
  45. Atamanyuk D. Synthesis and Biological Activity of New Thiopyrano[2,3-d]thiazoles Containing a Naphthoquinone Moiety. *Scientia Pharmaceutica*. 2013;81(2):423-436. <https://doi.org/10.3797/scipharm.1301-13>
  46. Atamanyuk D, Zimenkovsky B, Atamanyuk V, Lesyk R. 5-Ethoxymethylidene-4-thioxo-2-thiazolidinone as Versatile Building Block for Novel Biorelevant Small Molecules with Thiopyrano[2,3-d][1,3]thiazole Core. *Synthetic Communications*. 2013 Oct 29;44(2):237-244. <https://doi.org/10.1080/00397911.2013.800552>
  47. Lesyk R, Kaminskyy D, Vasylenko O, Atamanyuk D, Gzella A. Isorhodanine and Thiorhodanine Motifs in the Synthesis of Fused Thiopyrano[2,3-d][1,3]thiazoles. *Synlett*. 2011 May 26;2011(10):1385-1388. <https://doi.org/10.1055/s-0030-1260765>
  48. Zelisko NI, Finiuk NS, Shvets VM, Medvid YO, Stoika RS, Lesyk RB. Screening of spiro-substituted thiopyrano[2,3-d]thiazoles for their cytotoxic action on tumor cells. *Biopolymers and Cell*. 2017 Aug 31;33(4):282-290. <https://doi.org/10.7124/bc.00095a>
  49. Zelisko N, Atamanyuk D, Vasylenko O, Grellier P, Lesyk R. Synthesis and antitrypanosomal activity of new 6,6,7-trisubstituted thiopyrano[2,3-d][1,3]thiazoles. *Bioorganic & Medicinal Chemistry Letters*. 2012 Dec;22(23):7071-7074. <https://doi.org/10.1016/j.bmcl.2012.09.091>
  50. Lozynskiy A, Zimenkovsky B, Gzella AK, Lesyk R. Arylidene Pyruvic Acids Motif in the Synthesis of New 2H,5H-Chromeno[4',3':4,5]thiopyrano[2,3-d]thiazoles via Tandem Hetero-Diels–Alder–Hemiacetal Reaction. *Synthetic Communications*. 2015 Aug 3;45(19):2266-2270. <https://doi.org/10.1080/00397911.2015.1076004>
  51. Matiychuk VS, Lesyk RB, Obushak MD, Gzella A, Atamanyuk DV, Ostapiuk YV, Kryshchshyn AP. A new domino-Knoevenagel–hetero-Diels–Alder reaction. *Tetrahedron Letters*. 2008 Jul;49(31):4648-4651. <https://doi.org/10.1016/j.tetlet.2008.05.062>

# The Novel Coronavirus Disease (COVID-19) Outbreak: The Israeli Experience

Mohammad Yasser Sabbah


Tel Aviv Sourasky Medical Center, Tel Aviv, Israel

 <https://orcid.org/0000-0002-9451-1893>

Corresponding author: [hamodi\\_sabbah@yahoo.com](mailto:hamodi_sabbah@yahoo.com)

Published: 2020-01-30

**How to Cite:** Sabbah MY. The Novel Coronavirus Disease (COVID-19) Outbreak: The Israeli Experience. JMS [Internet]. 2020 Mar 31;89(1):e413. doi:10.20883/medical.413

 DOI: <https://doi.org/10.20883/medical.413>

**Keywords:** COVID-19, Coronavirus, World Health Organization, worldwide spread, infection, disease



© 2020 by the author(s). This is an open access article distributed under the terms and conditions of the Creative Commons Attribution (CC BY-NC) license. Published by Poznan University of Medical Sciences

## ABSTRACT

Coronaviruses are a large family of viruses that cause illness ranging from the common cold to more severe diseases such as Middle East Respiratory Syndrome (MERS-COV) and Severe Acute Respiratory Syndrome (SARS-COV). The Coronavirus Disease 2019 (COVID-19) refers to the cluster of viral pneumonia cases which first started occurring in Wuhan city, which has a population of 11 million people and is the largest city in Hubei province in central China, since December 2019. On Tuesday, the 11<sup>th</sup> of February 2020, the WHO officially named the disease caused by the new coronavirus "COVID-19", with more than 43,000 patients, and more than 1,000 deaths cases were reported in China. The Government of Israel, the Prime Minister's Office in collaboration with the Ministry of Health, the Ministry of Defense and the Treasury, have decided to take early first steps to prevent the spread of the virus in the Country. The first step was banning Chinese tourists from entering the country via Ben-Gurion International Airport, and this was only the beginning, as afterwards the decision was made to close all border crossings. The idea was to reduce the number of entrances to the State of Israel as much as possible, and every citizen coming back from countries such as China and European countries was directly sent to home quarantine for a period of 14 days.

## Coronaviruses

Coronaviruses are a large family of viruses that cause illnesses ranging from the common cold to more severe diseases, such as Middle East Respiratory Syndrome (MERS-COV) and Severe Acute Respiratory Syndrome (SARS-COV). They are transmitted between animals and humans, with SARS-COV transmitted from civet cats to humans and MERS-COV from camels to humans [1].

## The novel coronavirus 2019 (COVID-19)

COVID-19 refers to the cluster of viral pneumonia cases which first occurred in Wuhan city in December 2019, the largest city in Hubei province in central China with a population of 11 million people. According to investigations conducted by the Mainland health authorities, the novel coronavirus was found to be the causative agent [2]. COVID-19

is genetically related to SARS-COV, which caused a global epidemic with 8,096 confirmed cases in more than 25 countries in 2002–2003 [3].

Initially, 27 cases were reported on 31<sup>st</sup> December 2019. The patients were identified by local hospitals using a surveillance mechanism for “pneumonia of unknown aetiology” that was established in the wake of the 2003 SARS outbreak to allow timely identification of novel pathogens, such as 2019-nCoV. Recently, infections have been identified in other Chinese cities and more than a dozen countries around the world [4]. On 11<sup>th</sup> January 2020, the number increased to 41, with seven severe cases and one death. The geographical origin of the spread of the virus was linked to the Huanan Seafood Wholesale Market, which was subsequently reported by journalists to be selling freshly slaughtered game animals [5]. In addition to seafood, the market also sold live cats, dogs, snakes and marmots. A notice posted outside the Huanan Seafood Market said that according to regulations for public health emergencies, the Wuhan Municipal Health Commission’s Hanjiang District Bureau had decided to suspend the seafood market’s operations to improve its environment. On Tuesday 14<sup>th</sup> of that month, videos uploaded to the internet showed masked, white-clad medical workers spraying sanitiser in the market [6]. On the 20<sup>th</sup> January 2020, 282 laboratory-confirmed human cases were reported, with confirmed cases in travellers from Wuhan announced on the 13<sup>th</sup> and 17<sup>th</sup> January in Thailand, on the 15<sup>th</sup> January in Japan, and on 19<sup>th</sup> January in South Korea [7]. As of 10<sup>th</sup> March 2020, 72,314 cases reviewed by the Chinese Center for Disease Control and Prevention showed that less than 1% were in children younger than 10 years [8].

### Symptoms

The symptoms of coronavirus infection are similar to those of the common flu, typically appearing 2–14 days after exposure to the virus [9]:

- › Fever,
- › Cough,
- › Shortness of breath.

The virus can lead to severe pneumonia and severe respiratory symptoms, kidney failure and death.

### The spread of COVID-19

SARS-CoV-2 can spread from person to person, with the virus transmitted between people

who are in close contact, within about six feet, through respiratory droplets produced when an infected person coughs or sneezes. Additionally, it can spread when a person comes into contact with infected surfaces or objects contaminated by the virus, then touches their mouth, nose, or eyes [10].

Fortunately, SARS-CoV-2 is highly sensitive to all common cleaning and disinfecting agents, so increasing the frequency of cleaning using disinfectant, including hand sanitisers, is effective in combating the virus. There is no specific protocol for cleaning to eradicate the coronavirus, but the Centers for Diseases Control and Prevention issued guidelines for the daily cleaning of surfaces, especially those touched by people with suspected or confirmed coronavirus disease, recommending that high-touch surfaces are disinfected on a daily basis [11].

### Coronavirus pandemic

On Thursday 11<sup>th</sup> February 2020, WHO officially named the disease caused by the new coronavirus “COVID-19”. On that day, the number of reported cases was over 43,000 patients, with more than 1,000 deaths. Most of the patients diagnosed were from China, only 400 cases from other countries. Only one day later, the number of patients escalated sharply, reaching over sixty thousand, with 1,300 deaths, all from China, except for one death recorded outside China.

This novel coronavirus continued to spread globally, with 219 patients identified on the Diamond Princess cruise ship at Yokohama port near Tokyo, Japan on Thursday 13<sup>th</sup> February [12]. Among the passengers, 16 were Israeli civilians, three of them were diagnosed with coronavirus. These three patients had mild symptoms but were transferred to a hospital in Japan for further treatment. The Israeli Ministry of Foreign Affairs and the Israeli Ministry of Health began to take steps to return the citizens to Israel to continue their follow up. On 19<sup>th</sup> February 2020, the siege on the Diamond Princess cruise ship ended, with a total of 621 cases of coronavirus and six deaths [12]. The uninfected Israeli citizens were flown to Israel, where they were immediately transferred to home to quarantine for a period of 14 days [13]. One day after the arrival of the uninfected Israeli citizens, the Israeli Ministry of Health imposed strict guidelines on quarantine and banning tour-

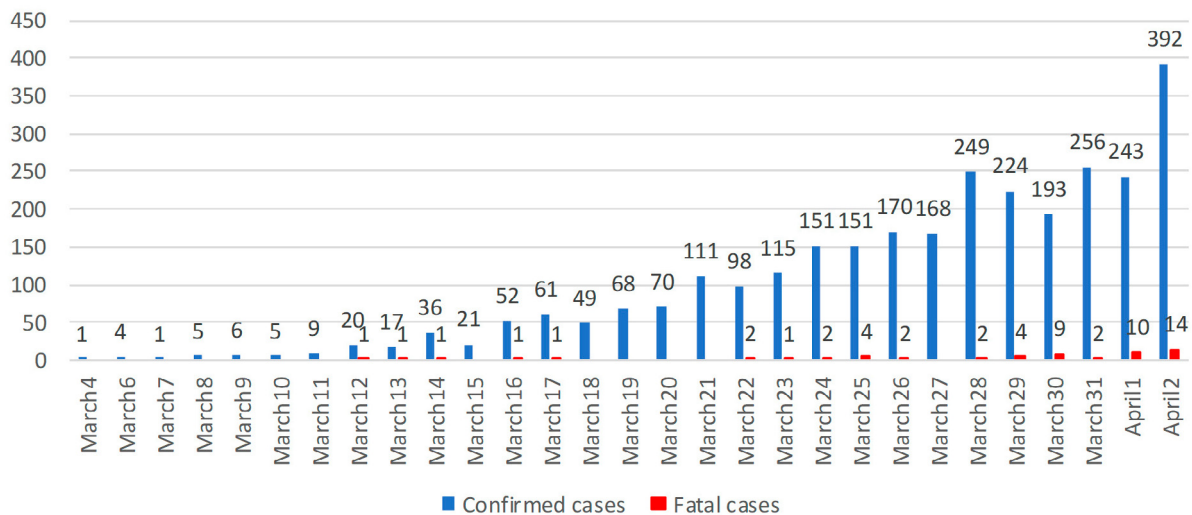


**Figure 1.** Number of new COVID-19 cases confirmed in Poland as of April 2, 2020. [18]

ists, with any Israeli citizen returning from South Korea and Japan to stay in home quarantine for 14 days. The Israeli Ministry of Foreign Affairs issued a travel warning to these countries, in addition to Thailand [13].

Towards the end of February, the largest outbreaks outside China were reported in South Korea, with more than 200 cases reported on 21<sup>st</sup> February. One day later, the number of cases in South Korea continued to escalate, 430 cases of coronavirus were identified and according to the WHO daily update, 77,809 cases and 2,372 deaths in 31 countries were reported. In the period from the 8<sup>th</sup> until the 18<sup>th</sup> February 2020, a group of nine tourists from South Korea visited the State of Israel and were diagnosed with coronavirus immediately after returning to their country. The Israeli Ministry of Health issued a warning to all people who came into contact with those tourists. Additionally, the Ministry of Health published a map showing the locations that these tourists visited, with 30 high school students who were in one of the locations visited by the tourists immediately sent to home quarantine for 14 days.

Despite its global spread, the WHO did not rush to declare coronavirus as a global pandemic. On Monday 25<sup>th</sup> of February, and according to Italian reports, the number of coronavirus cases in Italy was 2,019 with six deaths, which made it the most serious outbreak in Europe. Israel issued a travel warning to Israeli citizens travelling to Italy, especially the northern district, with anyone returning

from Italy being immediately sent to home quarantine for 14 days [13].

In Israel, the first coronavirus case was reported in a citizen who returned from the Diamond Princess cruise ship, which increased to four cases, and the patient was placed in home isolation. Simultaneously, global news channels, including Iran, Oman, Iraq, Kuwait, Afghanistan and Bahrain, continued to report the vast spread of the virus [13]. In response, the Israeli Ministry of Health issued another travel warning to European countries and all countries of the world in general. Citizens were advised to avoid trips to conferences and gatherings in which large numbers of people from different countries came together, as well as avoiding and cancelling any international conferences in Israel. On that same day (February 25<sup>th</sup>), it was reported that one Israeli citizen who was infected on the cruise ship and hospitalised in Japan had fully recovered from the virus and had returned to Israel. The rest of Israeli citizens in Japan were also in good shape and were later released on 28<sup>th</sup> February [13].

On Tuesday 25<sup>th</sup> February 2020, there were reports of the virus spread to other countries, including Croatia, Switzerland, Vietnam, Spain, Austria, Denmark and Estonia. The second Israeli citizen with coronavirus arrived from northern Italy and on that day, the number of infected people globally rose to 80,377 with 2,707 deaths. Israeli flight companies stopped all flights to Tokyo, Italy, Thailand and Hong Kong. As the virus con-

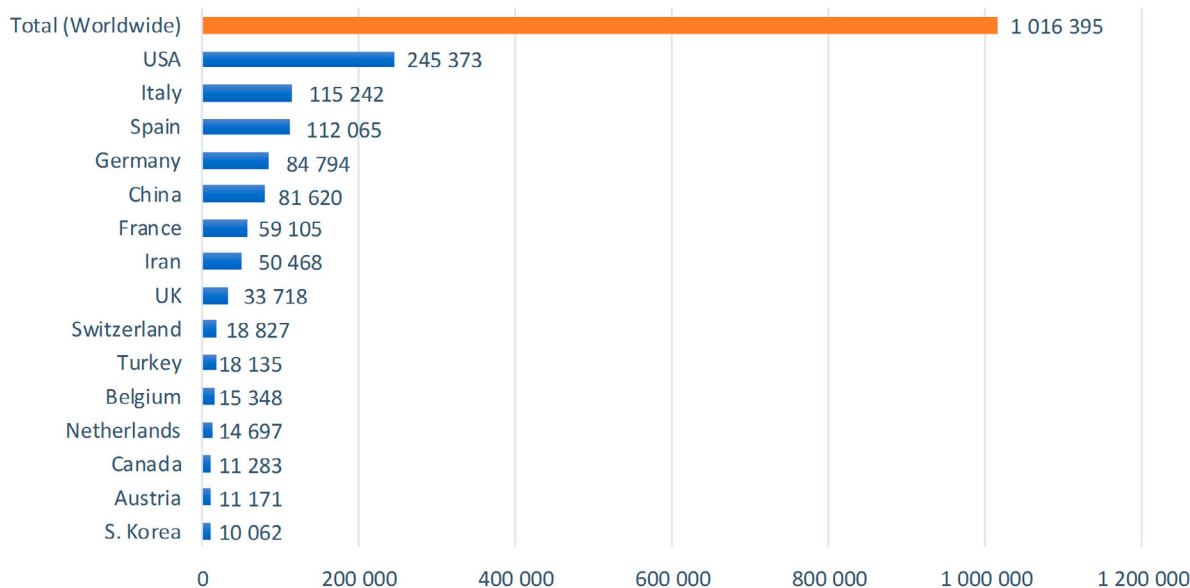


**Figure 2.** Number of new COVID-19 cases worldwide as of April 3, 2020, by country. [19]

tinued to spread to 59 countries, new cases were reported in seven other countries, Azerbaijan, Belarus, Lithuania, Iceland, Mexico, New-Zeeland and Nigeria. In the Middle East, Iran had the most serious outbreak, whereas Italy was the most seriously affected in Europe.

On 26<sup>th</sup> February 2020, there were seven cases of coronavirus in Israel, three infected from the Diamond Princess cruise ship, three others who returned from Italy, and one case (wife of one of the patients) that were infected in the country. The Israeli Ministry of Health imposed stricter instructions and published a list of places in which patients were to stay from the moment of their return to Israel until the onset of symptoms. Furthermore, the Ministry of Health warned that anyone close to the patients (about 2 metres away from the patients), or those who had been in the same area as the patients for 15 minutes, must stay in home quarantine and report immediately to the National Emergency Service, the Magen-David Adom (MDA). If within 14 days of contact with a diagnosed patient, an individual developed signs of fever of 38 degrees or over, cough, difficulty breathing or other respiratory symptoms appears, then they must call the MDA and not go to any clinics or hospitals.

On Tuesday 3<sup>rd</sup> March 2020, the Israeli Ministry of Health continued to issue travel warnings to various countries around the world, any per-

son returning from Spain, Switzerland, France and Austria were ordered to stay in home quarantine for 14 days. People who returned from other countries were instructed not to attend any public events. The Ministry of Health published instructions for maintaining personal hygiene, making sure to wash hands with soap and alcohol and to avoid shaking hands [13]. Coronavirus continued to spread and on Sunday 8<sup>th</sup> March 2020, there were 107,933 infected patients with 3,664 deaths documented in at least 104 countries [13]. Sixteen days after the virus outbreak in Italy, which was the most affected country in Europe, there were 6,000 cases of coronavirus, 570 of whom were seriously ill. The Italian government decided to take an unusual emergency measure and imposed full closure in the northern part of the country in an effort to reduce the spread of the virus. The closure affected around 16 million Italians living in the 14 counties in the north of Italy and included schools, universities, museums, cultural centres and sports events [13].

In the Palestinian Territories, the authorities decided to ban foreign tourists for two weeks and to close churches and mosques in Bethlehem after 19 cases of COVID-19 were diagnosed. In addition, 13 Americans tourists were placed in isolation at a hotel in Bethlehem city. With the evolving spread of the virus worldwide, the Israeli Ministry of Health continued to issue more instructions, any citizen

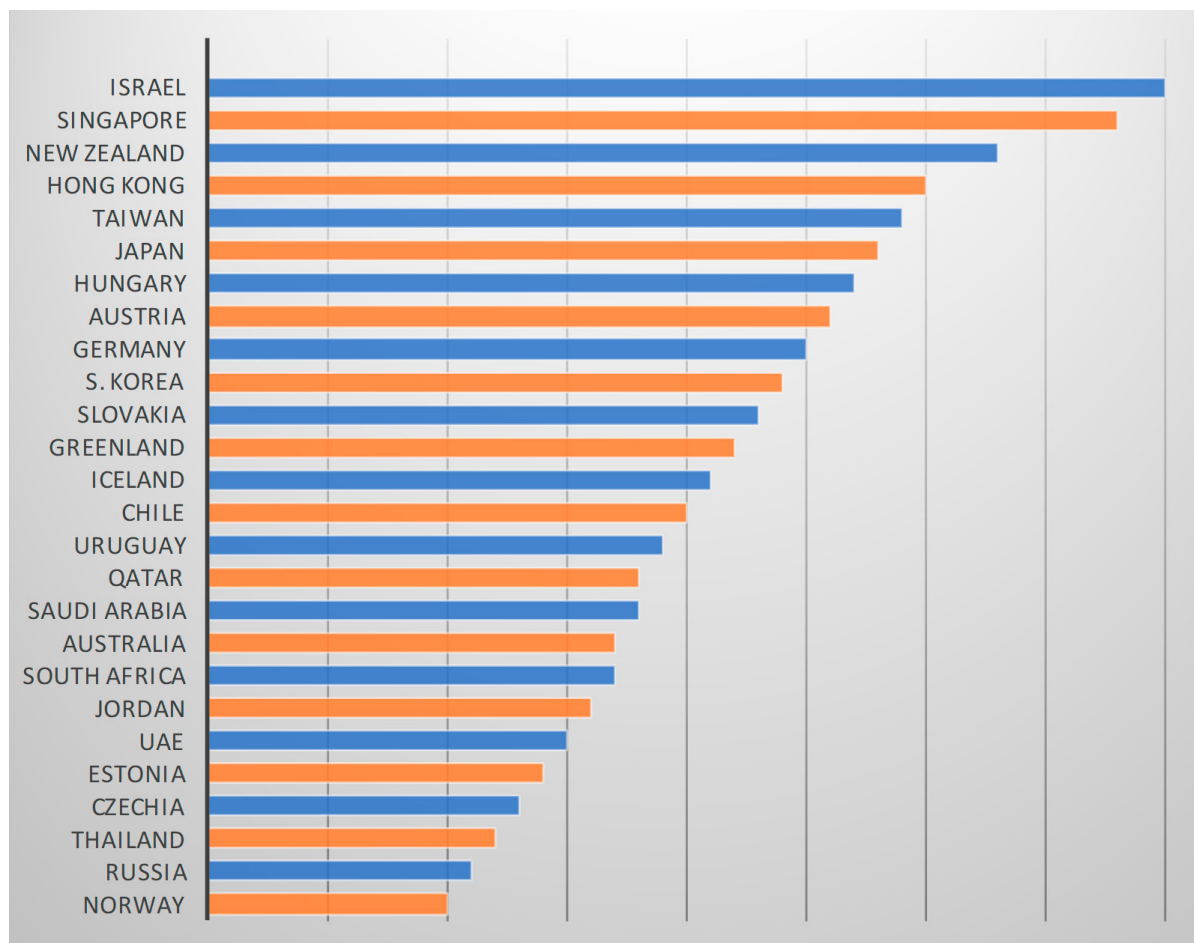


**Figure 3.** Coronavirus health Safety Country Ranking 2 April 2020, by country [26]

who returned from Australia or Taiwan with signs of a sore throat, cough, or fever were required to be immediately checked by the Emergency Response Services of MDA located in an incoming passenger lane of the transit hall at Tel-Aviv International Airport "Ben-Gurion". Moreover, Israel closed its land borders with Egypt, and the international flights terminal, Terminal 1, at Ben-Gurion Airport was also closed to all international flights [13]. The Israeli Ministry of National Security announced that it was considering declaring a national state of emergency to give the police additional authority to close certain areas as the virus continued to spread. The Israeli Prime Minister Benjamin-Netanyahu and US Vice president Mike Pence discussed the imposition of a potential closure order for people arriving in Israel from several destinations in the USA.

On Wednesday 11<sup>th</sup> March 2020, WHO announced the COVID-19 outbreak as a global pandemic, the first time since the announcement of the H1N1 pandemic in 2009. On that day, the Israeli Ministry of Health updated the number of corona

patients in Israel to 77, including a nine-year-old child. A total of 465 elementary school students from south Tel-Aviv and about 50 educators and school staff were placed in home quarantine after being in contact with the nine-year-old student who was diagnosed with the novel coronavirus [13]. The Israeli Ministry of Health continued publishing new guidelines for Israeli citizens, including banning any gathering of more than 50 people, such as wedding ceremonies, crowds at sports events, as well as shopping malls and stores.

In Israel, the updated number of individuals diagnosed with COVID-19 by the 13<sup>th</sup> March increased to 126, with 949 doctors in quarantine and unable to work, as well as 635 nurses and 171 paramedics also in solitary confinement. Some were exposed to patients with symptoms as part of their work, so also likely to become ill. The decision was made to close most of the educational system as a preventive measure [13].

As of the 19<sup>th</sup> March 2020, the total number of people diagnosed with COVID-19 globally

reached 220,229, with 9,000 deaths and 85,769 people who had recovered. In Israel, the number of coronavirus patients was 529, with 14 who had recovered from the illness. On the morning of 22<sup>nd</sup> March 2020, Palestinian and Israeli news channels reported the first two cases of COVID-19 in the Gaza Strip, people who had arrived from Pakistan and tested positive for COVID-19. In the Palestinian Territories, the total number of infected people reached 59 in both the West Bank and Gaza Strip according to official Palestinian Authority reports [14]. Globally, there was a rise in numbers diagnosed in Italy, Spain, the United States, Iran, France, Germany, Switzerland and the United Kingdom, with the virus spreading to other countries including Papua New Guinea and East Timor in the Pacific, as well as countries in several regions of Africa, Niger, Eritrea, Uganda, Fun Verde, Angola and Madagascar [13].

In Poland, the first confirmed case of COVID-19 was reported by Poland's Minister of Health on Wednesday 4<sup>th</sup> March 2020 [15], after which, cases were confirmed in seven other voivodeships throughout Poland during the period from the 5<sup>th</sup> to the 9<sup>th</sup> March 2020 [16]. Upon the emergence of these cases, Poland's Prime Minister announced some new restrictions and decisions, the major decisions included [17]:

- › Imposing a limit on the number of people allowed inside a store, up to three people per cash desk. At marketplaces, the limit of people allowed was three customers per sales point, and in post offices, two people per window.
- › From 10:00 to 12:00, stores and service points were allowed to receive and serve only people over 65 (in the remaining time, shops and service points were available to everyone, including seniors).
- › All customers must shop while wearing disposable gloves.
- › Large-space construction stores will be closed during weekends.
- › Pedestrians are to maintain a distance of at least two metres between one another. This also applies to families and relatives, except for children under 13 years of age and people with disabilities or those who are unable to move independently.
- › Children and adolescents under 18 years of age were not allowed to leave their homes unattended.

- › As of the 1<sup>st</sup> of April 2020, all household members living with a person who was quarantined was automatically quarantined.
- › Parks, beaches and boulevards were out of bounds, with city bike rental stores closed.
- › Hotels and other accommodation places, in addition to beauty and hair salons, were closed.
- › Rehabilitation treatments and massages were suspended, both in public and private facilities, except cases when rehabilitation was absolutely necessary.
- › A distance of one and a half metres should be maintained in the workplaces. Additionally, disinfectants should be provided in all workplaces.
- › The passenger seat limit also applied to private carriers.
- › Any person violating the above regulations was subject to a fine ranging from PLN 5,000 to PLN 30,000.

As of the 2<sup>nd</sup> 2020, 392 new cases of COVID-19 were confirmed in Poland, thus, the total number of cases in the country since 4<sup>th</sup> March 2020 increased to 2,946 (2,889 active cases), with over 48 thousand people under epidemiological supervision. According to the Minister of Health, 57 infected patients died, all of whom had underlying health conditions [18].

## The Israeli experience

The Government of Israel, the Prime Minister's Office in collaboration with the Ministry of Health, the Ministry of Defence and the Treasury decided to take early steps compared to other countries around the world to prevent the spread of coronavirus. The first step was preventing Chinese tourists from entering the country via Ben-Gurion International Airport, followed by full closure of all borders to reduce the number of entrances to Israel as much as possible. In addition, every citizen who returned to Israel from countries, such as China and Europe, were sent straight home to quarantine for a period of 14 days. Even before the first cases of COVID-19 were identified in Israel, Israeli authorities took preventive measures to prevent its spread. On 23<sup>rd</sup> January 2020, the Ministry of Health issued guidelines and information in case a person

developed any symptoms related to the disease and instructions on how to deal with such person to protect other individuals in close contact and how to protect medical staff. According to the orders of the Ministry of Health, anyone who had spent the previous two weeks in Wuhan city, China, or had been in contact with a person who was there and develops symptoms of the disease (fever, cough, pneumonia) was required to go to the closest hospital for medical examination. Suspected cases were to be placed in isolation on admission to the medical centre, with all healthcare staff working according to defined protocols to protect them against infection, and were to undergo all types of virus tests. All samples were sent to the Central Laboratory of the Ministry of Health, located in Sheba Tel-Hashomer Medical Center (located near Tel-Aviv), where the lab staff could identify the virus [20].

#### **Actions taken before the border was closed**

In all border crossings, information sheets and instructions were posted in different languages (Hebrew, Arabic, Chinese and English) detailing the guidelines for those coming from China. If any passenger reported fever or respiratory symptoms within two weeks prior to their arrival from China or upon arrival, then they were required to contact the first emergency response MDA (the Israeli first emergency response) [21]. Special workstations were installed and staffed in collaboration with the MDA in the transit hall at Ben-Gurion International Airport in Tel-Aviv, and equipped with a special space for isolation before sending a passenger suspected of infection to a hospital emergency room. In the case of a passenger reporting fever or respiratory symptoms while at the airport, the passenger was directed to the MDA station, which included an isolation compound. The MDA continually applied protective measures in accordance with the protocol and guidelines for coping with the SARS-CoV-2 virus outbreak. Upon the arrival of a suspected passenger, MDA staff provided the passenger with a face mask that they must wear, and measured their body temperature measurement. In the event of an emergency evacuation, MDA then transferred the passenger to the hospital in an ambulance containing special isolation equipment in accordance with the protocols of the

Israeli Ministry of Health and in cooperation with the hospital to receive the patient.

#### **Home isolation**

The Israeli Ministry of Health instructed those returning to the State of Israel from Austria, Italy, Germany, Hong Kong, Japan, Macau, China, Singapore, Spain, France, South Korea, Switzerland and Thailand, or those who have been in close contact with a COVID-19 patient (close contact is defined as a staying less than 2 metres far from a patient for 15 minutes) to stay in home quarantine for a period of 14 days from the date of their departure from these locations. Those who were instructed to go into home quarantine were forbidden from going to public places, educational institutions (universities or schools), workplaces, public transportation, recreational and shopping places, hospitals and clinics [22].

The Ministry of Health published a self-report method which could be completed as follows:

- › Reporting using the "Self-Reporting Form on Home Isolation" (electronic form found on the Ministry of Health's website).
- › Reporting using the "Form for those who came in contact with a patient" (electronic form).
- › Through the dedicated call centre using the number published by the Ministry of Health on its website.

Absence from work was considered as absence due to illness. If no signs of illness appeared, the quarantine ended on the 15<sup>th</sup> day and individuals could return to work and normal activities. The purpose of the home quarantine was to stop the infection and prevent the spread of the virus in the State of Israel. To do so, every citizen in solitary confinement was required to refrain from conducting any activity or being in public places as well as to ensure the protection of the rest of their family members with they lived with.

In case a citizen developed a fever of over 38 degrees, cough, difficulty in breathing or other respiratory symptoms within 14 days of returning from one of the high-risk destinations, or after close contact with a verified patient, the citizen should call the first emergency response services "MDA" [17]. In this case, the citizen should refrain from attending any hospital clinics and if necessary, a paramedic will be sent to the patient to perform laboratory tests at home (patient's home).



### Guidelines for home isolation issued by the Israeli Ministry of Health [23]

On the 19<sup>th</sup> March 2020, the State of Israel declared a state of emergency and took significant steps to combat the coronavirus outbreak, including disabling transportation lines, closing all educational institutions, including kindergartens, leisure and recreational sites in addition to any non-essential spaces. In his dramatic statement made on that day, the Israeli Prime Minister announced that the government would use the technology used in its war against terrorist organisations to locate corona patients across the state; the courts had approved the use of the technology and the tracking of all citizens of the State of Israel. From the day of infection and the onset of symptoms, the technology would text messages to the phone of any person who had been in contact with a COVID-19 patient, the content of the message was that the recipient of the message must stay in home quarantine for a period of 14 days, also providing some information regarding the disease and its symptoms, including vital phone numbers for the Ministry of Health. This technology was put into use as of Wednesday 18<sup>th</sup> of March, and according to the Israeli news channels, citizens were already receiving messages on their cell phones. Thus, even those who do not obey instructions, the technology would follow every citizen who violates the isolation or quarantine instructions.

As emergency measures, the Israeli Prime Minister's Office issued the following emergency guidelines for Israeli citizens [24]:

- › A person in home isolation should not be allowed to leave home except for transfer to a hospital.
- › The person should stay in a separate, well-ventilated room with a closed door, exiting the room when necessary and for a brief time only. When leaving the room, the person must cover their mouth and nose using a face mask.
- › The entry of other people into the isolation room should be reduced, with priority to one healthy person without a background of disease that can increase the risk of infection.
- › Health-workers should wear face masks and a full suit that includes gloves when contacting anyone in isolation. Contact with body fluids should be avoided, especially oral secre-

tions, airway secretions, urine and faeces of the person in isolation.

- › The laundry of the individual in isolation shall be placed in a dedicated bag in the isolation room until the date of washing the laundry. Any disposable products should be disposed of in a designated bag in the room until the time of disposal for external garbage.
- › Avoid co-using any items used or accessed by the infected person.
- › Reduce presence in public space: citizens cannot leave their home except for one of the following purposes: work, equipping food or medicine, for medical treatment, blood donation, demonstration, sports activity maximum two persons, attending wedding or funeral, helping a person with a medical condition.
- › Rules and behaviour in public places: maintain a distance of two metres between one person and the other, while driving a maximum of two passengers in the same car.
- › Delivery services: shipment must be placed near the home door.
- › Restrict trading activity: the following business locations/stores shall not operate: malls or any shopping centre containing over ten stores, nightclubs, bars, wedding venues, swimming pools, water parks, zoos, safaris, bathhouses, cinemas, museums and all cultural institutions, any business that do not provide medical treatment, national parks, and tourist attractions.
- › Restaurants: only for take away services.
- › Pharmacies: customers must maintain the recommended distance between each other (2 metres). The maximum number of customers inside a store at any given time should be four customers only.

As of the 2<sup>nd</sup> April 2020, the total number of confirmed COVID-19 cases in Israel increased to 6,211, with a total of 31 deaths. The Israeli Health Minister, Jacob Litzman, and his wife were diagnosed with COVID-19. The Ministry of Health instructed all Israeli citizens to wear protective face masks when leaving home. The number of people diagnosed globally was 976,249. As in recent days, the United States continued to lead the number of infections with approximately 215,000 people, followed by Italy and Spain. The global death toll was 50,000 people, and the number of recovered cases was 195,000

[13]. Despite the increase in the number of Israeli citizens infected with COVID-19, following the instructions of the Israeli Ministry of Health and the Government, Israel was ranked in first place in the COVID-19 Health Safety Countries Ranking on the Deep Knowledge Group Website [25].

## Summary

Up to the date of writing of this article, COVID-19 continues to spread to more countries worldwide, with an increasing number of people infected and rising death toll. There has been global panic, also affecting the stock markets, causing the worst economic losses in 30 years.

The first steps taken in the State of Israel were appropriate, their purpose was only to prevent the spread of the virus among the citizens of the country. The Israeli government was aware that COVID-19 was about to spread to Israel and the Israeli Ministry of Health issued a statement even before the first case was identified noting that "the spread of the virus in the State of Israel is only a matter of time."

Many countries are racing against time to develop a cure and a vaccine for the virus. Meanwhile, the virus will disappear with the arrival of spring and the increased temperature, but scientists believe that there will be a second wave next autumn when the virus will reappear.

## Acknowledgements

### Conflict of interest statement

The authors declare no conflict of interest.

### Funding sources

There are no sources of funding to declare.

## References

1. Coronavirus. <https://www.who.int/health-topics/coronavirus>. Accessed 2020 March 6.
2. Coronavirus Disease 2019 (COVID-19). [https://www.chp.gov.hk/files/pdf/severe\\_respiratory\\_disease\\_leaflet\\_en.pdf](https://www.chp.gov.hk/files/pdf/severe_respiratory_disease_leaflet_en.pdf). Accessed 2020 March 4.
3. Zou L, Ruan F, Huang M, Liang L, Huang H, Hong Z, Yu J, Kang M, Song Y, Xia J, Guo Q, Song T, He J, Yen H, Peiris M, Wu J. SARS-CoV-2 Viral Load in Upper Respiratory Specimens of Infected Patients. *New England Journal of Medicine*. 2020 03 19;382(12):1177-1179. <https://doi.org/10.1056/nejmc2001737>
4. Li Q, Guan X, Wu P, Wang X, Zhou L, Tong Y, Ren R, Leung KS, Lau EH, Wong JY, Xing X, Xiang N, Wu Y, Li C, Chen Q, Li D, Liu T, Zhao J, Liu M, Tu W, Chen C, Jin L, Yang R, Wang Q, Zhou S, Wang R, Liu H, Luo Y, Liu Y, Shao G, Li H, Tao Z, Yang Y, Deng Z, Liu B, Ma Z, Zhang Y, Shi G, Lam TT, Wu JT, Gao GF, Cowling BJ, Yang B, Leung GM, Feng Z. Early Transmission Dynamics in Wuhan, China, of Novel Coronavirus-Infected Pneumonia. *New England Journal of Medicine*. 2020 03 26;382(13):1199-1207. <https://doi.org/10.1056/nejmoa2001316>
5. Chan JF, Yuan S, Kok K, To KK, Chu H, Yang J, Xing F, Liu J, Yip CC, Poon RW, Tsoi H, Lo SK, Chan K, Poon VK, Chan W, Ip JD, Cai J, Cheng VC, Chen H, Hui CK, Yuen K. A familial cluster of pneumonia associated with the 2019 novel coronavirus indicating person-to-person transmission: a study of a family cluster. *The Lancet*. 2020 02;395(10223):514-523. [https://doi.org/10.1016/s0140-6736\(20\)30154-9](https://doi.org/10.1016/s0140-6736(20)30154-9)
6. Juan D. Wuhan wet market closes amid pneumonia outbreak. <https://www.chinadaily.com.cn/a/202001/01/WS5e0c6a49a310cf3e35581e30.html>. Accessed 2020 January 1.
7. Corman VM, Landt O, Kaiser M, Molenkamp R, Meijer A, Chu DK, Bleicker T, Brünink S, Schneider J, Schmidt ML, Mulders DG, Haagmans BL, van der Veer B, van den Brink S, Wijsman L, Goderski G, Romette J, Ellis J, Zambon M, Peiris M, Goossens H, Reusken C, Koopmans MP, Drosten C. Detection of 2019 novel coronavirus (2019-nCoV) by real-time RT-PCR. *Eurosurveillance*. 2020 01 23;25(3). <https://doi.org/10.2807/1560-7917.es.2020.25.3.2000045>
8. Lu X, Zhang L, Du H, Zhang J, Li YY, Qu J, Zhang W, Wang Y, Bao S, Li Y, Wu C, Liu H, Liu D, Shao J, Peng X, Yang Y, Liu Z, Xiang Y, Zhang F, Silva RM, Pinkerton KE, Shen K, Xiao H, Xu S, Wong GW. SARS-CoV-2 Infection in Children. *New England Journal of Medicine*. 2020 04 23;382(17):1663-1665. <https://doi.org/10.1056/nejmc2005073>
9. Coronavirus disease 2019 (COVID-19). <https://www.cdc.gov/coronavirus/2019-ncov/symptoms-testing/symptoms.html>. Accessed 2020 March 13.
10. Coronavirus disease (COVID-19). How COVID-19 spreads. <https://www.cdc.gov/coronavirus/2019-ncov/about/transmission.html>. Accessed 2020 March 4.
11. Knight V, Heredia CH. Planes, Trains and Automobiles: What does a deep clean mean?. *Scientific American*. 2020 Mar 17;
12. Pleasance C. Half of the infected coronavirus passengers on board Diamond Princess cruise ship had NO symptoms. <https://www.dailymail.co.uk/news/article-8109829/Half-infected-coronavirus-passengers-board-Diamond-Princess-cruise-ship-NO-symptoms.html>. Accessed 2020 March 13.
13. Coronavirus outbreak. <https://davidson.weizmann.ac.il/online/sciencenews/תוצרפתה-הנורוקה-מינוכד-הנורוקה-מינורו>. Accessed 2020 March 31.
14. Palestinian PM Orders West Bank Lockdown; More Than 1,000 Coronavirus Cases in Israel. <https://www.haaretz.com/israel-news/dozens-of-new-york-hasidic-jews-in-coronavirus-quarantine-after-arriving-in-israel-1.8689682>. Accessed 2020 March 22.

15. Poland Reports First Coronavirus Case - Health Minister. <https://www.usnews.com/news/world/articles/2020-03-04/poland-reports-first-coronavirus-case-health-minister>. Accessed 2020 April 3.
16. Pacjentka "nie była za granicą, nie miała kontaktu z osobą z podejrzeniem lub rozpoznaniem" zakażenia. <https://tvn24.pl/polska/koronawirus-w-polsce-nowe-przypadki-zakazenia-4328168>. Accessed 2020 March 9.
17. Prime Minister: We must maintain social distancing for the sake of the fight against the coronavirus. <https://www.premier.gov.pl/en/news/news/prime-minister-we-must-maintain-social-distancing-for-the-sake-of-the-fight-against-the.html>. Accessed 2020 March 31.
18. Number of new Coronavirus (COVID-19) cases confirmed in Poland in 2020, by date of report. <https://www.statista.com/statistics/1102374/poland-coronavirus-covid-19-new-cases-by-report/>. Accessed 2020 April 2.
19. Number of coronavirus (COVID-19) cases worldwide as of May 28, 2020, by country. <https://www.statista.com/statistics/1043366/novel-coronavirus-2019-ncov-cases-worldwide-by-country/>. Accessed 2020 April 3.
20. Ministry of Health: Guidelines for the Suspicion of Chinese Virus Issues. <https://www.ynet.co.il/articles/0,7340,L-5664783,00.html>. Accessed 2020 January 23.
21. Cross-border Protocol - Coping with the coronavirus's new disease. [https://www.health.gov.il/Subjects/disease/corona/Documents/coronavirus\\_med\\_guidelines.pdf](https://www.health.gov.il/Subjects/disease/corona/Documents/coronavirus_med_guidelines.pdf). Accessed 2020 January 30.
22. The new novel coronavirus. <https://www.health.gov.il/Subjects/disease/corona/Pages/default.aspx>. Accessed 2020 March 4.
23. Home Insulation Guidelines. [https://www.health.gov.il/Subjects/disease/corona/Pages/default.aspx?2702-9#home\\_quarantine\\_guidance](https://www.health.gov.il/Subjects/disease/corona/Pages/default.aspx?2702-9#home_quarantine_guidance). Accessed 2020 February 1.
24. Emergency regulations (new novel coronavirus-activity restrictions). [https://www.gov.il/he/General/corona\\_official](https://www.gov.il/he/General/corona_official). Accessed 2020 March 20.
25. Israel Ranked 1<sup>st</sup> in the Covid-19 Health Safety Countries Ranking on the Deep Knowledge Group Website. [https://www.gov.il/en/departments/news/spoke\\_ranking310320](https://www.gov.il/en/departments/news/spoke_ranking310320). Accessed 2020 March 31.
26. Coronavirus Health Safety Countries Ranking. Coronavirus Health Safety Countries Ranking. Accessed 2020 April 2.

# Monitoring the skin NADH changes during ischaemia and reperfusion in humans

Jan Niziński

Department of Cardiology-Intensive Therapy,  
Poznan University of Medical Sciences, Poland

 <https://orcid.org/0000-0002-5455-3845>

Lukasz Kamieniarz

University College London, London, United Kingdom

 <https://orcid.org/0000-0002-8427-9568>

Piotr Filberek

Department of Cardiology-Intensive Therapy,  
Poznan University of Medical Sciences, Poland

 <https://orcid.org/0000-0001-7575-8084>

Greta Sibrecht

Department of Cardiology-Intensive Therapy,  
Poznan University of Medical Sciences, Poland

 <https://orcid.org/0000-0002-8905-7921>

Przemysław Guzik

Department of Cardiology-Intensive Therapy,  
Poznan University of Medical Sciences, Poland

 <http://orcid.org/0000-0001-9052-5027>

Corresponding author: [pguzik@ptkardio.pl](mailto:pguzik@ptkardio.pl)

 DOI: <https://doi.org/10.20883/medical.405>

**Keywords:** 460-nm fluorescence, ischaemia, microcirculation, mitochondria, nicotinamide adenine dinucleotide, reperfusion

**Published:** 2020-01-31

**How to Cite:** Niziński J, Kamieniarz L, Filberek P, Sibrecht G, Guzik P. Monitoring the skin NADH changes during ischaemia and reperfusion in humans. *JMS [Internet]*. 2020 Mar 31;89(1):e405. doi:10.20883/medical.405



© 2020 by the author(s). This is an open access article distributed under the terms and conditions of the Creative Commons Attribution (CC BY-NC) licence. Published by Poznan University of Medical Sciences

## ABSTRACT

Nicotinamide adenine dinucleotide (NADH/NAD<sup>+</sup>) is involved in many important biochemical reactions in human metabolism, including participation in energy production by mitochondria. Flow Mediated Skin Fluorescence (FMSF) is a non-invasive method to study dynamic changes in the content of the reduced form of NADH by measuring the optical properties of NADH related to the emission of the autofluorescent light (460 nm) after an earlier excitation by ultraviolet light. This review summarises the available studies using this method to describe its potential and limitations.

## Introduction

Nicotinamide adenine dinucleotide (NADH/NAD<sup>+</sup>) is the most important cofactor involved in energy metabolism in live human cells. NADH/NAD<sup>+</sup> participates in glycolysis, the citric acid cycle and the mitochondrial respiratory chain, beta-oxidation, reduction of pyruvate to lactate, as well as the modification of RNA together with regulation of transcription. It is also a part of the second messenger system [1,2]. Some examples of NADH involvement in cellular metabolism are pictured in Figure 1.

Nicotinamide adenine dinucleotide exists in two forms: reduced NADH and oxidised NAD<sup>+</sup>. Both are found in the cytosol, cellular organelles, nucleus and the mitochondria [3]. However, the main site of NADH oxidation to NAD<sup>+</sup> are the mitochondria. The architecture of a mitochondrion is outlined in Figure 1: an intermembrane space separates the outer and inner membranes and the mitochondrial matrix with the electron transport chain and genome are contained within said inner membrane [4].

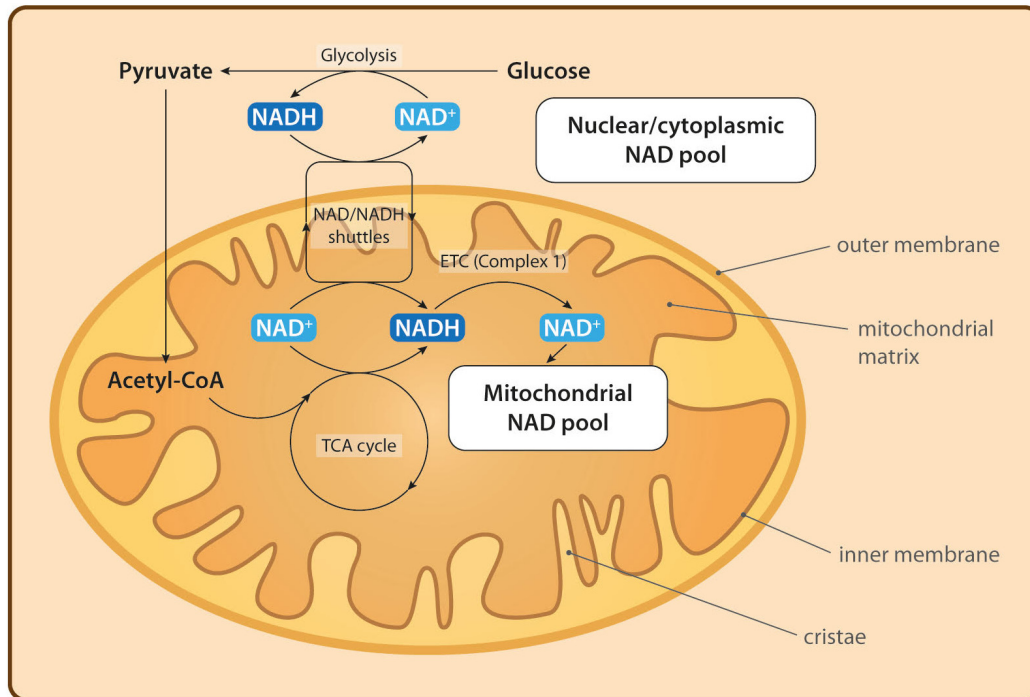


**Figure 1.** Metabolic pathways of NADH in cytosol and mitochondria. Abbreviations: ETC – electron transport chain; TCA cycle – tricarboxylic acid cycle

The intermembrane space is critical for storing protons involved in ATP production and both creatine kinase and adenine kinase are localised there. Both the outer and inner membranes are impermeable to most metabolites, including NADH. As NADH cannot cross the mitochondrial membranes, the transportation of high energy electrons from this molecule to the electron transport chain involves special reducing equivalents. The malate-aspartate and glycerophosphate cross membrane shuttles are two known pathways which transport reducing equivalents of NADH from cytoplasm to mitochondrial matrix.

The indirect, shuttle-based transportation of high energy electrons from NADH through the shuttling substrates across the mitochondrial membrane occurs only in aerobic conditions. Therefore, during anaerobic conditions (such as ischaemia), NADH produced by glycolysis accumulates in the cytoplasm, and its reducing equivalents cannot be passed further down to the mitochondrial matrix through the inner membrane. NADH inside mitochondria cannot be oxidised by Complex I to NAD<sup>+</sup> and thus the redox state changes in favour of NADH. Therefore, the amount of NADH may be utilised as a surrogate marker for

absolute (hypoxia) or relative (increased metabolism) oxygen deprivation [3].

The NADH content can be measured in several ways. Some of the examples include spectrophotometric, fluorometric [3,5] and bioluminescent enzyme assays [6,7]. Interestingly, exciting NADH with ultraviolet (UV) light in the 320–380 nm range produces autofluorescent light emission in the 420–480 nm range with peak intensity at 450–460 nm - this optical feature has been widely used for measuring NADH concentration or content in solutions, cells and tissues [3].

Chance applied the UV/fluorescence-based method to monitor the NADH amount in cells and tissues or concentration in liquids [8]. The first device that allowed for such measurement was developed in 1954 by Theorell and Nygaard [9], and in 1962 Chance et al. studied NADH content in the brain and kidneys of anaesthetized rats [10]. In 1966 Chance showed that the primary source of 420–480 nm UV photoemission is the NADH and not the oxidised NAD<sup>+</sup>, thus validating this method for NADH quantification [8,10]. Since then, the fluorescence method has been commonly used in many in-vivo studies. For instance, Mayevsky et al. studied NADH with this method in rats [11] and humans [12].

Mayevsky et al. showed that the majority of 460-nm fluorescence comes from mitochondria with an irrelevant contribution of cytoplasm on human and animal skin models [3]. Dunaev et al. showed that the UV and fluorescent light penetrates only the most superficial skin layers – up to 0.5 mm in depth – with the majority of photoemission coming from the depth up to 0.3 mm [13]. Thus, most of the fluorescence comes from the epidermis, which lacks a direct blood supply. Nutrients and oxygen are delivered to the epidermis directly from dermis and via dermal microcirculation [3,13]. Figure 2 outlines the penetration of UV light and the origin of the fluorescence derived from NADH in human skin.

sible for the NADH oxidation to NAD<sup>+</sup>, decreases and then ceases [15,16]. As a result NADH accumulates in mitochondria. Restoration of oxygen delivery to mitochondria and its matrix rapidly reverses this process. Complex I activity recovers and NADH is immediately oxidised to NAD<sup>+</sup>. Therefore, following ischaemia-induced hypoxia, reperfusion induces a rapid decline in NADH concentration [15,17].

The phenomenon of NADH accumulation during ischaemia and its reduction during reperfusion has been used by Piotrowski et al. to measure the dynamic changes in the NADH accumulation using the UV excitement and fluorescent emission method [18]. The method – termed

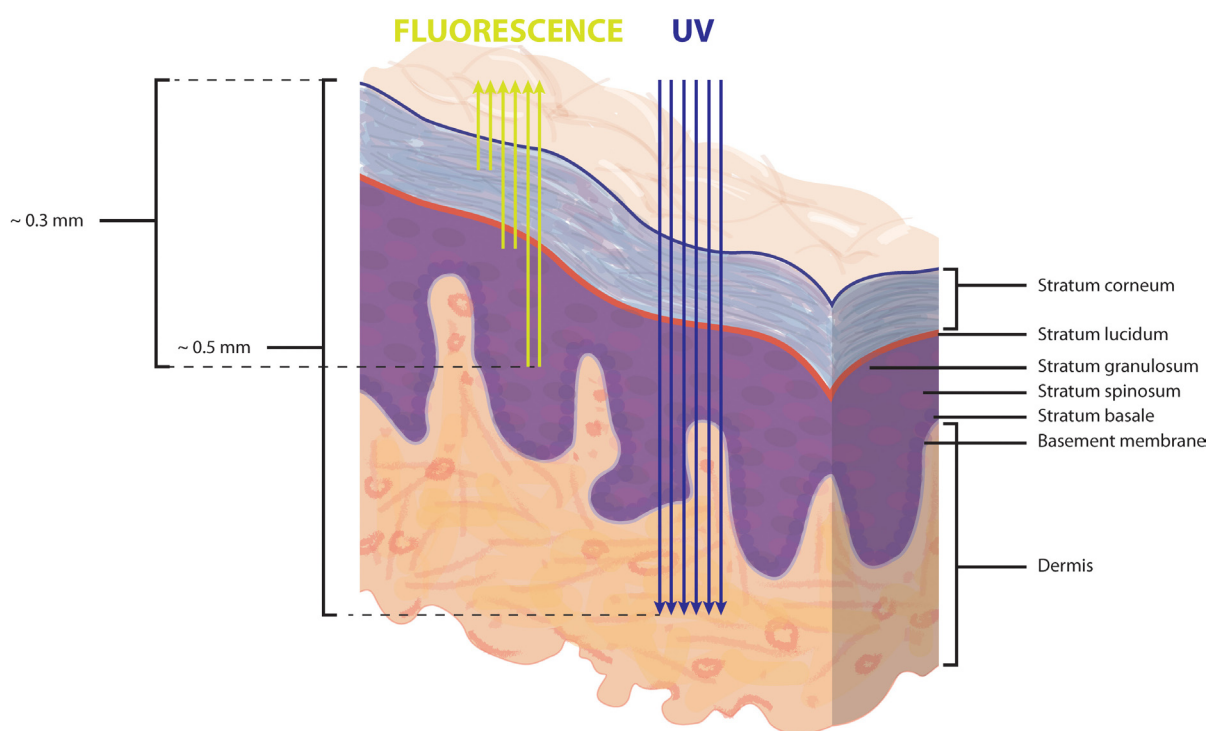


**Figure 2.** Penetration of the ultraviolet (UV) light through different skin layers and the source of the fluorescent light specific for NADH. Maximum penetration is about 0.5 mm, but the majority of the autofluorescence typical for NADH comes from the depth up to 0.3 mm

### Dynamic measurement of skin NADH content during ischaemia and reperfusion challenge

Cellular energy production in aerobic conditions depends on oxygen availability. During transient ischaemia, blood flow is ceased, leading to a decrease in oxygen supply. This leads to cellular metabolism switching into the anaerobic mode. The electron transfer through the electron transport chain stops [14], the activity of mitochondrial Complex I (NADH dehydrogenase), respon-

Flow Mediated Skin Fluorescence (FMSF) – involves continuous measurement of 460-nm fluorescence during ischaemia and reperfusion challenge. More specifically, the proposed FMSF method studies the dynamic changes in the 460-nm fluorescence after an earlier 340-nm ultraviolet excitation of the human forearm skin during a TIAR. Figure 3 shows a typical curve produced during FMSF plotting the intensity of photo emissions during an ischaemia-reperfusion episode.

During ischaemia, there is a gradual increase until the plateau of the 460-nm fluorescence intensity. The restoration of blood flow leads to a rapid decline in the strength of this signal (Figure 3) followed by its gradual recovery to the reference values. There are some grossly visible oscillations of the 460-nm fluorescence. Those are present at rest and reperfusion but not during ischaemia [19] (Figure 4). Their nature is unclear and under investigation. The FMSF method is

simple, fast and allows for real-time, dynamic and non-invasive measurement. The AngioExpert device (manufactured by Angionica in Lodz, Poland) is currently the only available device employing the FMSF method.

### Measurement of the flow-mediated skin 460-nm fluorescence

To record the FMSF with the AngioExpert device, the forearm of a study participant is immobilised

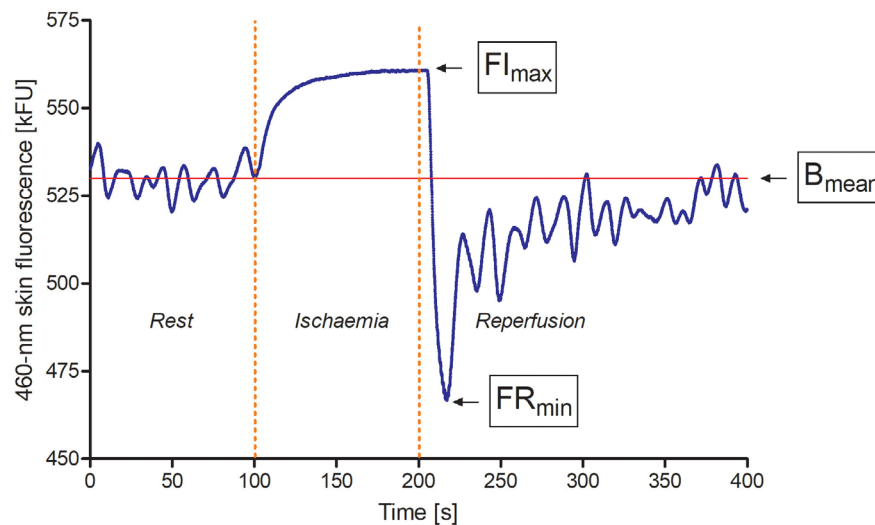


**Figure 3.** Typical changes of 460-nm forearm skin fluorescence during rest, ischaemia and reperfusion. At rest, NADH content is relatively stable, although some fluctuations are visible. During ischaemia, there is a rapid increase in NADH content. Reperfusion leads to fall of NADH, followed by slow recovery to the baseline level. For the abbreviations, please refer to the main text

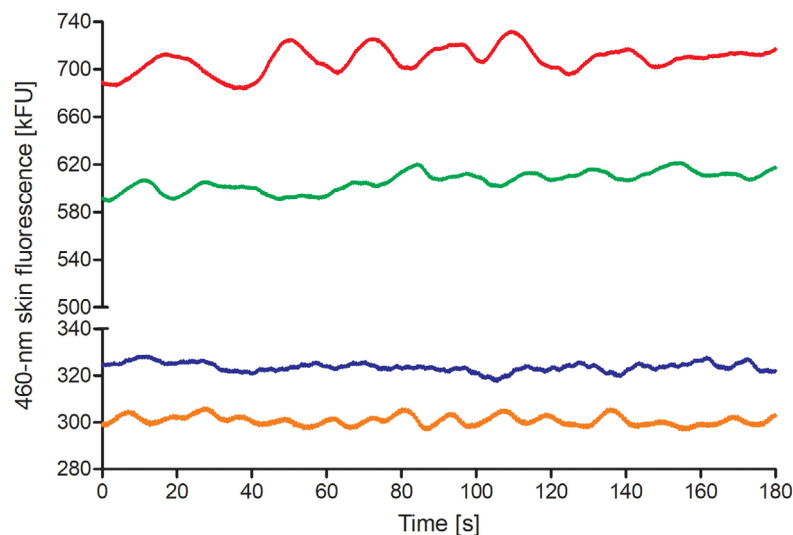


**Figure 4.** Four samples of the 460-nm fluorescence intensity and oscillations recorded in different young and healthy volunteers resting in a sitting position. There are natural differences in the baseline 460-nm fluorescence intensity between different people, depending for example, on the melatonin amount in the skin. All oscillations of different amplitude and frequency occur during normal blood flow. These oscillations disappear when blood supply is ceased during ischemia (please compare Figure 4 and Figure 6)

in special support to minimise recording noise. To induce TIAR, a deflated brachial cuff is placed on the studied arm for the baseline recording, and then it is inflated to 60 mmHg above Systolic Blood Pressure (SBP) for at least 100 seconds (in some studies 300 seconds [20]) to induce transient and controlled ischaemia. To allow for reperfusion, the brachial cuff is rapidly and wholly deflated.

The fluorescence data is obtained from a UV emitter-sensor device. The forearm completely covers the UV light emitter and fluorescence sensor. As the UV sensor is sensitive to movement, the study participant is required to remain still, and the forearm support is employed to improve the quality of readings. An example recording of 100-second ischaemia is shown in Figure 4. This procedure is safe and commonly applied in human studies [21,22], including both studies on healthy volunteers and studies on patients with an active disease process.

To quantify the FMSF response, we have proposed and use the following parameters [19,21]:

- › Bmean [kFU] – mean fluorescence at 460 nm recorded before each ischaemia as the baseline value;
- › FImax [kFU] – the maximal 460-nm fluorescence that increased above the baseline during each controlled forearm ischaemia;
- › FRmin [kFU] – the minimal 460-nm fluorescence after decreasing below the baseline during each reperfusion;
- › Imax [kFU] – the difference between FImax and Bmean;
- › Rmin [kFU] – the difference between Bmean and FRmin;
- › IRampl [kFU] – the maximal range of the 460-nm fluorescence change during ischaemia and reperfusion;
- › Clmax – Imax/IRampl ratio showing the relative contribution of the NADH increase during ischaemia to the maximal change in NADH during TIAR.

So far, the FMSF method has been applied in several studies, including both healthy people and patients with various diseases. Table 1 summarises all available publications describing this method.

Literature analysis and our current experience helped us identify some limitations of the FMSF method, which we describe below.

## Limitations related to the 460-nm fluorescence method of measuring NADH

### Skin properties

Skin parameters vary between individuals and ethnic groups, and it appears that the fluorescence intensity is affected by the melanin content of the skin. The percentage melanin content of the basal layer of the epidermis varies between 1% and 43% [23]. The study by Dremin and Dunaev suggests that the fluorescence signal decreases as the skin pigment increases [24]. Thus, comparing the results of skin fluorescence between participants from different ethnic groups at nominal value is inappropriate without appropriate statistical modelling that would account for this confounder. Additionally, the fluorescence signal is affected by epidermis thickness which varies between body sites. Epidermis thickness measured by Robertson and Rees using confocal microscopy differs between 55.6  $\mu\text{m}$  (upper back) to 62.5  $\mu\text{m}$  (back of the hand) [25]. Therefore, data comparison and pooling can only be attempted with measurements taken at the same body site.

### NADH/NAD<sup>+</sup> balance

The 460-nm fluorescence measures only NADH and not NAD<sup>+</sup> content [3]. NAD<sup>+</sup> does not possess optic properties similar to NADH and so does not allow for direct quantity measurement. However, in a short period, it is usually assumed that the total amount of NAD (sum of NADH and NAD<sup>+</sup>) remains close to constant [3]. Klein et al. confirmed the assumption in their study on dogs where the entire NAD content remained constant during the first 30 minutes of ischaemia [26]. However, during more extended ischaemia of over 30 minutes, the total NAD content depletes, and the interpretation of NADH/NAD<sup>+</sup> becomes less reliable.

### Uncertainty about cellular NADH origin

As already mentioned, NADH is present not only in the mitochondria but also in the cytoplasm and the nucleus. The 460-nm fluorescence measures total tissue or cellular NADH content. However, as shown by Anderson-Engels and Wilson, the 460-nm fluorescence, at least at resting aerobic conditions, comes primarily from mitochon-



drial NADH [3,27] with negligible input from the cellular NADH. This is supported by many other studies on various tissues [3,28,29]. It is therefore assumed that the 460-nm fluorescence informs about the redox state of mitochondrial NADH. It is also uncertain what is the main source of the 460-nm fluorescence increase – NADH from cytoplasm generated by glycolysis or NADH from the mitochondrial matrix as it cannot be oxidised to NAD<sup>+</sup> as hypoxia/anoxia stop the function of the electron transport chain. Regardless the processes which have the largest contribution to the NADH increase during ischaemia, it is more certain that the sudden drop in its content during reperfusion is caused by rapid oxidation of this molecule to NAD<sup>+</sup> in the mitochondrial matrix. In other words, the NADH drop during reperfusion appears to be mostly, if not exclusively, related to the function of the electron transport chain. For this reason, the rapid reduction in NADH content during reperfusion is a valuable index of the restoration of mitochondrial function after earlier ischaemia.

#### **Uncertainty about the mitochondrial pool of NADH**

NADH in mitochondria is divided into two pools: free NADH and protein-bound NADH. Protein-bound NADH makes up around 35% of the total NADH while contributing to almost 80% of the fluorescence signal [30]. Blinova et al. showed that the binding site of NADH molecules influences the intensity of NADH autofluorescence in mitochondria [31]. When NADH binds to the Complex 1, the NADH fluorescence is enhanced tenfold, but when it binds to other matrix enzymes, such as lactate dehydrogenase, then this fluorescence increases only 1.5–2 fold. The FMSF method does not inform about NADH relocation inside mitochondria.

#### **Spontaneous oscillations of the 460-nm fluorescence**

As already mentioned and shown in Figure 5, the resting 460-nm fluorescence is dynamic, with clearly visible oscillations. Their nature is unknown, they disappear during ischaemia and return, usually with a higher amplitude, during reperfusion. These oscillations are currently investigated by Angionica, i.e. the manufacturer of the AngioExpert device.

#### **Measurement of the skin fluorescence as an index of microvascular function**

Most of the studies on the post-UV skin 420–480 nm fluorescence repeatedly show that this method measures NADH content and mitochondrial function [3,8,10–13,18,19,21,23,24,28–32]. It is evident that mitochondrial function and oxidation of NADH to NAD<sup>+</sup> strictly depend on the blood flow through circulation and supply of oxygen. In other words, less available oxygen impairs mitochondrial function and attenuates NADH oxidation. Mayevsky has suggested that the monitoring of NADH by the autofluorescence also reflects the role of microvascular circulation [3,11,12]. For this reason, it is never definite what the most probable cause of the observed change in NADH skin content – mitochondria, microcirculation or both is? In some studies, the 460-nm fluorescence is only used for measuring the microvascular circulation [22,33–36].

#### **Limitations related to the FMSF method**

##### **Forearm skin as the target body part for studying**

This method, due to the construction of the measuring table and forearm support, allows measuring the FMSF in the forearm only. Although the 460-nm fluorescence can be measured anywhere in the skin or other tissues [3], the AngioExpert device allows measuring the FMSF signal only using one of two forearms.

##### **Atypical response**

Typical changes of the FMSF signal occurring during ischaemia and reperfusion in healthy individuals are presented in Figure 4 and Panel A of Figure 5. However, sometimes there are atypical FMSF responses noted in healthy people. Some examples of such atypical FMSF curves are shown in panels B, C and D in Figure 5.

Most commonly, the atypical FMSF response is limited to the ischaemic part of the recording. So far, there is no clear explanation for this phenomenon.

##### **Ambiguous and variable duration of the ischaemic challenge**

For the FMSF method, the optimal time for ischaemia duration is not established, and differ-

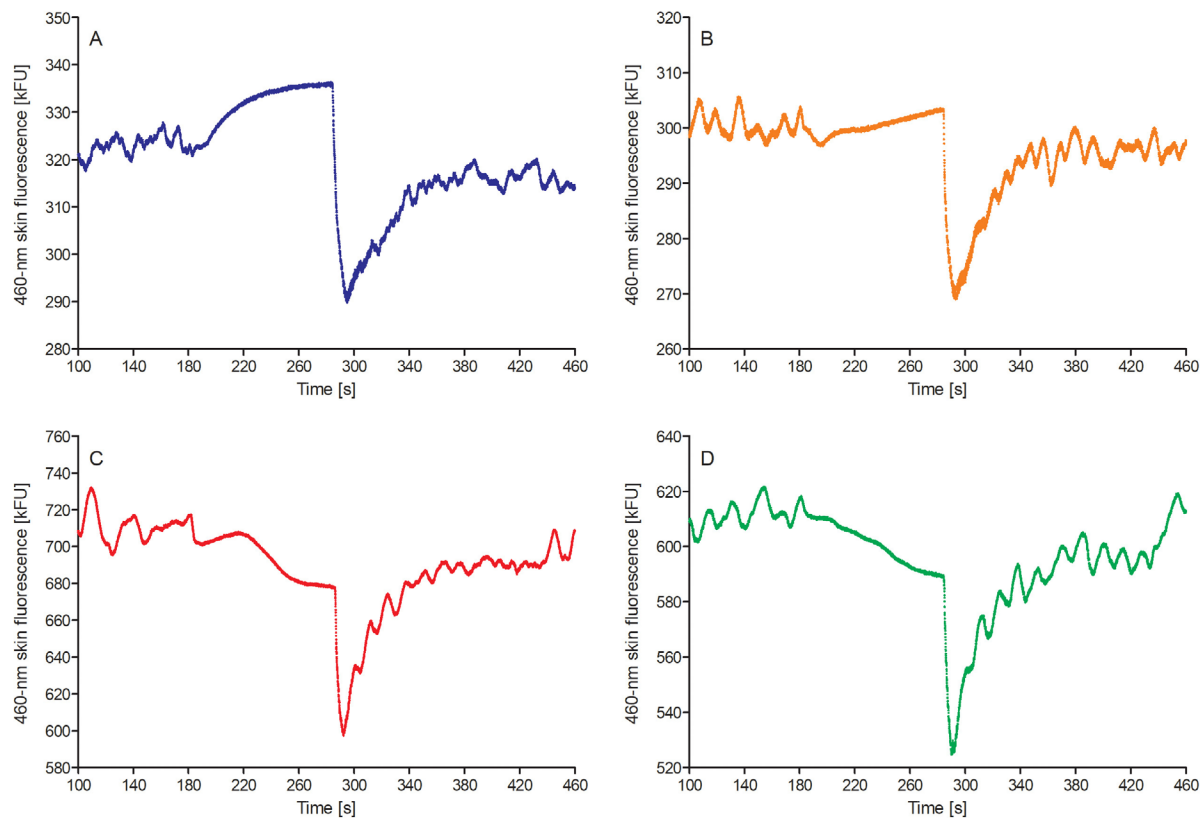


**Figure 5.** Examples of 460-nm skin fluorescence responses during ischaemia-reperfusion. Graph A represents the typical response, with an increase of FMSF signal during ischemia, its rapid fall during reperfusion, followed by restoration of the fluorescence to the baseline level. Graph B, C and D represent atypical responses found in young, healthy individuals

ent times are applied in various studies ranging from 100 seconds to 300 seconds [20]. A significant factor limiting ischaemia duration is numbness onset in the studied arm and forearm during ischaemia. Some patients may report pain of different severity, usually mild. Most commonly, however, the sensation experienced during the reperfusion phase is described by the participants as a transient feeling of warmth and itching lasting for 15–30 seconds. For these reasons, it is important to inform the participant about the potential uncomfortable symptoms which are, fortunately, short-lasting, tolerable and carry no risk.

#### **Ambiguous interpretation and terminology of the reperfusion phase**

The term proposed by the Angionica for the reperfusion phase was hyperaemia. Undoubtedly, as shown in Figure 6, during the first 20 seconds of reperfusion, there is a transient increase in the blood flow through the microcirculation. How-

ever, normalisation of the blood flow to the reference level is much faster than the normalisation of FMSF signal, which takes about 2–5 minutes to recover to the baseline level. It suggests that terming the entire reperfusion phase as “hyperaemia” is not right to the physiological phenomena occurring.

So far, most of the published studies with FMSF employ the prototype AngioExpert device, which is under development. Although there were no significant changes made to the construction, UV light emitter and fluorescent sensor, the proposed parameters used to quantify the FMSF were changing over time. This is a natural consequence of a very young method, and for this reason, there are significant differences in the definitions and names of parameters describing the same FMSF curve. On the other hand, Angionica appears flexible and puts no limits for the use of different descriptors (see Figure 4, compare with studies listed in Table 1).

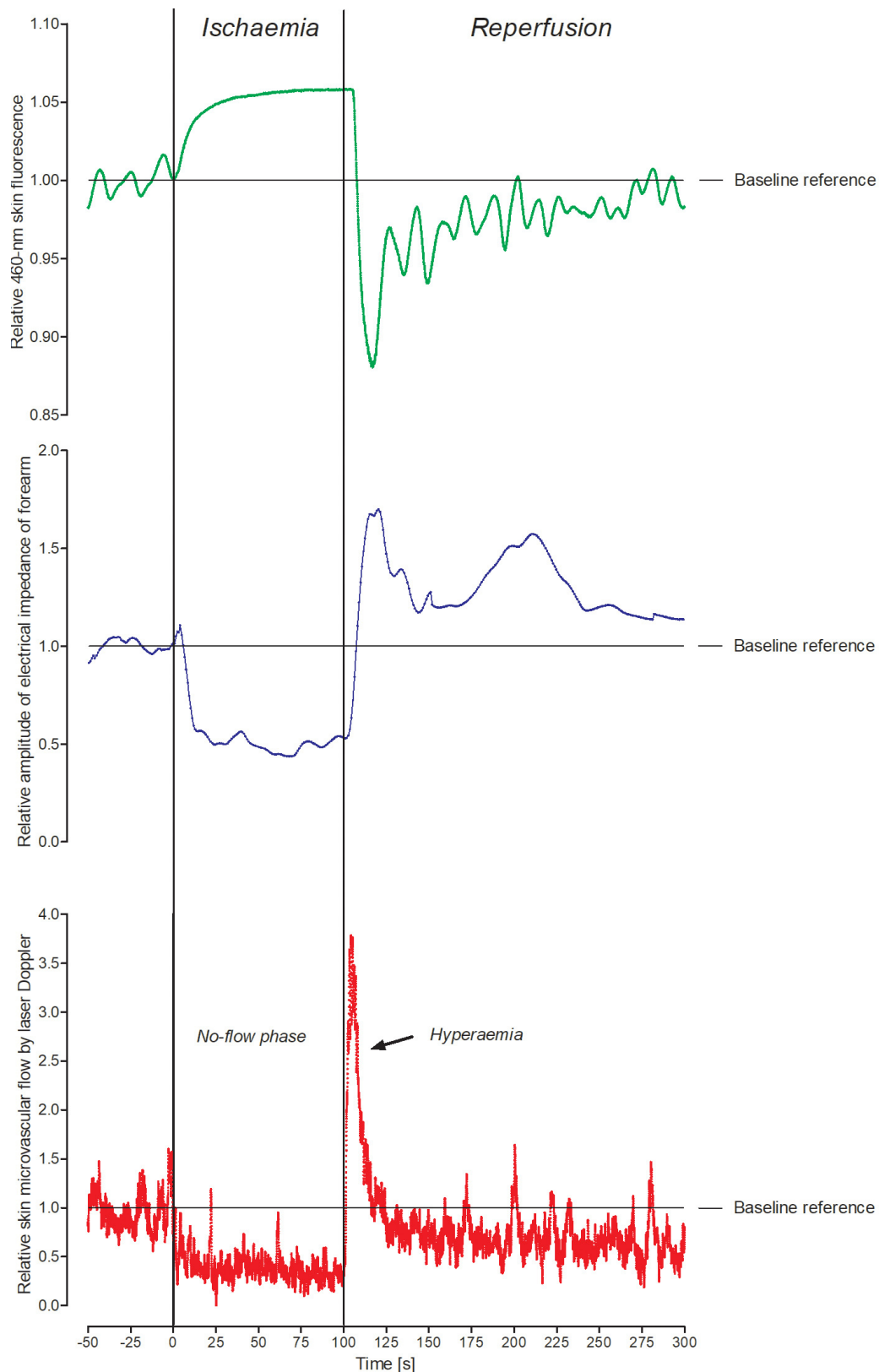


**Figure 6.** Example of simultaneous recording of FMSF, electrical impedance (showing the amount of water in the forearm) and laser Doppler (presenting the blood flow through skin microcirculation) during ischemia-reperfusion. The signals are synchronised according to the beginning and end of ischaemia. As shown, the dynamics of the changes in all three signals are not identical. It means that the FMSF signal is not a simple derivative of blood flow as assumed by some other authors [19,21,23,26]. FMSF is a more complex signal influenced by both NADH metabolism in mitochondria, the function of skin microcirculation and probably some other, yet unknown factors (e.g. water accumulation in the skin)

**Table 1.** Summary of studies using the FMSF method

| Authors                 | Studied subjects  | Summary   |
|-------------------------|---|---|
| Piotrowski et al. [22]  | 11 healthy volunteers and 11 patients with cardiovascular diseases  | FMSF curves have different characteristics between healthy volunteers and patients with cardiovascular disease  |
| Hellman et al. [20]     | 18 healthy volunteers and 18 patients with coronary artery disease  | Reduction of the value of NADH descriptors during reperfusion in patients with coronary artery disease compared with healthy subjects.  |
| Tarnawska et al. [24]   | 28 patients with coronary artery disease  | Ischaemic and reperfusion parts of the FMSF curves are blunted in patients with advanced coronary artery disease and diabetes. NADH fluorescence in patients with CAD is associated with plasma endothelial markers.  |
| Bugaj et al. [21]       | 121 highly trained athletes   | Exercise to exhaustion increases the skin NADH content at rest, during ischaemia and reperfusion but reduces the magnitude of NADH increase during ischemia both on men and women.  |
| Katarzynska et al. [25] | 31 healthy volunteers and 40 patients with type 1 diabetes (DM1)  | The 460-nm fluorescence drop during reperfusion is weaker in patients with type 1 diabetes than in healthy people. This reperfusion-induced drop of fluorescence attenuates with age in diabetic patients.  |
| Bogaczewicz et al. [26] | 34 healthy volunteers and 36 patients with systemic lupus erythematosus                                       | Patients with systemic lupus erythematosus have a reduction restoration of NADH during reperfusion compared to healthy people.  |
| Majewski et al. [27]    | 20 healthy volunteers, 23 patients with asthma, 26 patients with chronic obstructive pulmonary disease (COPD) | The 460-nm fluorescence increase during ischaemia is reduced in patients with COPD patients compared with healthy people. The 460-nm fluorescence drop during reperfusion is weaker in COPD patients compared to asthma and healthy subjects.   |
| Sibrecht et al. [19]    | One healthy individual  | Hyperaemic phase (measured by laser Doppler) of post-ischaemic reperfusion lasts app 20 seconds while the fluorescence signal during reperfusion recovers to baseline after over 200 seconds. Flow-related changes in the microvascular circulation contribute only to the early phase of reperfusion part of the FMSF curve. |
| Sibrecht et al. [28]    | 99 healthy volunteers   | Post-ischaemic preconditioning reduces NADH skin content and its increase during the following ischaemia episodes   |
| Nizinski et al. [29]    | 58 healthy volunteers   | An increased BMI is accompanied by a faster and higher increase of NADH during ischaemia and a delayed NADH recovery during reperfusion.  |
| Filberek [30]           | 99 healthy volunteers   | Men have more intense skin fluorescence during ischaemia and higher contribution of ischaemia to whole fluorescence change ( $C_{I_{max}}$ ).   |

## Conclusion

The 460-nm fluorescence intensity reflects the skin NADH content, which is mainly oxidised in mitochondria. However, mitochondrial function strictly depends on the oxygen supply by the skin microcirculation. Therefore it remains uncertain whether the dynamic alterations in this fluorescence recorded by the FMSF during TIAR reflect the function of either mitochondria or microvascular circulation or most probably both.

The FMSF is a unique scientific method to study the skin mitochondrial NADH content and its dynamic changes during transient and controlled ischaemia and reperfusion. This method is non-invasive, allows measuring NADH changes in a real-time and can be applied in many clinical and physiological scenarios. Although the FMSF has some limitations, its non-invasive character and scientific potential seem to merit further investigation. One of the most attractive features of this method is an opportunity to study mitochondrial function and/or microvas-

cular circulation during the clinically relevant challenge such as ischaemia and reperfusion. Another interesting feature is that the reduction in the 460-nm fluorescence during the reperfusion reflects the restoration of mitochondrial function after earlier ischaemia. For many reasons, the FMSF appears to have a lot of potential for implementation in physiological, clinical and pharmacological studies.

## Acknowledgements

### Conflict of interest statement

The authors declare no conflict of interest.

### Funding sources

This work was supported by the research grant „Najlepsi z Najlepszycy! 2.0” Programme of the Polish Ministry of Science and Higher Education (MNiSW/2017/118/DIR/NN2 – Pls: GS, PF & JN), and partially by a projects ANG/ZK/1/2017 (PI: PG) as a part of the project from the European Union from the resources of the European Regional Development Fund under the Smart Growth Operational Program, Grant No. POIR.01.01.01-00-0540/15.

## References

1. Brand MD, Affourtit C, Esteves TC, Green K, Lambert AJ, Miwa S, Pakay JL, Parker N. Mitochondrial superoxide: production, biological effects, and activation of uncoupling proteins. *Free Radical Biology and Medicine*. 2004 09;37(6):755-67. <https://doi.org/10.1016/j.freeradbiomed.2004.05.034>
2. Anderson KA, Madsen AS, Olsen CA, Hirschey MD. Metabolic control by sirtuins and other enzymes that sense NAD<sup>+</sup>, NADH, or their ratio. *Biochimica et Biophysica Acta (BBA) - Bioenergetics*. 2017 Dec;1858(12):991-8. <https://doi.org/10.1016/j.bbabi.2017.09.005>
3. Mayevsky A, Rogatsky GG. Mitochondrial function in vivo evaluated by NADH fluorescence: from animal models to human studies. *American Journal of Physiology-Cell Physiology*. 2007 02;292(2):C615-C640. <https://doi.org/10.1152/ajpcell.00249.2006>
4. Koga Y, Tanaka M, Ohta S, Wei Y. Biochemistry of mitochondria, life and intervention 2010. *Biochimica et Biophysica Acta (BBA) - General Subjects*. 2012 05;1820(5):551-552. <https://doi.org/10.1016/j.bbagen.2012.01.008>
5. Marín-García J, Akhmedov AT, Moe GW. Mitochondria in heart failure: the emerging role of mitochondrial dynamics. *Heart Failure Reviews*. 2012 06 17;18(4):439-456. <https://doi.org/10.1007/s10741-012-9330-2>
6. Vidugiriene J, Leippe D, Sobol M, Vidugiris G, Zhou W, Meisenheimer P, Gautam P, Wennerberg K, Cali JJ. Bioluminescent Cell-Based NAD(P)/NAD(P)H Assays for Rapid Dinucleotide Measurement and Inhibitor Screening. *ASSAY and Drug Development Technologies*. 2014 Dec;12(9-10):514-526. <https://doi.org/10.1089/adt.2014.605>
7. Levy B, Ambrosio G, Pries A, Struijker-Boudier H. Microcirculation in Hypertension. *Circulation*. 2001 08 07;104(6):735-740. <https://doi.org/10.1161/hc3101.091158>
8. Chance B, Cohen P, Jobsis F, Schoener B. Intracellular Oxidation-Reduction States in Vivo: The microfluorometry of pyridine nucleotide gives a continuous measurement of the oxidation state. *Science*. 1962 Aug 17;137(3529):499-508. <https://doi.org/10.1126/science.137.3529.499>
9. Theorell H, Nygaard A. Kinetics and equilibria in flavoprotein systems. I. A fluorescence recorder and its application to a study of the dissociation of the old yellow enzyme and its resynthesis from riboflavin phosphate and protein. *Acta Chem Scand*. 1954;:877-88.
10. Chance B. Mitochondrial NADH redox state, monitoring discovery and deployment in tissue. *Methods in Enzymology*. 2004;:361-70. [https://doi.org/10.1016/S0076-6879\(04\)85020-1](https://doi.org/10.1016/S0076-6879(04)85020-1) PMID 15130749
11. Mayevsky A, Chance B. A New Long-Term Method for the Measurement of NADH Fluorescence in Intact Rat Brain With Chronically Implanted Cannula. *Adv Exp Med Biol*. 1973;37A:239-44. [https://doi.org/10.1007/978-1-4684-3288-6\\_30](https://doi.org/10.1007/978-1-4684-3288-6_30) PMID 4378057
12. Mayevsky A, Sonn J, Luger-Hamer M, Nakache R. Real-Time assessment of organ vitality during the transplantation procedure. *Transplantation Reviews*. 2003 04;17(2):96-116. [https://doi.org/10.1016/s0955-470x\(02\)00007-1](https://doi.org/10.1016/s0955-470x(02)00007-1)
13. Dunaev AV, Dremin VV, Zherebtsov EA, Rafailov IE, Litvinova KS, Palmer SG, Stewart NA, Sokolovski SG, Rafailov EU. Individual variability analysis of fluorescence parameters measured in skin with different levels of nutritive blood flow. *Medical Engineering & Physics*. 2015 06;37(6):574-583. <https://doi.org/10.1016/j.medengphy.2015.03.011>
14. Chen Q, Camara AKS, Stowe DF, Hoppel CL, Lesnefsky EJ. Modulation of electron transport protects cardiac mitochondria and decreases myocardial injury during ischemia and reperfusion. *American Journal of Physiology-Cell Physiology*. 2007 01;292(1):C137-C147. <https://doi.org/10.1152/ajpcell.00270.2006>
15. Riess ML, Camara AKS, Chen Q, Novalija E, Rhodes SS, Stowe DF. Altered NADH and improved function by anesthetic and ischemic preconditioning in guinea pig intact hearts. *American Journal of Physiology-Heart and Circulatory Physiology*. 2002 07 01;283(1):H53-H60. <https://doi.org/10.1152/ajpheart.01057.2001>
16. Lesnefsky EJ, Chen Q, Moghaddas S, Hassan MO, Tandler B, Hoppel CL. Blockade of Electron Transport during Ischemia Protects Cardiac Mitochondria. *Journal of Biological Chemistry*. 2004 09 03;279(46):47961-47967. <https://doi.org/10.1074/jbc.m409720200>
17. Varadarajan SG, An J, Novalija E, Smart SC, Stowe DF. Changes in [Na<sup>+</sup>]<sub>i</sub>, compartmental [Ca<sup>2+</sup>]<sub>i</sub>, and NADH with dysfunction after global ischemia in intact hearts. *American Journal of Physiology-Heart and Circulatory Physiology*. 2001 01 01;280(1):H280-H293. <https://doi.org/10.1152/ajpheart.2001.280.1.h280>
18. Mayevsky A, Chance B. Oxidation-reduction states of NADH in vivo: From animals to clinical use. *Mitochondrion*. 2007 09;7(5):330-339. <https://doi.org/10.1016/j.mito.2007.05.001>
19. Sibrecht G, Bugaj O, Filberek P, Nizinski J, Kusy K, Zielinski J, Guzik P. Flow-Mediated Skin Fluorescence Method for Non-Invasive Measurement of the NADH At 460 Nm – a Possibility To Assess the Mitochondrial Function. *Postępy Biologii Komórki*. 2017;44(4):333-52.
20. Hellmann M, Tarnawska M, Dudziak M, Dorniak K, Roustit M, Cracowski J. Reproducibility of flow mediated skin fluorescence to assess microvascular function. *Microvascular Research*. 2017 09;113:60-64. <https://doi.org/10.1016/j.mvr.2017.05.004>
21. Bugaj O, Zieliński J, Kusy K, Kantanista A, Wieliński D, Guzik P. The Effect of Exercise on the Skin Content of the Reduced Form of NAD and Its Response to Transient Ischemia and Reperfusion in Highly Trained Athletes. *Frontiers in Physiology*. 2019 05 15;10. <https://doi.org/10.3389/fphys.2019.00600>
22. Piotrowski L, Urbaniak M, Jedrzejczak B, Marcinek A, Gebicki J. 10.1152/ajpheart.2001.280.1.H280 Note: Flow mediated skin fluorescence—A novel technique for evaluation of cutaneous microcirculation. *Review of Scientific Instruments*. 2016 03;87(3):036111. <https://doi.org/10.1063/1.4945044>

23. Jacques SL. Corrigendum: Optical properties of biological tissues: a review. *Physics in Medicine and Biology*. 2013 06 27;58(14):5007-5008. <https://doi.org/10.1088/0031-9155/58/14/5007>
24. Dremin VV, Dunaev AV. How the melanin concentration in the skin affects the fluorescence-spectroscopy signal formation. *Journal of Optical Technology*. 2016 01 01;83(1):43. <https://doi.org/10.1364/jot.83.000043>
25. Rees J, Robertson K. Variation in Epidermal Morphology in Human Skin at Different Body Sites as Measured by Reflectance Confocal Microscopy. *Acta Dermatologica Venereologica*. 2010;90(4):368-373. <https://doi.org/10.2340/00015555-0875>
26. Klein HH, Schaper J, Puschmann S, Nienaber C, Kreuzer H, Schaper W. Loss of canine myocardial nicotinamide adenine dinucleotides determines the transition from reversible to irreversible ischemic damage of myocardial cells. *Basic Research in Cardiology*. 1981 Nov;76(6):612-621. <https://doi.org/10.1007/bf01908051>
27. Andersson-Engels S, Brian C. In vivo fluorescence in clinical oncology: fundamental and practical issues. *J Cell Pharmacol*. 1992;3:66-79.
28. Nuutinen EM. Subcellular origin of the surface fluorescence of reduced nicotinamide nucleotides in the isolated perfused rat heart. *Basic Research in Cardiology*. 1984 01;79(1):49-58. <https://doi.org/10.1007/bf01935806>
29. Mayevsky A. Brain NADH redox state monitored in vivo by fiber optic surface fluorometry. *Brain Research Reviews*. 1984 03;7(1):49-68. [https://doi.org/10.1016/0165-0173\(84\)90029-8](https://doi.org/10.1016/0165-0173(84)90029-8)
30. Blinova K, Carroll S, Bose S, Smirnov AV, Harvey JJ, Knutson JR, Balaban RS. Distribution of Mitochondrial NADH Fluorescence Lifetimes: Steady-State Kinetics of Matrix NADH Interactions. *Biochemistry*. 2005 02;44(7):2585-2594. <https://doi.org/10.1021/bi0485124>
31. Blinova K, Levine RL, Boja ES, Griffiths GL, Shi Z, Ruddy B, Balaban RS. Mitochondrial NADH Fluorescence Is Enhanced by Complex I Binding. *Biochemistry*. 2008 09 09;47(36):9636-9645. <https://doi.org/10.1021/bi800307y>
32. Blacker TS, Duchon MR. Investigating mitochondrial redox state using NADH and NADPH autofluorescence. *Free Radical Biology and Medicine*. 2016 Nov;100:53-65. <https://doi.org/10.1016/j.freeradbiomed.2016.08.010>
33. Tarnawska M, Dorniak K, Kaszubowski M, Dudziak M, Hellmann M. A pilot study with flow mediated skin fluorescence: A novel device to assess microvascular endothelial function in coronary artery disease. *Cardiology Journal*. 2018;25(1):120-7. <https://doi.org/10.5603/CJ.a2017.0096> PMID 28840593
34. Katarzynska J, Borkowska A, Czajkowski P, Los A, Szczerbinski L, Milewska-Kranc A, Marcinek A, Kretowski A, Cypryk K, Gebicki J. Flow Mediated Skin Fluorescence technique reveals remarkable effect of age on microcirculation and metabolic regulation in type 1 diabetes. *Microvascular Research*. 2019 07;124:19-24. <https://doi.org/10.1016/j.mvr.2019.02.005>
35. Bogaczewicz J, Tokarska K, Wozniacka A. Changes of NADH Fluorescence from the Skin of Patients with Systemic Lupus Erythematosus. *BioMed Research International*. 2019 Dec 24;2019:1-7. <https://doi.org/10.1155/2019/5897487>
36. Majewski S, Szewczyk K, Białas AJ, Miłkowska-Dymanowska J, Kurmanowska Z, Górski P. Assessment of microvascular function in vivo using flow mediated skin fluorescence (FMSF) in patients with obstructive lung diseases: A preliminary study. *Microvascular Research*. 2020 01;127:103914. <https://doi.org/10.1016/j.mvr.2019.103914>

# ORBIS (Open Research Biopharmaceutical Internships Support) – building bridges between academia and pharmaceutical industry to improve drug development

## Emilia Jakubowska

Chair and Department of Pharmaceutical Technology, Faculty of Pharmacy, Poznan University of Medical Sciences, Poznan

 <https://orcid.org/0000-0002-7492-9045>

## Sharon Davin

Applied Process Consulting Ltd., Dublin, Ireland

 <https://orcid.org/0000-0003-0578-8741>

## Aleksandra Dumcic Dumcic

Zentiva k.s., Prague, Czech Republic

 <https://orcid.org/0000-0002-2347-1409>

## Grzegorz Garbacz

Physiolution GmbH, Greifswald, Germany

 <https://orcid.org/0000-0003-4511-0329>


## Anne Juppo

University of Helsinki, Division of Pharmaceutical Chemistry and Technology, Formulation and Industrial Pharmacy Unit, Helsinki, Finland

 <https://orcid.org/0000-0003-1805-8991>

## Bożena Michniak-Kohn

Center for Dermal Research and Ernest Mario School of Pharmacy, Rutgers, The State University of New Jersey, Piscataway, New Jersey, USA

 <https://orcid.org/0000-0002-3858-158X>

## Piotr J. Rudzki

Łukasiewicz Research Network – Pharmaceutical Research Institute, Warsaw, Poland

 <https://orcid.org/0000-0002-4622-4849>

## Wojciech Smułek

Institute of Technology and Chemical Engineering, Poznan University of Technology, Poznan, Poland

 <https://orcid.org/0000-0001-5377-9933>

## Clare Strachan

University of Helsinki, Division of Pharmaceutical Chemistry and Technology, Formulation and Industrial Pharmacy Unit, Helsinki, Finland

 <https://orcid.org/0000-0001-9180-5856>

## Oleg Syarkevych

JSC Farmak, Kyiv, Ukraine

 <https://orcid.org/0000-0002-4236-5927>

## Lidia Tajber

School of Pharmacy and Pharmaceutical Sciences, Trinity College Dublin, College Green, Dublin 2

 <http://orcid.org/0000-0003-1544-6796>

## Janina Lulek

Chair and Department of Pharmaceutical Technology, Faculty of Pharmacy, Poznan University of Medical Sciences, Poznan, Poland

 <https://orcid.org/0000-0002-5567-9909>

Corresponding author: [jlulek@ump.edu.pl](mailto:jlulek@ump.edu.pl)

 DOI: <https://doi.org/10.20883/medical.419>

**Keywords:** drug discovery and design, pharmaceutical formulation, research and development, solid state materials, pharmaceutical technology, biomedical analysis

**Published:** 2020-01-31

**How to Cite:** Jakubowska E, Davin S, Dumcic AD, Garbacz G, Juppo A, Michniak-Kohn B, Rudzki PJ, Smułek W, Strachan C, Syarkevych O, Tajber L, Lulek J. ORBIS (Open Research Biopharmaceutical Internships Support) – building bridges between academia and pharmaceutical industry to improve drug development. *JMS [Internet]*. 2020 Mar 31;89(1):e419. doi:10.20883/medical.419



© 2020 by the author(s). This is an open access article distributed under the terms and conditions of the Creative Commons Attribution (CC BY-NC) license. Published by Poznan University of Medical Sciences

## ABSTRACT

Open Research Biopharmaceutical Internships Support (ORBIS) is an international, Horizon 2020 project funded by Maria Skłodowska-Curie Actions, Research and Innovation Staff Exchange (RISE) programme. Six academic institutions and four pharmaceutical companies from seven countries cooperate with the

aim to improve the preclinical pathway of medicine development through increased Research and Development (R&D) productivity, especially focusing on processes and technologies which address the challenge of poor drug bioavailability. The RISE scheme supports secondments, meaning that early stage and experienced researchers are sent to consortium partner institutions to advance studies on pharmaceutical pre-formulation, dosage forms and drug delivery systems and methods of biopharmaceutical evaluation. The ORBIS project enables secondees to gain new skills and develop their competences in an international and intersectoral environment, strengthening the human capital and knowledge synergy in the European pharmaceutical R&D sector.

## Introduction

ORBIS (**O**pen **R**esearch **B**iopharmaceutical **I**nternships **S**upport, grant agreement no. 778051) is an international and intersectoral project awarded €2,268,000 by the European Commission under the Research and Innovation Staff Exchange (RISE) call of Marie Skłodowska-Curie Actions (MSCA), Horizon 2020 programme (H2020-MSCA-RISE-2017). This four-year project was launched on 1<sup>st</sup> March 2018.

ORBIS (Figure 1) is one of the largest projects and consortia of the RISE programme, comprising 10 beneficiaries and partners; these include six academic institutions and four pharmaceutical companies located in seven countries (Figure 2). This project will enable over 200 researchers to advance their research and other skills through secondment placements. Poznan University of Medical Sciences (PUMS, Poland) is the project coordinator and the grant is managed by the project chair, Professor Janina Lulek, Head of the Chair and Department of Pharmaceutical Technology at PUMS.



Figure 1. ORBIS official logo

## Research Project Objectives

The current process of drug development is lengthy and inefficient. When developing a new chemical entity only one out of approximately 10,000 molecules enters the market as a drug. The situation is no better for generic or value-

added medicinal products, where the active pharmaceutical ingredient (API) is already well-known: commencing from the first laboratory trials, it takes a minimum of four years of intensive activities for the simplest generic drug product to reach the market. The societal demand for more effective medicines has created a challenge of supply within the pharmaceutical industry. To address this gap, ORBIS proposes that the time for the medicinal product to reach the patients might be reduced by improving early stage R&D productivity. The overarching objective of ORBIS is to form an international and intersectoral academic and industrial network to address this challenge (Table 1). This consortium was built on pre-existing collaboration that has expanded into the current ORBIS group (Figure 2). The project aims to improve the preclinical pathway of medicine development, concentrating on processes and technologies to address poor drug bioavailability.

The close research cooperation between the project partners, as well as knowledge synergy and transfer between the academic and industrial sectors, has created a stimulating environment for employees and PhD students to advance their individual career and transferrable skills during research visits (ORBIS secondments) and those interactions are the core enablers of the consortium objectives (Table 2).

## Research Plan and Basic Concept

The core and vehicle for accomplishing the ORBIS project objectives are secondments, i.e. 1- to 12-month long research and training visits of early stage and experienced researchers at partner institutions. PhD students and employees from the European universities can travel abroad



**Table 1.** Institutions participating in ORBIS project

| Institution name and acronym   | Location               | Project role/ short description   |
|--|------------------------|---|
| Poznan University of Medical Sciences (PUMS)                           | Poznan, Poland         | Project beneficiary and coordinator. Apart from the project management and organization, several departments of Faculty of Pharmacy are engaged in sending and hosting secondees. PUMS expertise includes: pharmaceutical preformulation, drug design and delivery, physical chemistry, pharmaceutical and biopharmaceutical analysis, pharmacokinetics.          |
| APC Ltd. (APC)   | Dublin, Ireland        | Project beneficiary. APC specializes in integrating innovative process performance across a medicine's life cycle, from early Phase development to manufacturing support. APC's research platforms and associated information deliverables help the global bio/pharma sector accelerate the development and launch of their medicines.                            |
| JSC Farmak (FMK)   | Kyiv, Ukraine          | Project beneficiary. FMK is the leading Ukrainian developer of generic and innovative dosage forms. Small, pilot and large-scale manufacturing facilities.  |
| Łukasiewicz Research Network - Pharmaceutical Research Institute (PRI) | Warsaw, Poland         | Project beneficiary. PRI develops API manufacturing technologies, translating academic research into practical solutions for industry. Expertise covers laboratory scale synthesis and scale-up, development of formulations, analytics and pharmacokinetic studies. API manufacturing facilities.  |
| Physiolution GmbH (PHY)  | Greifswald, Germany    | Project beneficiary. PHY develops biorelevant test methods for assessing <i>in vitro</i> biopharmaceutical properties of the drug substances and drug products.   |
| Poznan University of Technology (PUT)                                  | Poznan, Poland         | Project beneficiary. Researchers of the Institute of Chemical Technology and Engineering, Faculty of Chemical Technology, provide knowledge in areas of inorganic and organic chemical technology, chemical engineering, polymer technology, chemical analysis and biotechnology.   |
| University of Helsinki (UH)  | Helsinki, Finland      | Project beneficiary. The Formulation and Industrial Pharmacy unit of the Division of Pharmaceutical Chemistry and Technology focuses on the translation of a drug molecule into a medicine. Expertise is offered in novel spectroscopic techniques and manufacturing technologies of oral solid dosage forms.   |
| Trinity College Dublin (TCD)   | Dublin, Ireland        | Project beneficiary. Trinity Pharmacy & Pharmacology is joint 45 in the world by subject (Pharmacy and Pharmacology) and the School of Pharmacy and Pharmaceutical Sciences is the leading Pharmacy educator in Ireland. The expertise includes pharmaceutical preformulation, engineering of solid-state materials and advanced oral and pulmonary formulations. |
| Zentiva (ZNT)  | Prague, Czech Republic | Project beneficiary. ZNT is an international pharmaceutical company that develops, manufactures and distributes generic and value-added medicinal drug products for oral and parenteral drug delivery.  |
| Rutgers, the State University of New Jersey (RUTG)                     | New Jersey, USA        | Project partner. RUTG is a member of the "Big 10" top universities in the U.S. with 70,000 undergraduates & graduates & over \$750.8 million in research monies. The School of Pharmacy is in the top ten pharmacy schools in the US. Center for Dermal Research founded in 2011 is the only academic Center in NJ dedicated to pharmaceutical skin research.     |

to pharmaceutical companies and Rutgers University, while staff from the industrial members visit foreign academic partners, meaning that all secondments must be international and mostly intersectoral.

ORBIS activities are organized in 7 Work Packages (WP), each addressing a specific project objective to streamline the scientific progress, knowledge transfer or dissemination.

The aim of **WP1: Drug substances and pharmaceutical preformulation** is to translate the discovery synthesis of a drug substance (API) into technology development and investigate the solid-state physicochemical characteristics of APIs. The overarching goal is to improve unfavourable

biopharmaceutical characteristics of APIs, i.e. poor solubility and/or dissolution. To accelerate small molecule process design, several technological platforms are explored to deliver an improved product better suited for further formulation development. Research employs advanced analytical equipment to investigate the intrinsic, solid state and derived properties of the APIs and their forms.

The purpose of **WP2: Dosage forms and drug delivery systems** is to design, develop and test new drug carriers and dosage forms for oral and topical delivery of drugs. Examples of oral formulations are novel liposomes, polymeric nano- and microparticles, minitables, self-microemul-

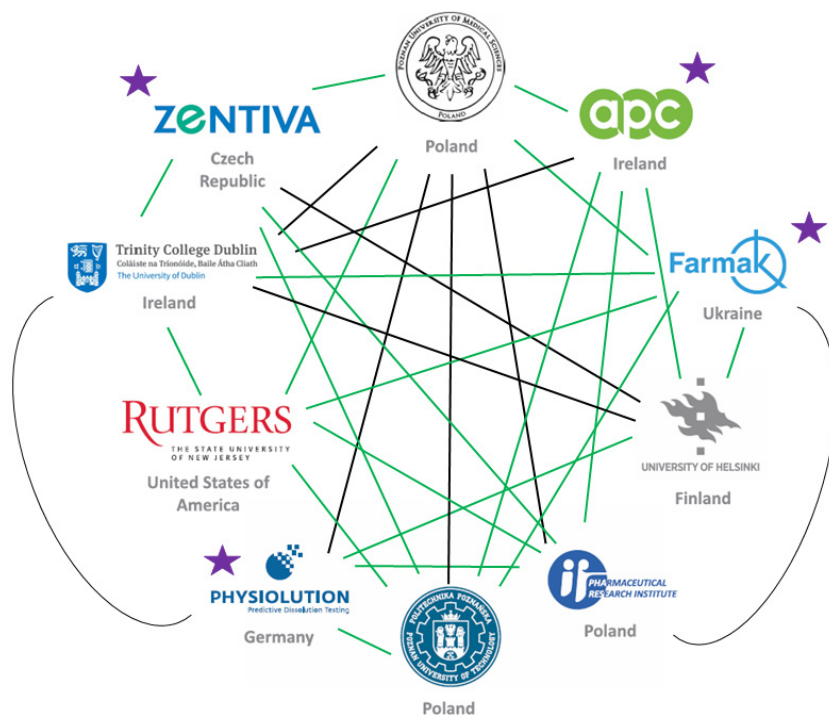


**Figure 2.** ORBIS network. Pre-ORBIS collaboration (black lines) and new ORBIS collaboration (green lines). Industry partners are marked with a star

**Table 2.** ORBIS project objectives

|  |   |
|--|---|
| To improve the process development of drug substances by innovating synthesis and evaluation of active materials and their physical forms.                                     | To enable hands-on and relevant industrial training of early stage researchers including a range of "soft skills".                        |
| To advance pharmaceutical preformulation studies by developing new industry-relevant methods of evaluation of drug substances physical forms in the biopharmaceutical context. | To foster "communal" academia-industry open collaboration.  |
| To formulate advanced drug delivery systems and optimize manufacturing of oral dosage forms.   |   |
| To better understand drug transport across the skin and develop topical and transdermal delivery systems.  | To support industry-academia research leading to joint publications, presentations and enabling staff transfer between these two sectors. |
| To innovate the biopharmaceutical evaluation of dosage forms and drug delivery systems by improving the testing approaches and methods of bioanalysis.                         |   |

**Table 3.** Overview of ORBIS summer schools and workshops

| Event name  | Organizing institutions | Place and date  |
|---|-------------------------|---|
| 1 <sup>st</sup> School on pharmaceutical preformulation testing of APIs and dosage forms.                   | TCD & APC               | Dublin, 12–14 <sup>th</sup> June 2019                             |
| Open Workshop on process development of drug substances.  | FMK                     |   |
| 2 <sup>nd</sup> ORBIS Summer School on Oral Dosage Forms: Fundamentals, Challenges and Future Opportunities | UH & ZNT                | Helsinki, 18–20 <sup>th</sup> September 2019                      |
| ORBIS Workshop on Dosage Forms and Drug Delivery Systems.   | UH                      |   |
| 3 <sup>rd</sup> School on topical and transdermal drug delivery systems.                                    | PUMS & RUTG             | Poznan, 29 <sup>th</sup> September – 1 <sup>st</sup> October 2020 |
| 4 <sup>th</sup> School on biopharmaceutical evaluation of dosage forms and drug delivery.                   | ZNT & PRI               | Prague, September 2021  |
| Open Workshop on biopharmaceutical evaluation of dosage forms and drug delivery systems.                    | PHY                     |   |

sifying systems or mesoporous materials, while topical pharmaceutical dosage forms include liquid (ionic liquids, microemulsions), semi-solid (hydrogels, organogels, creams) and adhesive (patches). This work package employs a variety of advanced methods to analyse the developed formulations, including novel imaging and structure analysis techniques and in vitro skin permeation tests.

**WP3: Biopharmaceutical evaluation of dosage forms and drug delivery systems** focuses on the development of biorelevant methods for in vitro dissolution and release testing, simulating conditions that act on dosage forms during their gastro-intestinal passage. An additional aim is to advance bioanalytical methods, including biological sample preparation techniques, reducing HPLC analysis time and assessing validation parameters according to the European Medicines Agency guidelines [1].

In addition to the scientific WPs, ORBIS is supported by four other WPs. **WP4: Training** especially concerns early stage researchers. Secondments are an opportunity to become familiar with new research topics and intersectoral environments, learn new methodologies and techniques as well as develop transferrable scientific and “soft” skills, further increasing employability of the young researchers. **WP5: Management** deals with the strategic management and organization of this large consortium, while **WP6: Communication and dissemination** increases the project impact, visibility and dissemination of results. **WP7: Ethics** monitors the handling of ethical issues related to the project and it is supported by the Honorary Ethical Advisory Board, an independent body of external experts.

## Research Methodology

Methods include API synthesis, preformulation studies, manufacturing, analytics (including bioanalytics), continuous processing, quality by design and new testing methodology design. Also, a blend of experimental and computational techniques is used to accomplish the research goals. Experts in the various research areas from the consortium are involved in the design of the methods and approaches, amalgamating the expertise in the multidisciplinary, international

and intersectoral consortium. The partners are integrating their common research protocols and filling gaps in individual infrastructures.

## Measurable effects and expected results

Several deliverables and milestones are aligned with the objectives of the ORBIS project. The WP1 team will demonstrate a continuous operation of synthesis/crystallisation processes for APIs relevant to ORBIS and develop a strategy to improve the solubility/permeability of BCS class II and IV APIs. A public report on perspectives of API manufacturing and advances in preformulation studies will be jointly prepared.

The WP2 milestones comprise the demonstration of oral formulation advancements accomplished as a part of ORBIS (e.g. minitables, novel drug carriers) and improvements in formulation of transdermal dosage forms. A WP2 deliverable will be a public report on new insights into oral dosage forms and delivery systems as well as novel approaches in topical and transdermal drug delivery.

The main impact of WP3 will be the successful evaluation of bioanalytical methods for selected APIs. The WP3 team will prepare a report on pharmacokinetics driven development of dosage form specifications and estimation of pharmacokinetics based on in vitro data.

To date, after 24 months of project activity, 221 months of secondments have been completed and have started to deliver tangible research outputs, such as new research collaborations and publications [2-6].

Apart from the scientific deliverables and milestones, the progress of the ORBIS project is measured by completing activities related to training, management and dissemination. Four summer schools and workshops for ORBIS participants are the outcomes of WP4 (Table 3). These events involve lectures delivered by world-class researchers, hands-on workshops and demonstrations of relevant techniques, as well as are an opportunity to showcase the organizing partners' capabilities and the results of secondments. The summer schools and workshops are also excellent networking events for strengthening the relationships and formulating new ideas

for cooperation between the ORBIS partners and reaching beyond the timeframe of this project.

To date, the project has also successfully achieved its managerial deliverables – including two out of the three major consortium meetings (kick-off, mid-term and planned final conference) and one out of the two progress reports. Project activities and outputs can be followed on the ORBIS website and social media channels established as dissemination deliverables [7].

A goal of ORBIS is to have 504 months of secondments achieved by February 2022. This will lead to over two hundred researchers from European academia and pharmaceutical companies gaining new skills and experience in an international and interprofessional environment. A key impact of the ORBIS project will be increased competence and employability of researchers in the European pharmaceutical sector. Through new personal ties, academic and industrial institutions will form close cooperation and partnerships beyond the scope and duration of ORBIS. The project will enhance the transfer of knowledge in the pharmaceutical sector, ultimately strengthening human capital in research and innovation under the MSCA-RISE action.

## Acknowledgements

### Conflict of interest statement

The authors declare no conflict of interest.

### Funding sources

This project has received funding from the European Union's Horizon 2020 Research and Innovation Programme under the Marie Skłodowska-Curie grant agreement No. 778051 and the Ministry of Science and Higher Education of Poland fund for supporting internationally co-financed projects in 2018–

2022 (agreements No 3898/H2020/2018/2 and 3899/H2020/2018/2). This article reflects the authors' view only. Neither the Research Executive Agency nor the Polish Ministry of Science and Higher Education may be held responsible for any use of the information contained therein.

The authors gratefully acknowledge Prof. Andrzej Kutner, Dr. Bartłomiej Milanowski and Bożena Raducha for their contribution to grant proposal preparation and project launching. The ORBIS project team, including researchers and administrative staff, is acknowledged for excellent cooperation and commitment.

## References

1. Guideline on bioanalytical method validation. <https://www.ema.europa.eu/en/bioanalytical-method-validation>. Accessed 2020 March 11.
2. Kaza M, Karaźniewicz-Łada M, Kosicka K, Siemiątkowska A, Rudzki PJ. Bioanalytical method validation: new FDA guidance vs. EMA guideline. Better or worse?. *Journal of Pharmaceutical and Biomedical Analysis*. 2019 02;165:381-385. <https://doi.org/10.1016/j.jpba.2018.12.030>
3. Rudzki PJ, Milanowski B, Tajber L, Garbacz G, Jakubowska E, Rychter M, Kutner A, Lulek J. Otwarcie międzynarodowego i międzysektorowego projektu ORBIS (Horyzont 2020). *Polskie Towarzystwo Farmaceutyczne*. 2018 Jul;74(7):413-6.
4. Rudzki PJ, Biecek P, Kaza M. Incurred Sample Reanalysis: Time to Change the Sample Size Calculation?. *The AAPS Journal*. 2019 02 11;21(2). <https://doi.org/10.1208/s12248-019-0293-2>
5. Gryniewicz G, Maruszak W. Open Space Knowledge and Data and Their Influence on Natural Products Based Self-Medication Trends. *Cancer Studies and Therapeutics*. 2019 Aug;4(3):1-3.
6. Hincker A, Frey K, Rao L, Wagner-Johnston N, Ben Abdallah A, Tan B, Amin M, Wildes T, Shah R, Karlsson P, Bakos K, Kosicka K, Kagan L, Haroutounian S. Somatosensory predictors of response to pregabalin in painful chemotherapy-induced peripheral neuropathy. *PAIN*. 2019 08;160(8):1835-1846. <https://doi.org/10.1097/j.pain.0000000000001577>
7. ORBIS project website. <https://orbisproject.eu>. Accessed 2020 March 17.

# Longitudinal assessment of changes in psychosocial functioning of patients with adolescent idiopathic scoliosis using virtual reality before, during and after treatment: a quantitative and qualitative study

Ewa Misterska

The University of Safety, Department of Pedagogy and Psychology

 <https://orcid.org/0000-0001-9726-9214>

Corresponding author: [emisterska1@wp.pl](mailto:emisterska1@wp.pl)

Maciej Głowacki

Department of Pediatric Orthopaedics and Traumatology, Poznan University of Medical Sciences, Poland

 <https://orcid.org/0000-0002-9932-670X>

Published: 2020-01-31

**How to Cite:** Misterska E, Głowacki M. Longitudinal assessment of changes in psychosocial functioning of patients with adolescent idiopathic scoliosis using virtual reality before, during and after treatment: a quantitative and qualitative study. *JMS [Internet]*. 2020 Mar 31;89(1):e370. doi:10.20883/medical.370



© 2020 by the author(s). This is an open access article distributed under the terms and conditions of the Creative Commons Attribution (CC BY-NC) license. Published by Poznan University of Medical Sciences

 DOI: <https://doi.org/10.20883/medical.370>

**Keywords:** adolescent idiopathic scoliosis, body image, mental health, projective tests, cognitive-behavioural therapy, virtual reality

## ABSTRACT

This project aims to longitudinally assess changes in the psychosocial functioning of females with adolescent idiopathic scoliosis before and after completion of surgical treatment and implementation of cognitive-behavioural therapy. The planned study is a longitudinal randomised trial with 1-year follow-up. The cross-sectional aspect of the research concerns differences in perception of body shape from the perspective of the patients, their doctors, and healthy female adolescents. This study will recruit 106 patients treated at the Department of Pediatric Orthopaedics and Traumatology, Poznan University of Medical Sciences, their doctors and 106 healthy female controls. It will be the first study to use biometric self-avatars in virtual reality to investigate changes within body representation in scoliosis. The study findings will inform the development of guidelines for interdisciplinary rehabilitation of scoliosis patients following surgical treatment.

## General information

The project entitled „Longitudinal assessment of changes in psychosocial functioning of patients with adolescent idiopathic scoliosis before, during and after treatment. Quantitative and qualita-

tive study" was founded by the National Science Centre, Poland within Opus 14 competition (grant number 2017/27/B/NZ5/02109). The project is planned for 36 months, and it is run by the Department of Pedagogy and Psychology, The University of Safety, Poland, in the cooperation

with the Department of Pediatric Orthopaedics and Traumatology, Poznan University of Medical Sciences, Poland. The head of the project is Ewa Misterska, M.Sc, Ph.D, and the principal investigator is Maciej Głowacki, M.D, Ph.D. The total grant value is 579761 PLN. The study was approved by the ethics committee at the Poznan University of Medical Sciences (Decision No. 695/18).

## Research Project Objectives

The aim of the project, designed as a randomized trial with a 1 year follow-up, is a longitudinal assessment of changes in the psychosocial functioning of female patients with adolescent idiopathic scoliosis (AIS) before and after completion of surgical treatment and implementation of cognitive-behavioral therapy (CBT) interventions. A control group of healthy females will also be selected for comparative purposes.

This is the first project planning to use biometric self-avatars in virtual reality (VR) to investigate body image in AIS. This method will allow performing a realistic manipulation of body shape of personalized avatars and investigating perception of other bodies in a well-controlled way by changing the identity of the avatar while keeping the underlying body shape identical. Specifically, a stereoscopic virtual reality life-size stereo display, a three-dimensional (3D) body scanner and a body model will allow for body shape manipulations of photo-realistic virtual avatars and naturalistic mirror-scenario presentation of these avatars. Importantly, this technology will also enable to create artificial other persons that have the participant's body shape.

In recent years, VR generated both excitement and confusion [1]. The first healthcare applications of VR started in the early '90s due to the need of medical staff to visualize complex medical data, particularly during surgery and for surgery planning [2]. In behavioural sciences, where immersive devices are used by more than 50% of the applications, VR is described as "an advanced form of human-computer interface that allows the user to interact with and become immersed in a computer-generated environment in a naturalistic fashion" [3]. During the exposing, patients can thus experience the feeling of being there" [1]. All these definitions underline two dif-

ferent focuses of VR in medicine: VR as a simulation tool and VR as an interaction tool. For physicians and surgeons, the simulation focus of VR prevails over the interaction one: the ultimate goal of VR is the presentation of virtual objects to every human sense in a way identical to their natural counterpart [9]. For clinical psychologists and rehabilitation specialists the ultimate goal is different [4,5]. They use VR to provide a new human-computer interaction paradigm in which users are no longer simply external observers of images on a computer screen but active participants within a computer-generated 3D virtual world (VW). VR was verified in the treatment of six psychological disorders, e.g. panic disorders with agoraphobia [6], body image disturbances [7] or binge eating disorders [8].

The aim of the project is related to the core hypothesis which assumes that CBT interventions should prevent AIS patients from sustained body image and mental health disturbances following operative treatment. Therefore, the following questions will be investigated:

- › Do women with AIS after CBT intervention differ in their body-shape estimation, body image disturbances and mental health as compared to scoliosis patients not subjected to this intervention?
- › Do women with AIS overestimate perception of scoliosis-related body deformity before and after surgical treatment?
- › How do women with AIS differ from controls with regard to their desired body?
- › Are estimated own body shape or desired body shape correlated with scoliosis-related parameters, e.g. Cobb angle, apical translation or rib hump angle? Furthermore, to investigate the influence of a scoliosis-related body deformity on perception of other persons' body shape, we will conduct another experiment asking.
- › Do shape estimates and most attractive body shape change when patients refer no longer to the own body but to another person who is matched in body shape? Finally, we will assess the following issues.
- › Will scoliosis patients vary their behavior toward female avatars based on their body image disturbances?
- › Is there any difference between patients and their doctors in esthetic evaluation of patient's

body shape at various stages of surgical scoliosis treatment?

- › Is there any difference, depending on the stage of surgical treatment, in the patients' drawings of the body shape, as well as quantitative evaluation of BID and mental health disturbances?
- › Is there any relationship between the qualitative and VR-related evaluation of desired body shape before and following AIS surgical treatment?

## Research Plan and Basic Concept

### Work plan

In order to realize detailed goals listed above, the planned study concerns evaluation of changes within body image and mental health of AIS patients subjected (CBT scoliosis sample) or not (control scoliosis sample) to psychotherapeutic intervention, at three time points:

- › before operative treatment, at the Department of Pediatric Orthopaedics and Traumatology, Poznan University of Medical Sciences, Poland (1st A study phase);
- › within 2 weeks following operative treatment, at the Department of Pediatric Orthopaedics and Traumatology, Poznan University of Medical Sciences, Poland (1st B study phase);
- › minimum 12 months after operative treatment, after spondylodesis (spinal fusion) has stabilized and natural compensatory mechanisms have emerged, in relation to the area affected by fusion, via correspondence (2nd study phase).

The cross-sectional aspect of the research concerns differences in perception of body shape from the perspective of the patients, their doctors, and healthy female adolescents.

### Study design

Considering the study design, the random assignment to treatment groups aims to ensure that the characteristics of the participants, which may affect the results, are balanced [10].

Both scoliosis samples (experimental and control) will be fully informed of the study type. To prevent contamination, the groups will be asked not to mention the intervention to anyone outside of the group until the study was completed.

For the requirements of this project, no patients will be required to return to the clinic.

Participation will be voluntary and the patient and their carer can withdraw from the study at any point, without this affecting their right to pursue further treatment at the same Clinic. The protocol of the study will be described in details to all subjects at the time of recruitment. After hospital discharge, continuity of care and support through telecommunication devices (e-mail, chat, and telephone as preferred) will be offered to each patient. Contacts will not be scheduled and will depend only on each patient's needs.

## Research Methodology

Considering radiological and clinical research methodology, X-rays of the patient in a standing position including the pelvis from a posterior-anterior angle will be taken before and after surgery. Parameters submitted for analysis will include i.e. the value of Cobb angle, apical translation, the range of instrumentation and percent of scoliosis correction after operative treatment. Sociodemographic data will be assessed as well.

Considering psychological quantitative evaluation, patients and healthy controls will be assessed using the Polish versions of: the Trunk Appearance Perception Scale (TAPS), Spinal Appearance Questionnaire-for patients (SAQ for patients), the Strengths and Difficulties Questionnaire-25 for patients (SDQ-25 for patients) and The Trunk Aesthetic Clinical Evaluation (TRACE). Doctors will be assessed using the TRACE. Concerning qualitative analysis, participants will be assessed using the Draw a Person Test (DAP). They will be asked to draw themselves, then a female and a male body. The scoring of the DAP will be performed using the Koppitz's Human Figure Drawing Scoring System with our original modification [11-22].

Concerning virtual reality tasks, based on a three-dimensional (3D) body scan, realistic virtual 3D bodies (avatars) for each participant that will be varied through a range of  $\pm 20\%$  of the participants' Cobb angle, will be created. Avatars will be presented in a virtual reality mirror scenario. Participants will identify their actual and their desired body shape.

The cognitive-behavioral therapy for the experimental group will consist of eight sessions, each of two hours duration and will be aimed at supporting patients in accepting their actual

body shape, and in feeling positive about cosmetic results of surgical treatment.

## Patients and samples

### Patient sample

Recruitment to the study will be in accordance with the inclusion criteria (females; aged 12–18 years; qualified to surgical treatment due to AIS by means of anterior or posterior spinal fusion) and the exclusion criteria (previous spinal surgery; previous diagnosis of mental impairment). Specifically, a simple random sampling will be chosen as random allocation process. In this case, a full list of patients qualified for surgical treatment due to AIS (sample basis) and fulfilling the inclusion criteria will be available, and we will randomly select individuals using a table of random numbers, either to the CBT scoliosis sample (experimental group,  $n = 53$ ) or control scoliosis sample ( $n = 53$ ). Simple randomization can be trusted to generate similar numbers in the two trial groups and to generate groups that are roughly comparable in terms of known (and unknown) prognostic variables.

The required sample size suitable for the study was determined using the following general formula:  $n = N / (1 + (4d^2(N-1)) / u\alpha^2)$ , where  $u\alpha = 0,05$ , estimation error  $d = 0.10$  and  $N = 180000$  (based on the epidemiological data, revealing that scoliosis is diagnosed in 2–3% of children and adolescents and on GUS report indicating 6000000 children and adolescents in Poland; therefore, the population of AIS in Poland is about 180000) [23]. Based on this formula, a sample size of 96 patients was deemed suitable. In addition, sample size will be increased by 10% to compensate for potential nonresponses (refusals/losses) [24]. Finally, recruitment to the study will take place with 106 patients who were qualified for operative treatment due to scoliosis, at the Department of Pediatric Orthopaedics and Traumatology, Poznan University of Medical Sciences, their doctors and 106 healthy female controls. Simple random sampling will be chosen as random allocation process.

### Healthy controls

The following entry criteria to the healthy controls will be applied: (1) females; (2) age range of 12 to

18; and (3) no scoliosis or other spinal deformities confirmed in the clinical examination. Healthy controls will be matched at a 1:1 ratio for (i) sex and (ii) age corresponding to the minimum 1-year follow-up for the scoliosis patients. The school attended by the students in the control group will be chosen at random, as will be the class tutors to whom we will send study participation request containing information for students and parents. Adams forward bend test will be used to assess suspected scoliosis, according to the methodology proposed by Santos [25]. The evaluator will be positioned behind the student and will ask the child to undertake a trunk flexion, inclining the head and allowing the arms to fall towards the ground. The evaluator will observe the symmetry of the thoracic and lumbar spine in order to identify the presence of spinal deformity. Gibbosity will be defined as the condition of over-curvature opposed to a contralateral flattening. The possible results for this test would be: suspicion of scoliosis (gibbosity presence) or absence of scoliosis (gibbosity absence) [25].

## Data analysis

Quantitative data analysis and processing methods: In terms of descriptive statistics of quantitative features, the following will be determined: mean, median, minimum and maximum values, standard deviation, 95% confidence interval. To compare differences in results between the three time points, a Friedman two-way ANOVA will be utilized. Significant omnibus tests will be followed-up using multiple Wilcoxon signed-rank tests with a Bonferroni adjustment to protect against Type I errors. Spearman's rank correlation coefficient will be used for calculating correlations between quantitative variables. The Mann-Whitney test or the Kruskal-Wallis test will be used to determine dependencies between quantitative and qualitative characteristics. The accepted border level of statistical significance will be  $p = 0.05$  and, therefore, any test results where the  $p$  value exceeded this level will be treated as insignificant.

Qualitative data analysis and processing methods: In respect to the descriptive statistics of the qualitative features, the number of units that belong to the described categories of a giv-



en feature and their relative percentage values will be given. The scoring of the DAP will be performed using the Koppitz's Human Figure Drawing Scoring System [21] by two independent evaluators [E1,E2].

VR tasks analysis and processing methods: from the different experimental tasks, we will extract for all experiments:

- › the degree of inaccuracy/distortion of the estimated body shape as compared to participants' actual body shape at the time of the experiment (1AFC and MoA),
- › the desired body shape change (MoA),
- › the discrepancy between desired and actual body shape (MoA).

To quantify the degree of distortion, we will analyze the over- or underestimation relative to actual individual body shape.

## Measurable Effects and Expected Results

This would be the first study to use biometric self-avatars in virtual reality to investigate changes within body representation in scoliosis. This method will allow performing a realistic manipulation of body shape of personalized avatars and investigating perception of other bodies in a well-controlled way by changing the identity of the avatar while keeping the underlying body shape identical. Specifically, a stereoscopic virtual reality life-size stereo display, a three-dimensional (3D) body scanner and a body model will allow for body shape manipulations of photo-realistic virtual avatars and naturalistic mirror-scenario presentation of these avatars. Importantly, this technology will also enable to create artificial other persons that have the participant's body shape.

It is important to underline that VR is an exciting area offering opportunities in every healthcare areas, from teaching to clinical interventions [1]. The results of the referred study may have a significant contribution to development of guidelines for interdisciplinary rehabilitation of scoliosis patients following surgical treatment. Considering future research implications, the current set of virtual reality could be used in exposure-based treatments. Such methods may inform the development of interventions to reduce stigmatized beliefs about persons with easily recogniz-

able body deformities, difficult to modify through more traditional therapeutic approaches.

## Acknowledgements

### Conflict of interest statement

The authors declare no conflict of interest.

### Funding sources

The paper is a part of the project supported by the National Science Centre, Poland (grant number: 2017/27/B/NZ5/02109).

## References

1. Pensieri C, Pennacchini M. Overview: Virtual Reality in Medicine. *Journal For Virtual Worlds Research*. 2014 01 19;7(1). <https://doi.org/10.4101/jvwr.v7i1.6364>
2. Chinnock C. Virtual reality in surgery and medicine. *Hosp Technol Ser*. 1994;13(18):1-48. PMID 10172193
3. Schultheis MT, Rizzo AA. The application of virtual reality technology in rehabilitation. *Rehabilitation Psychology*. 2001;46(3):296-311. <https://doi.org/10.1037/0090-5550.46.3.296>
4. Szekely G, Satava RM. Virtual reality in medicine. *BMJ*. 1999 Nov 13;319(7220):1305-1305. <https://doi.org/10.1136/bmj.319.7220.1305>
5. Riva G, Rizzo A, Alpini D, Attree EA, Barbieri E, Bertella L, Buckwalter JG, Davies RC, Gamberini L, Johansson G, Katz N, Marchi S, Mendozzi L, Molinari E, Pugnetti L, Rose FD, Weiss PL. Virtual Environments in the Diagnosis, Prevention, and Intervention of Age-Related Diseases: A Review of VR Scenarios Proposed in the EC VETERAN Project. *CyberPsychology & Behavior*. 1999 Dec;2(6):577-591. <https://doi.org/10.1089/cpb.1999.2.577>
6. Vincelli F, Anolli L, Bouchard S, Wiederhold BK, Zurloni V, Riva G. Experiential Cognitive Therapy in the Treatment of Panic Disorders with Agoraphobia: A Controlled Study. *CyberPsychology & Behavior*. 2003 06;6(3):321-328. <https://doi.org/10.1089/109493103322011632>
7. Riva G, Bacchetta M, Cesa G, Conti S, Molinari E. Six-Month Follow-Up of In-Patient Experiential Cognitive Therapy for Binge Eating Disorders. *CyberPsychology & Behavior*. 2003 06;6(3):251-258. <https://doi.org/10.1089/109493103322011533>
8. Riva G, Bacchetta M, Baruffi M, Silvia Rinaldi, Molinari E. Virtual reality based experiential cognitive treatment of anorexia nervosa. *Journal of Behavior Therapy and Experimental Psychiatry*. 1999 09;30(3):221-230. [https://doi.org/10.1016/s0005-7916\(99\)00018-x](https://doi.org/10.1016/s0005-7916(99)00018-x)
9. Riva G, Bacchetta M, Baruffi M, Molinari E. Virtual-reality-based multidimensional therapy for the treatment of body image disturbances in binge eating disorders: a preliminary controlled study. *IEEE Transactions on Information Technology in Biomedicine*. 2002 09;6(3):224-234. <https://doi.org/10.1109/titb.2002.802372>
10. Polit DF, Gillespie BM. Intention-to-treat in randomized controlled trials: Recommendations for

- a total trial strategy. *Research in Nursing & Health*. 2010 06 01;33(4):355-368. <https://doi.org/10.1002/nur.20386>
11. Bago J, Sanchez-Raya J, Perez-Grueso FJS, Climent JM. The Trunk Appearance Perception Scale (TAPS): a new tool to evaluate subjective impression of trunk deformity in patients with idiopathic scoliosis. *Scoliosis*. 2010 03 25;5(1). <https://doi.org/10.1186/1748-7161-5-6>
  12. Misterska E, Glowacki M, Latuszewska J, Adamczyk K. Perception of stress level, trunk appearance, body function and mental health in females with adolescent idiopathic scoliosis treated conservatively: a longitudinal analysis. *Quality of Life Research*. 2012 Nov 28;22(7):1633-1645. <https://doi.org/10.1007/s11136-012-0316-2>
  13. Sanders JO, Harrast JJ, Kuklo TR, Polly DW, Bridwell KH, Diab M, Dormans JP, Drummond DS, Emans JB, Johnston CE, Lenke LG, McCarthy RE, Newton PO, Richards BS, Sucato DJ. The Spinal Appearance Questionnaire. *Spine*. 2007 Nov;32(24):2719-2722. <https://doi.org/10.1097/brs.0b013e31815a5959>
  14. Bago J, Climent JM, Pineda S, Gilperez C. Further evaluation of the Walter Reed Visual Assessment Scale: correlation with curve pattern and radiological deformity. *Scoliosis*. 2007 Dec;2(1). <https://doi.org/10.1186/1748-7161-2-12>
  15. Pineda S, Bago J, Gilperez C, Climent JM. Validity of the Walter Reed Visual Assessment Scale to measure subjective perception of spine deformity in patients with idiopathic scoliosis. *Scoliosis*. 2006 Nov 08;1(1). <https://doi.org/10.1186/1748-7161-1-18>
  16. Misterska E, Glowacki M, Harasymczuk J. Assessment of spinal appearance in female patients with adolescent idiopathic scoliosis treated operatively. *Medical Science Monitor*. 2011;17(7):CR404-CR410. <https://doi.org/10.12659/msm.881852>
  17. Goodman R. The Strengths and Difficulties Questionnaire: A Research Note. *Journal of Child Psychology and Psychiatry*. 1997 07;38(5):581-586. <https://doi.org/10.1111/j.1469-7610.1997.tb01545.x>
  18. GOODMAN R. Psychometric Properties of the Strengths and Difficulties Questionnaire. *Journal of the American Academy of Child & Adolescent Psychiatry*. 2001 Nov;40(11):1337-1345. <https://doi.org/10.1097/00004583-200111000-00015>
  19. Mazur J, Tabak I, Kololo H. W kierunku lepszej oceny zdrowia psychicznego dzieci i młodzieży. Polska wersja kwestionariusza mocnych stron i trudności. Doświadczenia dwóch badań populacyjnych. *Med Wieku Rozwoj*. 2007;11(1):13-24. PMID 17965460
  20. Goodenough FL. Measurement of intelligence by drawings. *Yonkers-on-Hudson, New York, Chicago: World Book Company; 1926.*
  21. Koppitz EM. Psychological Evaluation of Children's Human Figure Drawings. *New York: Grune & Stratton, Inc.; 1968.*
  22. Machover K. Personality projection in the drawing of the human figure: A method of personality investigation.. *Charles C Thomas Publisher; 1949.* <https://doi.org/10.1037/11147-000>
  23. Witold M, Andrzej S. Wiktora Degi ortopedia i rehabilitacja. Tom 2. *Warszawa: Wydawnictwo Lekarskie PZWL; 2002.*
  24. Martínez-Mesa J, González-Chica DA, Bastos JL, Bonamigo RR, Duquia RP. Sample size: how many participants do I need in my research?. *Anais Brasileiros de Dermatologia*. 2014 07;89(4):609-615. <https://doi.org/10.1590/abd1806-4841.20143705>
  25. Santos C, Cunha A, Braga V, Saad I, Ribeiro M, Conti P. Occurrence of postural deviations in children of a school of Jaguariúna, Sao Paulo, Brazil. *Rev Paul Pediatr*. 2009;(27):74-80.

**Journal of Medical Science (JMS)** is a PEER-REVIEWED, OPEN ACCESS journal that publishes original research articles and reviews which cover all aspects of clinical and basic science research. The journal particularly encourages submissions on the latest achievements of world medicine and related disciplines. JMS is published quarterly by Poznan University of Medical Sciences.

#### ONLINE SUBMISSION:

Manuscripts should be submitted to the Editorial Office by an e-mail attachment: nowinylekarskie@ump.edu.pl. You do not need to mail any paper copies of your manuscript.

All submissions should be prepared with the following files:

- Cover Letter
- Manuscript
- Tables
- Figures
- Supplementary Online Material

**COVER LETTER:** *Manuscripts* must be accompanied by a *cover letter* from the author who will be responsible for correspondence regarding the manuscript as well as for communications among authors regarding revisions and approval of proofs. The cover letter should contain the following elements: (1) the full title of the manuscript, (2) the category of the manuscript being submitted (e.g. Original Article, Brief Report), (3) the statement that the manuscript has not been published and is not under consideration for publication in any other journal, (4) the statement that all authors approved the manuscript and its submission to the journal, and (5) a list of at least two referees.

**MANUSCRIPT:** Journal of Medical Science publishes Original Articles, Brief Reports, Review articles, Mini-Reviews, Images in Clinical Medicine and The Rationale and Design and Methods of New Studies. From 2014, only articles in English will be considered for publication. They should be organized as follows: Title page, Abstract, Introduction, Materials and Methods, Results, Discussion, Acknowledgments, Conflict of Interest, References and Figure Legends. All manuscripts should be typed in Arial or Times New Roman font and double spaced with a 2,5 cm (1 inch) margin on all sides. They should be saved in DOC, DOCX, ODT, RTF or TXT format. Pages should be numbered consecutively, beginning with the title page.

#### Ethical Guidelines

Authors should follow the principles outlined in the Declaration of Helsinki of the World Medical Association ([www.wma.net](http://www.wma.net)). The manuscript should contain a statement that the work has been approved by the relevant institutional review boards or ethics committees and that all human participants gave informed consent to the work. This statement should appear in the Material and Methods section. Identifying information, including patients' names, initials, or hospital numbers, should not be published in written descriptions, illustrations, and pedigrees. Studies involving experiments with animals must be conducted with approval by the local animal care committee and state that their care was in accordance with institution and international guidelines.

#### Authorship:

According to the International Committee on Medical Journal Ethics (ICMJE), an author is defined as one who has made substantial contributions to the conception and development of a manuscript. Authorship should be based on all of the following: 1) substantial contributions to conception and design, data analysis and interpretation; 2) article drafting or critical advice for important intellectual content; and 3) final approval of the version to be published. All other contributors should be listed as acknowledgments. All submissions are expected to comply with the above definition.

#### Conflict of Interest

The manuscript should contain a conflict of interest statement from each author. Authors should disclose all financial and personal relationships that could influence their work or declare the absence of any conflict of interest. Author's conflict of interest should be included under Acknowledgements section.

#### Abbreviations

Abbreviations should be defined at first mention, by putting abbreviation between brackets after the full text. Ensure consistency of abbreviations throughout the article. Avoid using them in the title and abstract. Abbreviations may be used in tables and figures if they are defined in the table footnotes and figure legends.

#### Trade names

For products used in experiments or methods (particularly those referred to by a trade name), give the manufacturer's full name and location (in parentheses). When possible, use generic names of drugs.

#### Title page

The first page of the manuscript should contain the title of the article, authors' full names without degrees or titles, authors' institutional affiliations including city and country and a running title, not exceeding 40 letters and spaces. The first page should also include the full postal address, e-mail address, and telephone and fax numbers of the corresponding author.

#### Abstract

The abstract should not exceed 250 words and should be structured into separate sections: Background, Methods, Results and Conclusions. It should concisely state the significant findings without reference to the rest of the paper. The abstract should be followed by a list of 3 to 6 Key words. They should reflect the central topic of the article (avoid words already used in the title).

*The following categories of articles can be proposed to the Journal of Medical Science:*

#### ORIGINAL RESEARCH

**Original articles:** Manuscripts in this category describe the results of original research conducted in the broad area of life science and medicine. The manuscript should be presented in the format of Abstract (250-word limit), Keywords, Introduction, Material and Methods, Results, Discussion, Perspectives, Acknowledgments and References. In the Discussion section, statements regarding the importance and *novelty of the study* should be presented. In addition, the limitations of the study should be articulated. The abstract must be structured and include: Objectives, Material and Methods, Results and Conclusions. Manuscripts cannot exceed 3500 words in length (excluding title page, abstract and references) and contain no more than a combination of 8 tables and/or figures. The number of references should not exceed 45.

**Brief Reports:** Manuscripts in this category may present results of studies involving small sample sizes, introduce new methodologies, describe preliminary findings or replication studies. The manuscript must follow the same format requirements as full length manuscripts. Brief reports should be up to 2000 words (excluding title page, abstract and references) and can include up to 3 tables and/or figures. The number of references should not exceed 25.

#### REVIEW ARTICLES

**Review articles:** These articles should describe recent advances in areas within the Journal's scope. Review articles cannot exceed 5000 words length (excluding title page, abstract and references) and contain no more than a combination of 10 tables and/or figures. Authors are encouraged to restrict figures and tables to essential data that cannot be described in the text. The number of references should not exceed 80.

**A THOUSAND WORDS ABOUT...** is a form of Mini-Reviews. Manuscripts in this category should focus on *latest achievements of life science and medicine*. Manuscripts should be up to 1000 words in length (excluding title page, abstract and references) and contain up to 5 tables and/or figures and up to 25 most relevant references. The number of authors is limited to no more than 3.

## OTHER SUBMISSIONS

**Invited Editorials:** Editorials are authoritative commentaries on topics of current interest or that relate to articles published in the same issue. Manuscripts should be up to 1500 words in length. The number of references should not exceed 10. The number of authors is limited to no more than 2.

**Images in Clinical Medicine:** Manuscripts in this category should contain one distinct image from life science or medicine. Only original and high-quality images are considered for publication. The description of the image (up to 250 words) should present relevant information like short description of the patient's history, clinical findings and course, imaging techniques or molecular biology techniques (e.g. blotting techniques or immunostaining). All labeled structures in the image should be described and explained in the legend. The number of references should not exceed 5. The number of authors is limited to no more than 5.

**The Rationale, Design and Methods of New Studies:** Manuscripts in this category should provide information regarding the grants awarded by different founding agencies, e.g. National Health Institute, European Union, National Science Center or National Center for Research and Development. The manuscript should be presented in the format of Research Project Objectives, Research Plan and Basic Concept, Research Methodology, Measurable Effects and Expected Results. The article should also contain general information about the grant: grant title, keywords (up to five), name of the principal investigator and co-investigators, founding source with the grant number, *Ethical Committee permission number*, code in clinical trials (if applicable). Only grant projects in the amount over 100,000 Euro can be presented. Manuscripts should be up to 2000 words in length (excluding references) and can include up to 5 tables and/ or figures. The abstract should not exceed 150 words. The number of authors is limited to the Principal Investigator and Co-investigators.

### Acknowledgements

Under acknowledgements please specify contributors to the article other than the authors accredited. List here those individuals who provided help during the research (e.g., providing language help, writing assistance or proof reading the article, etc.). Also acknowledge all sources of support (grants from government agencies, private foundations, etc.). The names of funding organizations should be written in full.

### References

**All manuscripts should use the 'Vancouver' style for references.** References should be numbered consecutively in the order in which they appear in the text and listed at the end of the paper. References cited only in Figures/Tables should be listed in the end. Reference citations in the text should be identified by Arabic numbers in square brackets. Some examples:

- This result was later contradicted by Smith and Murray [3].
- Smith [8] has argued that...
- Multiple clinical trials [4–6, 9] show...

Journal names should be abbreviated according to Index Medicus. If available always provide Digital Object Identifier (DOI) or PubMed Identifier (PMID) for every reference.

Some examples

### Standard journal articles

1. Petrova NV, Kashirskaya NY, Vasilyeva TA, Kondratyeva EI, Marakhonov AV, Macek Jr M, Ginter EK, Kutsev SI, Zinchenko RA. Characteristics of the L138ins (p.Leu138dup) mutation in Russian cystic fibrosis patients. *JMS* [Internet]. 2020 Mar 31;89(1):e383. doi: 10.20883/medical.383.

## Books

Personal author(s)

1. Rang HP, Dale MM, Ritter JM, Moore PK. *Pharmacology*. 5th ed. Edinburgh: Churchill Livingstone; 2003.

Editor(s) or compiler(s) as authors

2. Beers MH, Porter RS, Jones TV, Kaplan JL, Berkwitz M (editors). *The Merck manual of diagnosis and therapy*. 18th ed. Whitehouse Station (NJ): Merck Research Laboratories; 2006.

Chapter in the book

1. Phillips SJ, Whisnant JP. Hypertension and stroke. In: Laragh JH, Brenner BM, editors. *Hypertension: pathophysiology, diagnosis, and management*. 2nd ed. New York: Raven Press; 1995. p. 465–478.

**TABLES:** Tables should be typed on sheets separate from the text (each table on a separate sheet). They should be numbered consecutively with Arabic numerals. Tables should always be cited in text (e.g. table 2) in consecutive numerical order. Each table should include a compulsory, concise explanatory title and an explanatory legend. Footnotes to tables should be typed below the table body and referred to by superscript lowercase letters. No vertical rules should be used. Tables should not duplicate results presented elsewhere in the manuscript (e.g. in figures).

**FIGURES:** All illustrations, graphs, drawings, or photographs are referred to as figures and must be uploaded as separate files when submitting a manuscript. Figures should be numbered in sequence with Arabic numerals. They should always be cited in text (e.g. figure 3) in consecutive numerical order. Figures for publication must only be submitted in high-resolution TIFF or EPS format (*minimum 300 dpi resolution*). Each figure should be self-explanatory without reference to the text and have a concise but descriptive legend. All symbols and abbreviations used in the figure must be defined, unless they are common abbreviations or have already been defined in the text. Figure Legends must be included after the reference section of the Main Text.

*Color figures:* Figures and photographs will be reproduced in full colour in the online edition of the journal. In the paper edition, all figures and photographs will be reproduced as black-and-white.

**SUPPLEMENTARY ONLINE MATERIAL:** Authors may submit supplementary material for their articles to be posted in the electronic version of the journal. To be accepted for posting, supplementary materials must be essential to the scientific integrity and excellence of the paper. The supplementary material is subject to the same editorial standards and peer-review procedures as the print publication.

### Review Process

All manuscripts are reviewed by the Editor-in-Chief or one of the members of the Editorial Board, who may decide to reject the paper or send it for external peer review. Manuscripts accepted for peer review will be blind reviewed by at least two experts in the field. After peer review, the Editor-in-Chief will study the paper together with reviewer comments to make one of the following decisions: accept, accept pending minor revision, accept pending major revision, or reject. Authors will receive comments on the manuscript regardless of the decision. In the event that a manuscript is accepted pending revision, the author will be responsible for completing the revision within 60 days.

### Copyright

The copyright to the submitted manuscript is held by the Author(s), who grants the Journal of Medical Science (JMS) a nonexclusive licence to use, reproduce, and distribute the work, including for commercial purposes.